NASA Contractor Report 198312

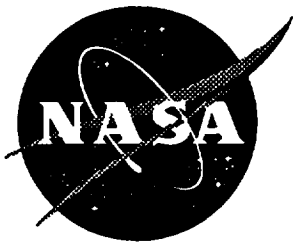

Results of Tests Performed on the Acoustic Quiet Flow Facility Three-Dimensional Model Tunnel

Final Report on the Modified D.S.M.A. Design

P. S. Barna
Lockheed Martin Engineering & Sciences Company
Hampton, Virginia

Contract NAS1-19000

April 1996

National Aeronautics and
Space Administration
Langley Research Center
Hampton, Virginia 23681-0001

RESULTS OF TESTS PERFORMED ON THE ACOUSTIC QUIET FLOW FACILITY THREE-DIMENSIONAL MODEL TUNNEL

FINAL REPORT ON THE MODIFIED D.S.M.A. DESIGN

by

P.S.BARNA

SUMMARY

Numerous tests were performed on the original ACOUSTIC QUIET FLOW FACILITY THREE-DIMENSIONAL MODEL TUNNEL, scaled down from the full-scale plans, shown in figure 1, which were submitted to NASA by Messrs. D.S.M.A. Corporation in July 1992 [1]. Results of tests performed on the original scale model tunnel were reported in April 1995, which clearly showed that this model was lacking in performance.

Subsequently this scale model was modified to attempt to possibly improve the tunnel performance.

The modification included: (a) redesigned diffuser;
(b) addition of a collector;
(c) addition of a Nozzle-Diffuser;
(d) changes in location of vent-air.

Tests performed on the modified tunnel showed a marked improvement in performance amounting to a nominal increase of pressure recovery in the diffuser from 34 percent to 54 percent.

Results obtained in the tests have wider application. They may also be applied to other tunnels operating with an open test section not necessarily having similar geometry as the model under consideration.

LIST OF SYMBOLS

A	area, sqft or sqin.
Ai	inlet area
Ae	exit area
AR	area ratio Ai/Ae for contraction
AR	area ratio Ae/Ai for diffusers
AS	aspect ratio at diffuser inlet, b/w
b	width at diffuser inlet,
B	blockage at diffuser inlet,
Cp	specific heat at constant pressure
d	diameter,
g	gravitational acceleration 32.2 ft/secsq.,
h	enthalpy, u+pv, B.T.U.,or vertical traverse height ins.
J	work equivalent, 778 ftlbs/BTU
k	ratio of specific heats, Cp/Cv
M	Mach number,
l	length of traverse along tunnel centerline, ins.
L	length of diffuser, ins.
Ps	static pressure, p.s.f.,
Pt	total pressure, p.s.f.,
R	gas constant, for air 53.3
Rd	energy recovery in diffuser, percent
deg.R	absolute temperature,
Re	Reynolds number
T	stagnation temperature, deg R.
u'	horizontal fluctuations, ft/s
v'	vertical fluctuations, ft/s
U,V,	stream velocity, ft/s
Uc	stream velocity in the tunnel centerline, ft.s
w	diffuser inlet height, horizontal travel distance, ins.
W	massflow, lb/sec.
X	horizontal distance normal to flow, ins.
Y	vertical distance normal to flow, ins.
Z	horiz.,longitudinal distance along tunnel centerline, ins.
u'/U	relative r.m.s. fluctuations,
ρ	air density, slugs per cuft.
θ	static temperature, deg.R, or collector/diffuser side angle

Abbreviations:

p.s.f.	pound per sqft.
p.s.i.	pound per sqins.,
CFM	cuft. per minute,
CFS	cuft. per second,
r.m.s.	root mean square,

HP = horsepower

Subscripts

ave	average,
e	exit,
i	inlet,
c	center
1	diffuser inlet
2	diffuser outlet

SECTION I

DESIGN CHANGES AND STUDIES OF COMPONENT PERFORMANCE

An improved environment in the test chamber, a more suitable jet in which to conduct tests, and an improved overall efficiency were the targets of these modifications. Details of the flow in the test chamber, and of the jet performance will be discussed in Section II to be presented later. Herein the emphasis is on the improved efficiency; specifically that of the collector, and diffuser.

SOME DESIGN DETAILS OF THE ORIGINAL AND MODIFIED MODEL TUNNEL

In order to understand the difference between the original and the modified D.S.M.A. model tunnel refer to figures 2 and 3 where the essential dimensions of the test chamber enclosure and main components are shown in inches both in plan view and elevation. These dimensions were reduced from the original D.S.M.A design in a ratio of 1:48.

Figure 2/a shows the plan view of the original design, where a parallel duct leads to the contraction protruding into the test chamber and discharging air into the test area. (The flow is from left to right). Having crossed the test area, the air then moves into the diffuser, a portion of which is also protruding into the test chamber. An air-vent intake is located on top of the chamber as shown in figure 2/b. Having entered horizontally, the vent-air is turned downward by the corner and is expected to flow around the parallel duct as well as to move horizontally with the main flow issuing from the contraction.

Figure 3 shows essential details of the modified design in which the size of both, the test chamber and the test area, remain the same. In the plan view, figure 3/a, one observes the following changes: an extension to the contraction, in form of a short diverging duct called the Nozzle-Diffuser (abbreviated to N/D); the addition of a collector which replaces the protruding part of the diffuser; alterations to the diffuser entry to produce an air gap between the collector and diffuser and other changes in the diffuser design. (Details of the original and modified diffuser and the reasons for the changes will be discussed further on). Finally, the air-vent ducts were relocated in order to to permit air to enter from both sides of the chamber. The air-vent intake on the top of the chamber was eliminated, as shown in figure 3/b.

It is noted that while the center of the test area moved slightly to the right, the size of the testing area remained the same.

SOME PROBLEMS EXPERIENCED WITH THE DSMA DESIGN ALTERATIONS

It is of interest to recount the various steps taken in the course of alterations which ultimately lead to the final design.

Relocation of the air-vent from the top of the test chamber to side vents opposite each other was a straightforward move without problems. This change allowed the flow around the contraction to be more symmetrical and it also required from the vent-air to turn only once 90 degrees. (From practical considerations: cleaning a vertical passage equipped with filters deemed easier than climbing on top of the chamber).

Problem with collectors

The problem of eliminating reverse flow at the diffuser entry and thus increasing diffuser recovery became a rather tedious process. It started first with the proposition of testing collectors. Some time ago various collector designs were tested at NASA in the 24th scale model of the 14- by- 22 ft. Low Speed Tunnel. The results were published in a NASA T.& M. [2].

Briefly: a collector is a short duct employed in wind-tunnels operating with an open test section. Placed upstream of the diffuser it resembles a contraction and is best formed with straight walls which are detached and located upstream from the diffuser. A suitable air gap between collector and diffuser entrance allows for flow equalization.(Allowing some gap-flow).

Installation of a collector demanded the diffuser to be permanently withdrawn from the test chamber (the portion protruding) and so to create space for the collector. Designs with various side angles were fabricated as shown in figure 4. The results were disappointing because tests already with the first test collector showed reverse flow at the collector inlet. Again low diffuser recovery was experienced. Thus it became clear that further studies were needed to resolve this tough problem.

Guidance was received from the tests performed earlier on the two-dimensional model [3]. It appeared from the tests that not only the side angle of the collector affected the flow, the throat width

(where the passage is the narrowest) had effects as well. And while the two-dimensional model allowed easy access to changes, in the three dimensional model such changes became very cumbersome. It was clear that both, a new diffuser and a new collector was needed, but it remained problematical how to design them.

Ultimately, the following procedure was adopted for the collector: the flow was traversed both, horizontally and vertically, and the velocity distribution was obtained along the center lines. This was performed in the exit plane of the contraction as well as immediately upstream of the collector. This method allowed to establish the volumetric flow rates by graphical integration. A sample is shown in APPENDIX A.

Since the flow rate entering the collector is larger than the flow rate leaving the contraction (because of the entraied vent-air),one can estimate from the integral curves the dimension of areas needed for continuity. It is noted that this procedure establishes first the required area at the collector inlet. The outlet area of the collector then can be established from the results of earlier tests which showed that for optimum flow conditions the side angles of the collector to be about 4 degrees.

Having established the exit area of the collector, the inlet area of the diffuser can be estimated which may be equal or slightly larger than the exit area of the collector. This is a matter of choice. On one hand, if one assumes that all flow moves through the collector passage then the areas may be equal, because there would be no flow expected through the gap. On the other hand, one may assume the rate of vent-air to bypass the collector and move through the gap, in which case the inlet area of the diffuser may be slightly larger to accomodate this flow as well.

The calculations showed the need for a smaller collector compared to what the original plan called for, as shown in figure 5 where the "new" collector and the first test collector appear side by side.

Problems with the diffuser

Having established the exit area of the collector, a different inlet area to the diffuser became available. Thus it became apparent that the original diffuser had to be discarded and a new one designed. In the new design, it was resolved to let the vent-air pass through the gap and to adjust the diffuser inlet area in order to accomodate the vented air flow amounting to about 10 percent of the main jet flowrate. This 10 percent is an arbitrary figure as the rate of vent-air may be adjusted by the ambient pressure prevailing inside the test chamber. However, experience gained fom the tests show that 10 percent is an "acceptable" figure considering results obtained under normal operating conditions. Except for the inlet area which was smaller, the new diffuser had the same length and aproximately the same exit area.

It is noted that the new diffuser proved to be superior to the old one for two reasons as further explained in APPENDIX B. On one hand it had the advantage of an increase in area ratio A2/A1 and in length to inlet diameter ratio L/d as well. On the other hand, the flow distribution at diffuser inlet showed a markedly smaller blockage, all contributing to a much improved diffuser. In figure 6 changes of dimensions from the original to the new diffuser are shown for comparison.

Problems with the Nozzle-Diffuser

Problems with the N/D were originally thought to be minimal because numerous tests performed with it, prior to the present project, proved the usefulness of its application [4,5]. Results in the project under consideration showed similar benefits; the details to be presented in a subsequent report. Nevertheless, while prior tests consistently showed optimum performance with a side angle of approximately six degrees, recent tests indicated that the length of the N/D may also affect performance. This aspect requires some further studies in future. Details of the N/D employed in this project, as attached to the contraction, is shown in figure 7.

THE MODIFIED TEST EQUIPMENT

Description of the first test model scaled from the original DSMA design was adequately presented in the Progress Report of April 1995 and it will not be repeated here. The modified test model is shown in more detail in figure 8 where all components are shown and some changes in pressure ports are also noted.

Static pressure ports 1,2,3,4,6,11 and 12 remain the same, while attention is called for the the following ports: 5 is moved to the exit of the N/D while 7 is located in the parallel portion of the diffuser inlet section and 8 at its exit. Please note that while ports 7 and 8 are pressure tappings at the walls, ports 9 and 10 are static ports of Pitot-static tubes (for the sake of comparison) positioned in the center of the ducts . Ports 16 to 22 are located along the center of the collector wall, while ports 13 and 14 are located on the walls of the vent-air passages.

INSTRUMENTATION

Since instrumentation has already been adequately presented in the previous Progress Report, details will be omitted here. It is noted that no additional instruments were introduced.

TEST RESULTS

Test results may be classified into two categories: (a) results on pressures over the entire circuit; (b) results of flow through each component.

Pressures

Results on the entire circuit may be simply represented by the pressure distribution: it readily shows the "energy" changes along the circuit, including the pressure recovery in the diffuser. A typical pair of examples is shown in figures 9 and 10. In both figures the horizontal abscissa shows the port location and the vertical ordinate represents gage pressure in p.s.f. The various port locations also appear on a sketch at the bottom of the graph.

Figure 9 shows the pressure distribution along the circuit with the 3.5 inch orifice plate located between ports 11 and 12. Looking at the distribution, one finds the fan pressure at 55 p.s.f. with no change between 1 and 2. The drop between 2 and 3 is due to the presence of the honeycomb and screen . While practically no significant change occurs between 3 and 4, a large conversion of pressure into kinetic energy is experienced between 4 and 5. (Please note that the pressure at 5 was measured with the static port of a Pitot - static tube located near the N/D wall with the port in alignement with the N/D exit plane). Port 6 shows the chamber pressure near the wall of the enclosure. (And so do ports 13 and 14 in vent-air passages).

Having traversed the testing area one observes ports 16 to 22 on the collector wall. These pressures are not shown on the figure but will be discussed later. The large rise in pressure between 7 and 8 signifies the pressure recovery in the diffuser, while the small rise between 8 and 11 is a limited diffusion due to an area increase at the corner. The pressure drop between 11 and 12 is caused by the orifice metering the flow rate, while the drop between 12 and the atmospheric exit represents "exit loss". This exit loss is the conversion of the remaining pressure into kinetic energy of the flow "going out the chimney".

It is noted that in this circuit pressure at port 1 and the atmospheric exit pressure remain fixed, while all other pressures along the circuit may be manipulated, e.g. by changing the N/D, or the orifice plate, or the hight H of the flow control plug, etc.

Figure 10 shows the pressure changes with the 4 inch orifice plate installed in the system. It appears at once that the flowrate increased because the pressure drop between port 4 and 5, representing kinetic energy, is larger than on figure 9. It also appears that pressures at 5 and downstream from 5 have shifted downward. Pressure at 5 dropped from +2.5 to -7.5, and at port 6 it changed from + 0.11 to -0.37, while at port 7 it dropped to -17.1 and so on. Notice the pressure drop at ports 13 and 14 from +0.14 with the 3 1/2 in. orifice plate, to -0.38 with the 4 in. orifice plate.

The sign change indicates a reversal of vent-air flow direction because negative pressures experienced at port 13 and 14 signify that vent-air was drawn into the test chamber, while positive pressures mean the opposite. Thus, results obtained with the 3.5 and 4 inch orifice plates clearly show the importance of pressure distribution tests.

Axial variation of pressure inside the collector passage (ports 16 to 22) leads to understanding internal flow distribution which was one of the subjects of discussion presented earlier in the Final Report on the Two-Dimensional Tunnel tests, January 1994 [3]. In that report it was concluded that optimum conditions were obtained with a 4 degree side angle of the collector, and that at higher side angles reverse flow was experienced at collector entry. In the present, Three-Dimensional Tunnel tests, two collectors were tested and the passage pressure variation is shown in figure 11 for both collectors.

It appears, that collector No.1, (first test collector) had an exit area of 6.18 sqin. while collector No.2 had 3.84 sqin. In going downstream from the inlet, both collectors first showed a pressure rise and attained a maximum pressure. Further downstream the pressure decreased gradually towards the exit. It is understood that pressure rise indicates deceleration while fall is accompanied by acceleration. However, pressure rise results in reverse flow because of the unfavorable gradient it creates, while pressure decrease results in acceleration of the flow which creates a favorable gradient that effectively controls boundary layer growth. There was a marked difference in the location of the maximum pressure, which in No. 1 collector was found farther downstream than in that of No.2. Under ideal flow conditions the stagnation point should be on the leading edge of the collector and in this case there would be little, if any, reverse flow.

Hence one concludes that No.1 collector suffered from reverse flow at the inlet which was confirmed with flow-visualization by using tufts of short length. Obviously the No.1 collector proved too large.

Flow distributions

Generally, along the circuit, flow pattern changes are experienced in all types of wind-tunnels small or large, because of the growth of the boundary layer along the flow. This is not quite the case in tunnels operating with an open test section because of the transfiguration of the jet. As it moves along the test area the jet core decreases in size while the total flow width increases. Figure 12 shows these effects schematically. Having traversed the test area the flow enters the collector where a fresh boundary layer is formed at the leading edge. In order to keep this boundary layer as thin as possible flow acceleration is required from the leading to the trailing edge. In the presence of an adverse pressure gradient flow reversals appear which must be prevented in order to produce a flow of low blockage at the inlet to the diffuser. It is known [6] that blockage has a major effect on diffuser performance. Since blockage is depending on history of the flow it is prudent to explore the flow distributions from contraction exit to diffuser inlet.

Various flow distributions

Flow distributions were obtained at relevant locations by measuring the stream velocity at numerous points across the flow. Accordingly, distributions across the flow were measured:

in the exit plane of the N/D;
in the inlet plane of the collector;
in the exit plane of the collector (inside the gap);
at diffuser intake, halfway down from the inlet.

In most tests attempts were made to measure both, horizontally and vertically, along the center lines of the cross section under study. (Measurements were obtained with hotwire, Pitot-Static tube and Pitot cylinder, as required).

Figure 13 shows the horizontal and figure 14 the vertical flow distribution in the exit plane of the N/D. Save for a small bounday-layer build up, the horizontal results appear satisfactory as uniformity was maintained over a major part of the traverse. However, the vertical traverse showed some adverse effects, probably due to some inaccuracy that may have occured during the manufacture of this component.

While the jet is traversing the test area marked changes occur in the flow pattern. The physics of jet flow is very well known and the subject is adequately discussed in the literature [7]. However, there is, remarkably, much less known how to collect the flow efficienly and how to design a suitable collector. We have discovered, some procedures which can lead to the desired results.

Consider first the far end of the jet, where it reaches the collector inlet. At this location the horizontal center flow distribution vastly differs from the flow pattern emerging from the contraction as shown in figure 15 where U/Umax is plotted against the horizontal distance x/w. Because the flow spreads out downstream the distribution curve is shown to cover an increasing width with distance from the nozzle exit. In this instance a traverse w = 10 ins. was used.(that is plus and minus 5 ins. from the centerline). On the bottom of the graph the N/D exit is shown schematically and at the top, the collector appears. The bell-shaped distribution of flow first needs to be "collected" (hence the name of the collector) and then must be made as uniform as possiblet to meet the requirement of low blockage entering the diffuser. Thus the collector faces a double task.

DESIGN MODIFICATIONS TO THE COLLECTOR AND DIFFUSER

The first set of tests performed on the original DSMA model [8] clearly showed a reverse flow at the diffuser entry. This was clearly illustrated in the report of April 1995 by the graphs of velocity distributions where flow velocities attained zero value at some distance from the walls because there the flow turned around. The diffuser recovery then was then estimated only 34% due to the

unsatisfactory flow distribution. This meant that 66% of kinetic energy had to be sacrificed.

Subsequent efforts lead to changes in the test set-up necessitating the withdrawal of the diffuser from the test chamber and the installation of an experimental collector. To accept a nozzle-diffuser, the contraction was moved back by a short distance allowing the test area to remain the same size.

The problem was: how to reduce the tunnel "blockage" to a reasonable level and at the same time increase diffuser recovery as well. Briefly, tunnel blockage is a relation of the actual flow rate through the tunnel to the "ideal" flow rate based on the assumption of perfectly uniform flow distribution. (See APPENDIX B for details). Results of tests published in the DIFFUSER DATA BOOK [6] suggest that blockage up to 12 percent may be considered reasonable.

As mentioned earlier, blockage under reverse flow conditions cannot be easily established because the rate of reverse flow is most difficult to obtain. Thus blockage of the original diffuser design has not been established. After the withdrawal of the diffuser and following the installation of both, an experimental collector and the N/D, some improvement in diffuser recovery was experienced amounting to about 39.7 percent.

At this point of the proceedings the experimental collector was replaced by a new collector having the length of the test collector and was provided with 4 degrees side angles. The dimensions for the entry and exit area were obtained by graphical integration of the velocity distribution upstream of the experimental collector, as explained in APPENDIX A. In this design it was assumed that all the flow from the contraction to pass through the collector while the ventilating airflow to pass through the gap.

Combination of the new collector with the old diffuser.

When the new collector was installed in its proper place upstream of the original diffuser, a short parallel duct was added to its intake to ensure parallel flow at the diffuser inlet. Flow traverses obtained in the parallel duct produced a 17.7 percent blockage in the horizontal plane and 20.75 percent blockage in the vertical plane. As a result of the high blockage diffuser recovery remained - disappointingly low at 42.5 percent.

The difference between the horizontal and vertical blockages indicated that a mismatch existed between collector exit and diffuser inlet. A comparison of the two dimensions of the new collector exit to the old diffuser inlet showed a 9 percent decrease in width but a hefty 29 percent decrease in height. It was then found expedient to look for a new diffuser.

Combination of the new collector with a new diffuser

Consultation with the DIFFUSER DATA BOOK on FLAT DIFFUSERS proved extremely useful. This book presents experimental data for both, conical and flat, diffusers. Diffusers under consideration were flat, the type where the side walls run parallel with each other. In order to eliminate the significantly large difference in dimensions between collector exit and diffuser inlet, the diffuser inlet height was reduced from 2.25 ins. to 1.75 ins. and its width, from 2.75 to 2.5 ins. (The small difference in height between 1.75 and collector height 1.60, amounting to 0.15 ins., was an allowance for the by-pass air to enter through the gap.) The length of the new diffuser remained the same 22.5 ins. A short parallel duct was again added to the diffuser inlet for the purpose of establishing parallel flow into the diffuser.

Flow traverses obtained at diffuser inlet showed a marked impro-ment in blockage as shown in figures 16 and 17 where the flow distributions at inlet are shown for both, the old and the new diffuser. It appears the the new diffuser has a blockage of about 11.7 percent in the horizontal plane (# 161) and 10.2 percent in

the vertical plane.(Test 162). As a result the new diffuser attained about 54 percent efficiency.

This result compares favourably with those presented in the DIFFUSER DATA BOOK graph which is reproduced here as figure 18, showing the various "parameters" affecting performance. (This graph, which is one of many graphs presented in the DATA book, shows results of tests obtained with "flat" diffusers). Figure 18 shows the constant efficiency curves for a variety of diffusers which have an aspect ratio AS=1, throat Mach number Mt = 0.2, blockage B = 0.12 and Reynoldds number R = 279,000. The abscissa represents the diffuser length to throat ratio L/w while the ordinate is the area ratio AR = A2/A1. The parallel lines inclined of about 45 degree represent the diffuser divergence angle 2θ.

The new diffuser has a divergence angle 2θ = 7 degree, area ratio of about 2.5 and length-to-throat ratio L/w = 13. These data yield an efficiency of about 58 percent on figure 18. (For details see APPENDIX C.) The discrepancy between 58 and 54 percent may be due to the difference in aspect ratio, the new diffuser having an aspect ratio AS = 1.4. The DATA BOOK shows that recovery efficiencies fall with increasing aspect ratio. This may be one reason for the lower efficnecy result obtained in the tests and the other may be the difference in Reynolds number. (2x10E5 vs. 2.79x10E5).

RECAPITULATION OF SECTION I

Tests were conducted on the modified three-dimensional AQFF 1:48 scale model tunnel in order to establish the results of the modifications.

These tests concerned mainly with studies with each component's performance rather than flow patterns. Performance of the test tunnel was considerably improved by: 1) adding a suitable collector: 2): re-designing the diffuser.

Studies of flow patterns will be discussed in SECTION II.

REFERENCES

1. Raimondo, S., Clark P. : The Quiet Flow facility, L.R.C. Final Review Submission, CMSS Architects, July 17, 1992.

2. Manuel, G.S. et al.: Effects of Collector Configuration on Test Section Turbulence Levels in an Open-Jet Wind Tunnel. NASA TM 4333, July 1992.

3. Barna, P.S. : Results of Tests Performed on the Acoustic Quiet Flow Facility Modified Two-Dimensional Model Tunnel. Final Report, Phase 1, Lockheed Engineering & Sciences Company, January 1994.

4. Barna, P.S. : Investigations of the Detail Design Issues for the High Speed Acoustic Wind Tunnel Using a 60th Scale Model Tunnel. Final Report. Part I. Tests with Open Circuit. Lockheed Engineering & Sciences Company, March 1991.

5. U.S.A. Patent-Barna, P.S. : Nozzle Diffuser for Use with an Open Test Section of a Wind Tunnel. Patent # 5,211,057 May 18, 1993.

6. Runstadler, P.W. et al. : Diffuser Data Book, CREARE Inc. TN-186 May 1975.

7. Abramovitch, G.N. : The Theory of Turbulent Jets, M.I.T. 1963.

8. Barna, P.S. : Results of Tests Performed on the Acoustic Quiet Flow Facility Three-Dimensional Model Tunnel. Progress Report on the D.S.M.A. Design, NASA CR-198311, April 1995.

APPENDIX A

Volumetric flow rates by graphical integration to establish dimensions of collector intakes

To establish the dimensions of the collector intake, consideration must be given to a jet which - in this case - is surrounded by co-flowing air introduced into the test chamber through the air vents. The size of a collector is to be established such that it will accept a volume flow rate, based on the velocity distribution, equal to or larger than that discharged from the contraction.Thus traversing the flow across a wide width of the chamber upstream of the test collector seems justified.

Mixing of the jet with the surrounding co-flowing air results in a non-uniform flow by the time it reaches the intake of the collector. As an example: a typical traverse is shown in figure AP/a where the velocity U is plotted against the horizontal distance x. The traverse width (or length) w was 11 inches. Since the jet was assumed to be symmetrical, half of the width, 5.5 ins., sufficed to establish half the flow rate. In addition, the depth of the area was assumed to be unity, that is 1 inch. Thus the half flow rate Q/2 may be expressed as

$$Q/2 = b\int_{0}^{w/2} U\,dx$$

where b = 1 inch.

Integration was performed with a planimeter and the integral curve is shown in figure AP/b. The integral curve shows the halved flow rate as 12.42 "units" on the ordinate. To understand this unit consider one square inch area on figure 16/a where one inch on the ordinate is represented as 20 ft/sec velocity. Thus 1 sqin represents (1x20)/144=0.1389 . Therefore, 12.42x0.1389 = 1.725 cubic ft. per second would be the total half-flow rate across 5.5 inch traverse.

The total flow rate through the N/D, being equal to 254.7 c.f.m. was based on an average flow velocity, Vave = 172 ft/s, through an

area of 2.2055 x 1.612 sqins. (See sketch below). For half flow rate, this works out across the 1 in. wide strip as 1.317 c.f.s. and upon dividing this by the factor 0.1389, one obtains 9.48.

Let us start the procedure with the half width of the collector thus considering that portion of the jet which was measured from the centerline and contains a volume flow rate of 9.48 "units". However, to establish half-width of the collector, one needs to start the integration from the jet centerline so that the resulting curve will be the mirror image of the one obtained when the integration started from the wall or near the wall. Upon finding 9.48 on the ordinate, the width can be found from the intersection of the horizontal line with the "mirror" curve. This yields a half-width equal to 1.1 ins. which, incidently, is about the same as the N/D half width. (These dimensions were slightly increased for vent-air).

Let us consider for a moment the streamline pattern of the flow, which emerges from the exit plane of the N/D. By noting the particular streamline springing from the lip of the N/D as the ZERO STREAMLINE one may follow this streamline until it contacts the collector. If one assumes that all the flow from the N/D under the zero streamline is "collected", the stagnation point may be located on the leading edge of the collector. Hence the collector needs to be no wider than the width derived from the integration. However, one may also consider to provide for the vent-air flow, estimated to be about 10-12 percent. To accomodate this, the collector ought to be made larger otherwise a quantity of air, bypassing the collector, may flow through the gap.

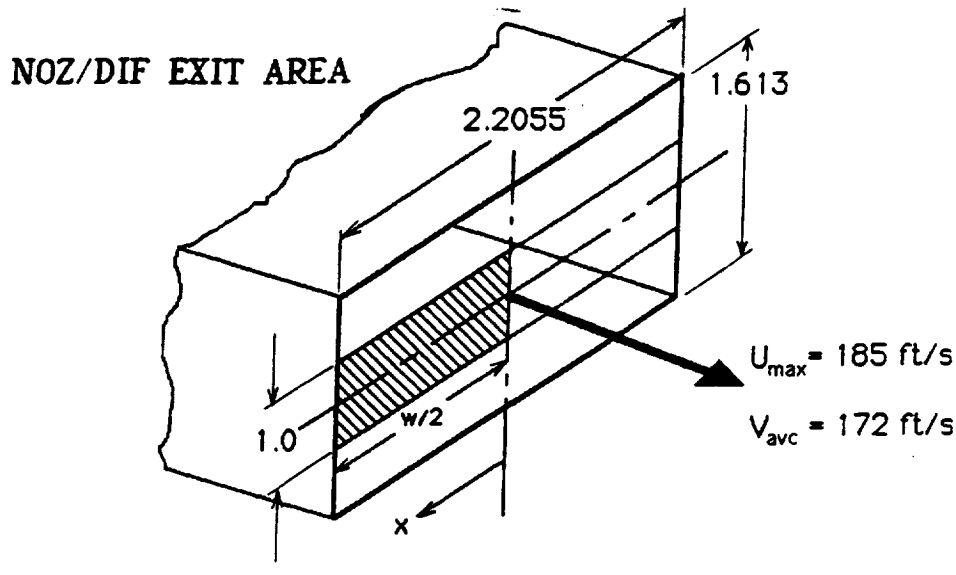

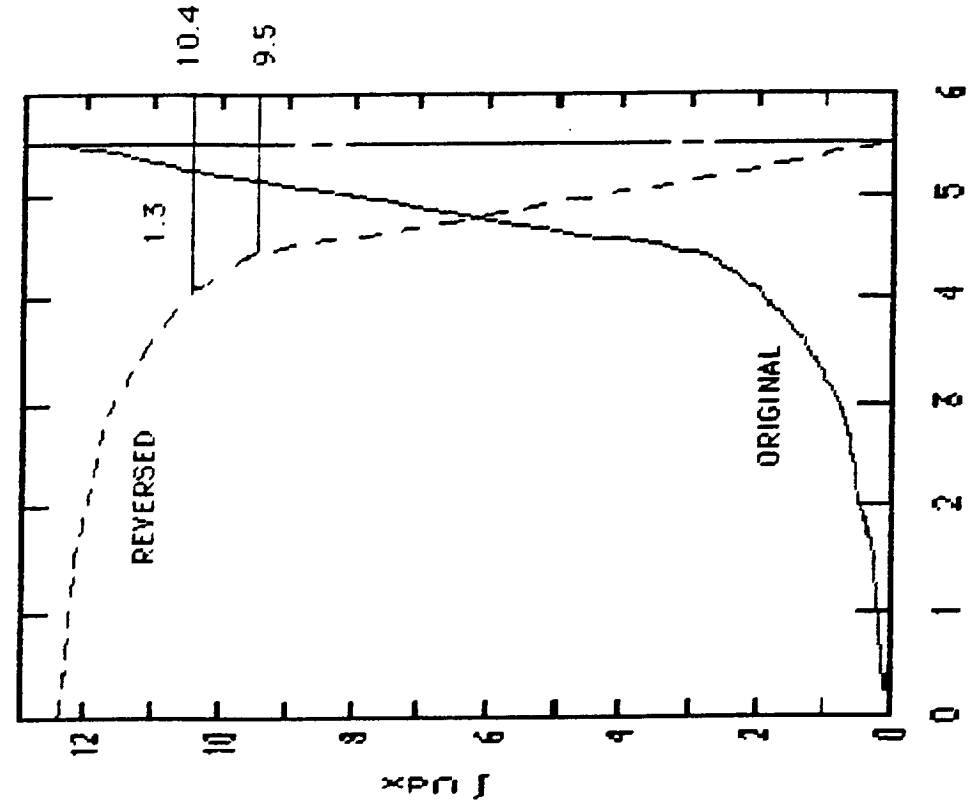

Figure AP/b. Results of integration of curve of Figure AP/a.

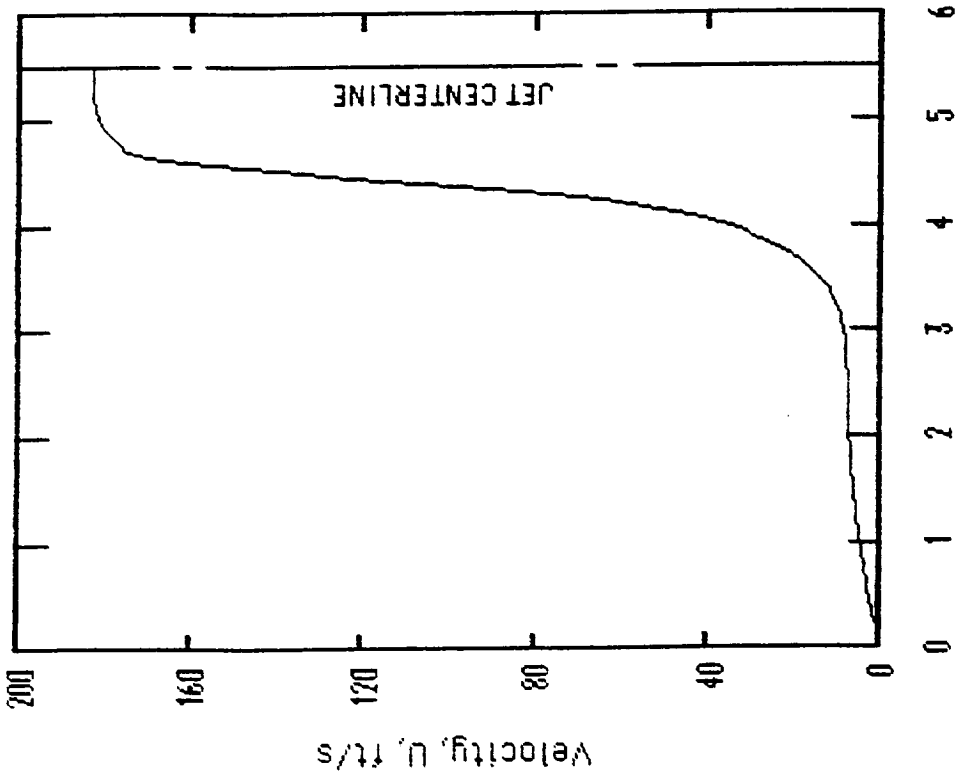

Figure AP/a. Velocity distribution upstream from test collector.

APPENDIX B

FUNDAMENTALS OF DIFFUSER RECOVERY

Reference is made to figure 18, (reproduced from the DIFFUSER DATA BOOK), where the solid curves represent diffuser recovery Rd as a function of numerous variables affecting performance. Derived from test data, recovery is defined as

$$Rd = (P2 - P1)/ 1/2 \rho U_c^2$$

where P2 - P1 is the static pressure rise from inlet to outlet of the diffuser and $1/2 \rho U_c^2$ is the kinetic head right in the center of the flow entering the diffuser. The DATA BOOK presents various graphs for both, conical and flat, diffusers.

The factors affecting diffuser recovery are:

1. Geometry
2. Blockage
3. Mach number
4. Reynolds number.

Diffuser geometry, for either conical or flat diffusers, depends on the area ratio AR = A2/A1, aspect ratio AS = b/w1, length ratio L/w1, side angle θ (usually given as the enclosed side angle 2θ). For a narrow range of Mach and Reynolds numbers, and for a specified geometry, it is BLOCKAGE that affects performance predominantly.

As an example consider a FLAT DIFFUSER operating with Mach = 0.2, Re = 214,000 and having a length ratio L/w1 = 12, area ratio AR = 2.5, an aspect ratio AS = 5.

For blockages, 2,4,6,8,10 and 12 percent, diffuser recovery is found to be : 74, 70.8, 65, 63, 59 and 55 percent, respectively. While the difference in percentage is 19, the ratio of best and worst is about 34 percent. This figure may make a marked difference in power requirements and noise production of a large wind tunnel!

Blockage is defined as the actual volumetric flow rate through the diffuser related to the ideal flow rate that is based on the assumption of perfectly uniform flow distribution. (For uniform flow distribution blockage would be zero). Since blockage depends on the flow distribution at entry to the diffuser, traverses must be taken to establish the actual shape U = f(x) for horizontal, and f(y) for vertical traverses.

The procedure followed in this project was simplified and traverses were only taken along the horizontal and vertical centerlines of the diffuser's entry area. Subsequently both, velocity and distance, were normalized and it may be shown that blockage

$$B = 1 - \int_0^1 (U/Umax)\ dx/w$$

for the horizontal line and

$$B = 1 - \int_0^1 (U/Umax)\ dy/h$$

for the vertical line. Ultimately, the two blockages were averaged.

APPENDIX C

Diffuser Dimensions

1) Original DSMA scale model diffuser.

Inlet Area : $A_1 = 2.25 * 2.75 = 6.1875$ sq. ins.

Exit Area : $A_2 = 4.50 * 2.75 = 12.375$ sq. ins.

Area Ratio : $AR = 12.375/6.1875 \cong 2.0$

Aspect Ratio : $AS = b/w = 2.75/2.25 = 1.22$

Length to width Ratio : $L/w = 22.5/2.25 = 10$

Blockage at inlet : $B \cong 20\%$ (average)

Enclosed side angle $2\Theta = 5.72°$

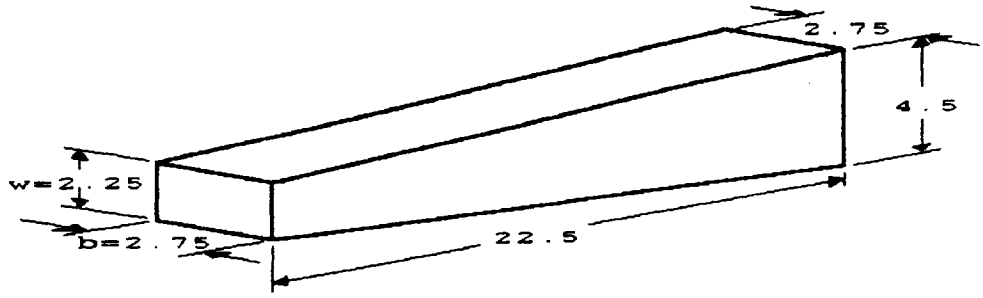

2) Modified diffuser

$A_1 = 1.75*2.5 = 4.375$ sq. ins.

$A_2 = 4.5*2.5 = 11.25$ sq. ins.

$AR = 11.25/4.37 = 2.57$

$AS = 2.5/1.75 = 1.428$

$L/w = 22.5/1.75 = 12.87 \cong 13$

$B = 11\%$ (ave.)

Enclosed side angle : $2\Theta \cong 7°$

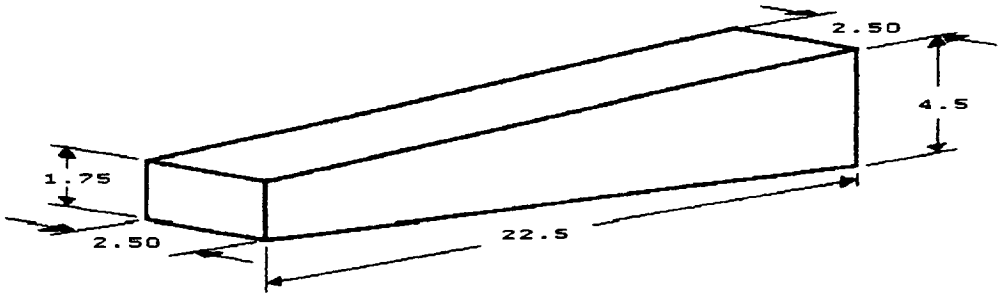

Reynolds number : Re = 206,000 (based on a hydraulic diameter of 2.06 in. and an inlet velocity of 200 ft/s.)

nas3figs

FIGURES ACCOMPANYING TEXT

1. Original DSMA full scale tunnel design
2. Essential components of model scaled from original in ratio 1:48
3 Modified DSMA scale model tunnel
4. Series of test collectors
5. Design of new collector as compared with test collector
6. Details of the original and the modified diffuser
7. Nozzle-diffuser details
8. Complete line diagram of the modified tunnel showing press. ports
9. Pressure distribution with 3.5 inch orifice
10 ditto with the 4 inch orifice plate
11 Pressure distribution along collector walls.
12 Jet traversing the test area- schematic (from text book)
13 Horizontal flow distribution of N/D exit plane
14 Vertical ditto ditto
15 Flow distribution at the collector inlet (146/A)
16 Flow traverses at diffuser inlet- horizontal
17 ditto - vertical
18 Performance curves of flat diffusers reproduced from DATA BOOK

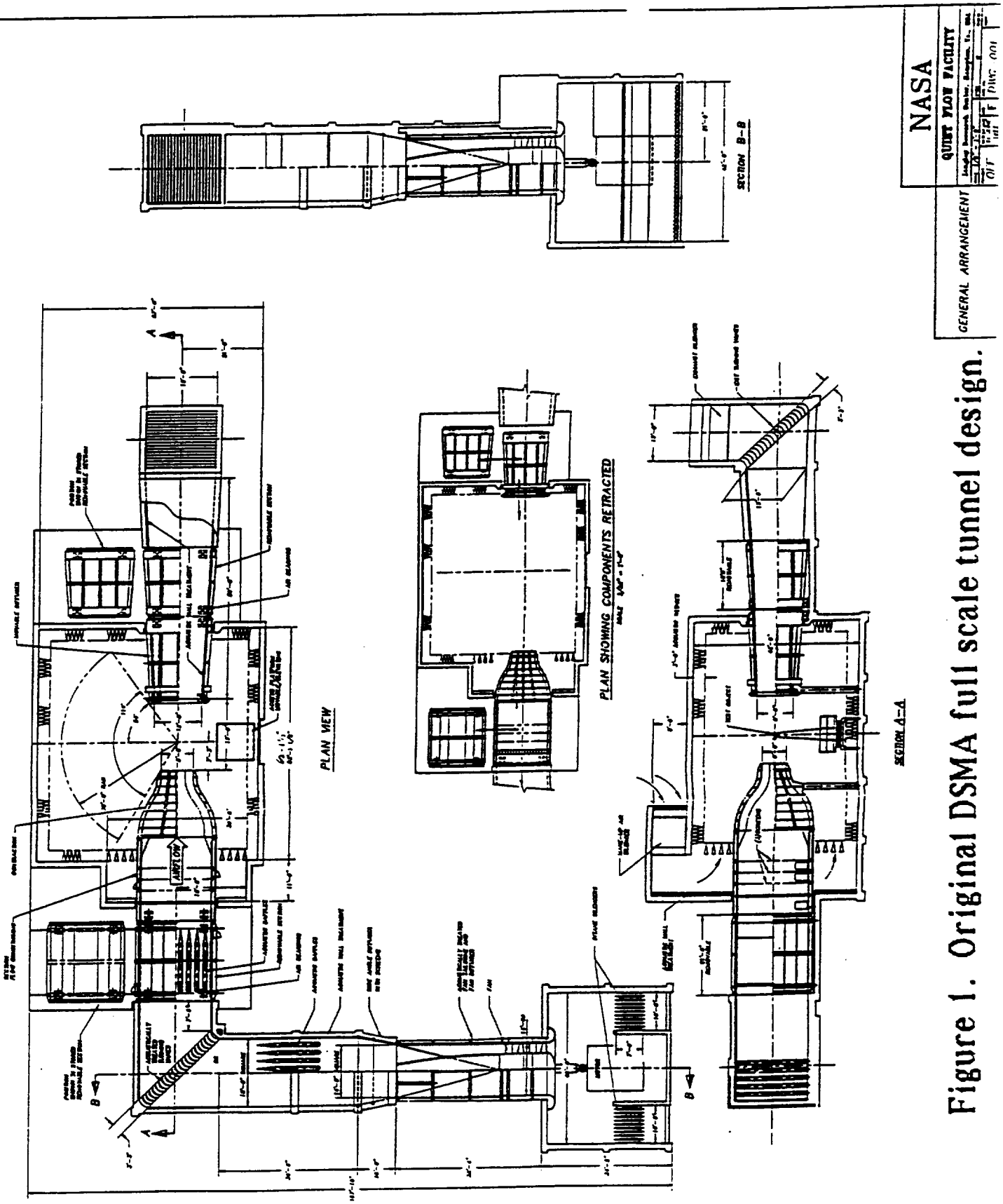

Figure 1. Original DSMA full scale tunnel design.

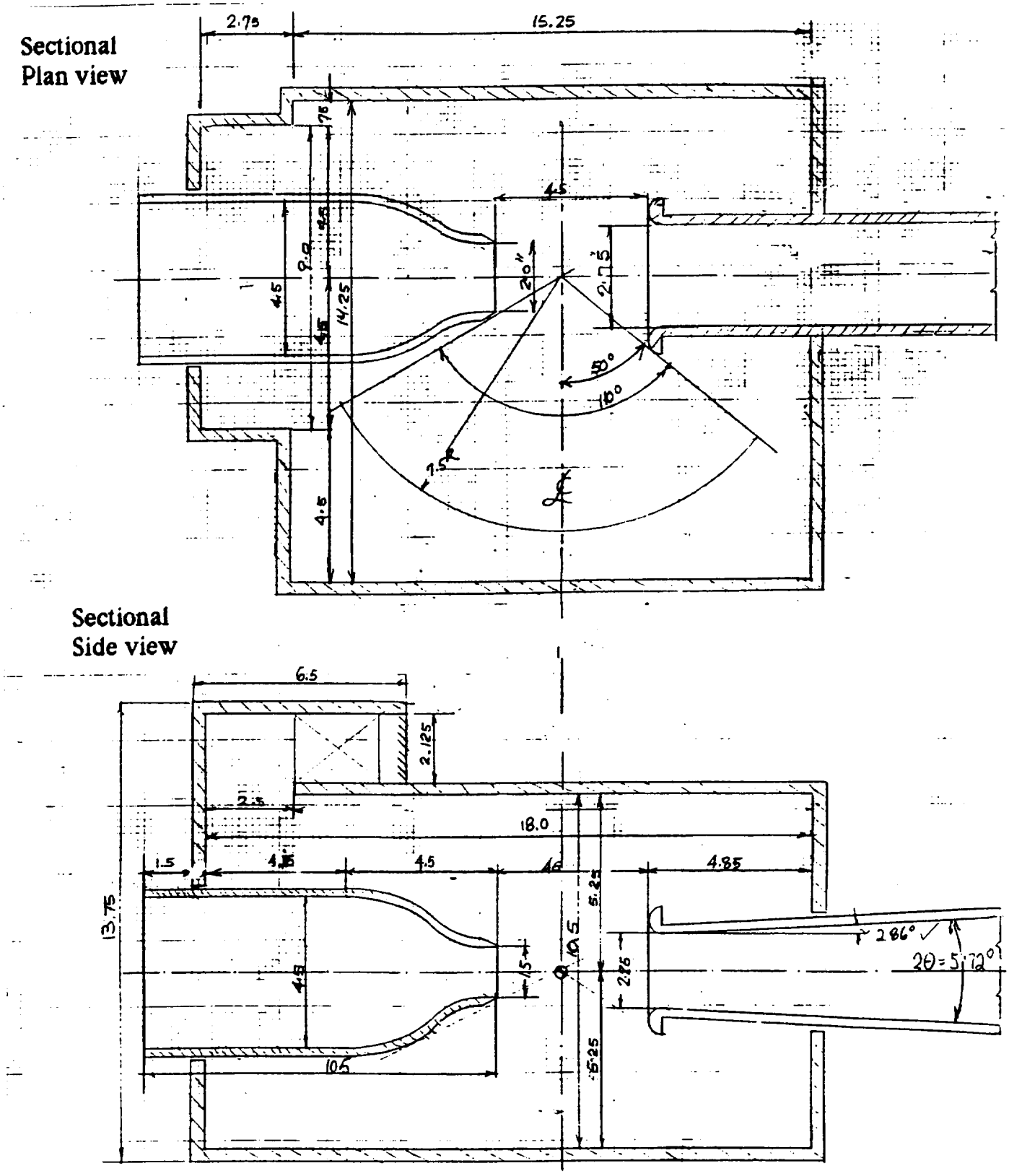

Figure 2. Essential components of model scaled from original in ratio 1:48.

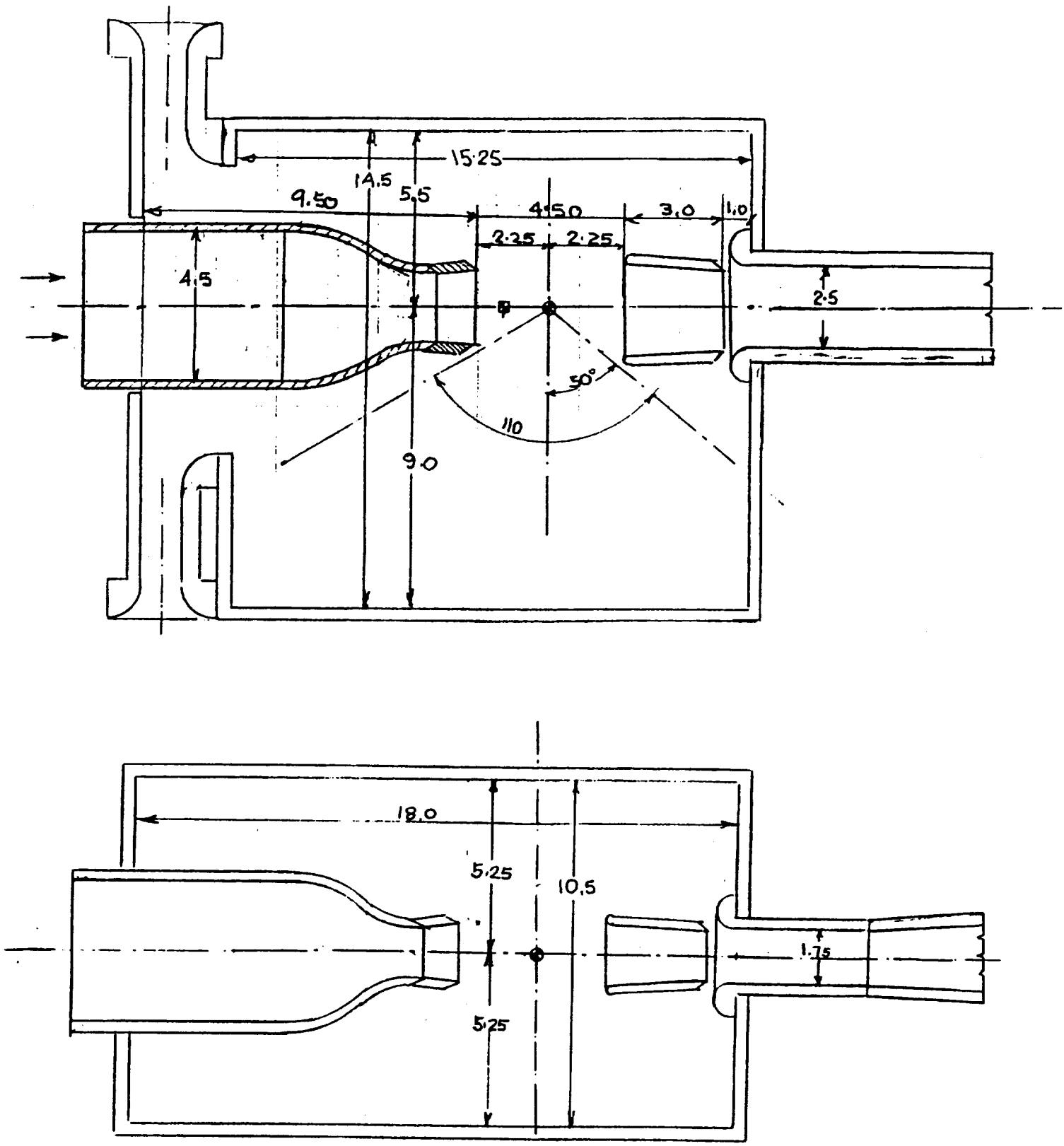

Figure 3. Modified DSMA scale model tunnel.

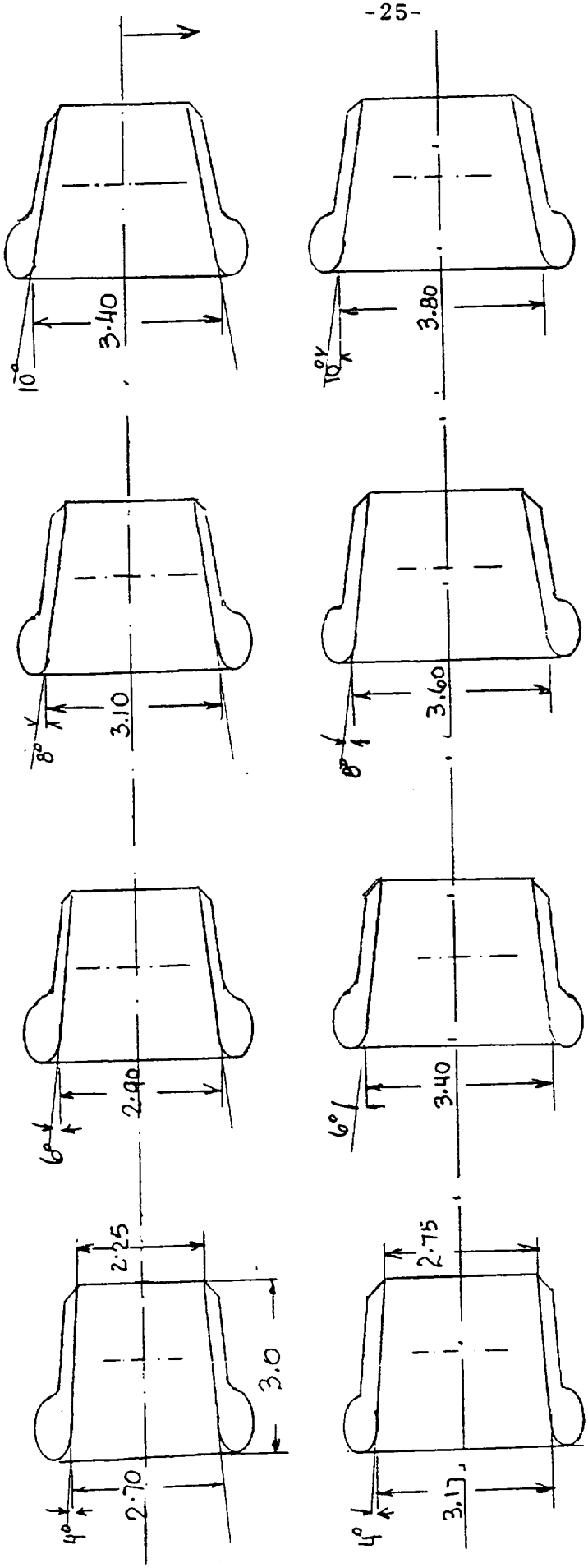

Figure 4. Series of test collectors.

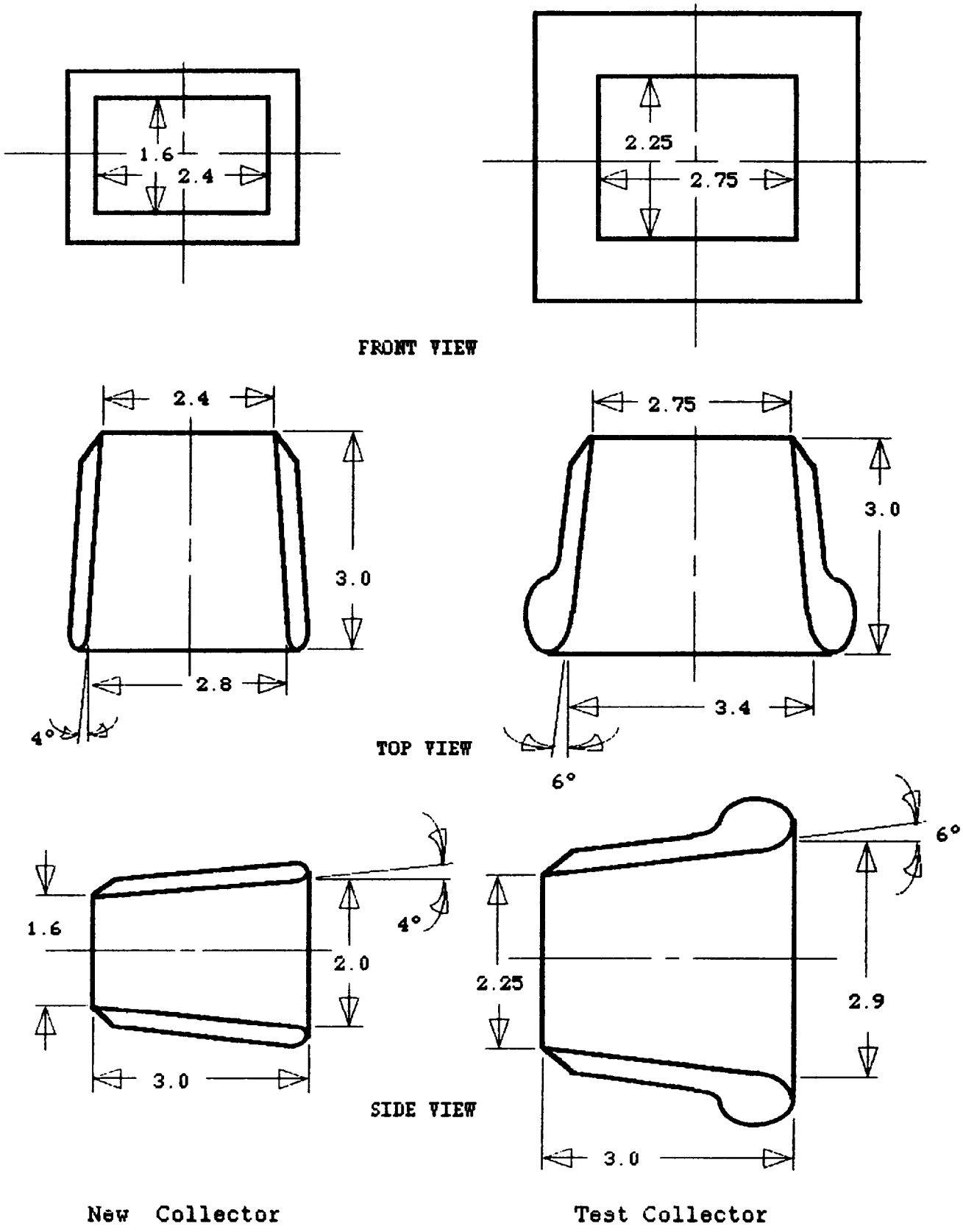

Figure 5. Design of new collector as compared with the test collector.

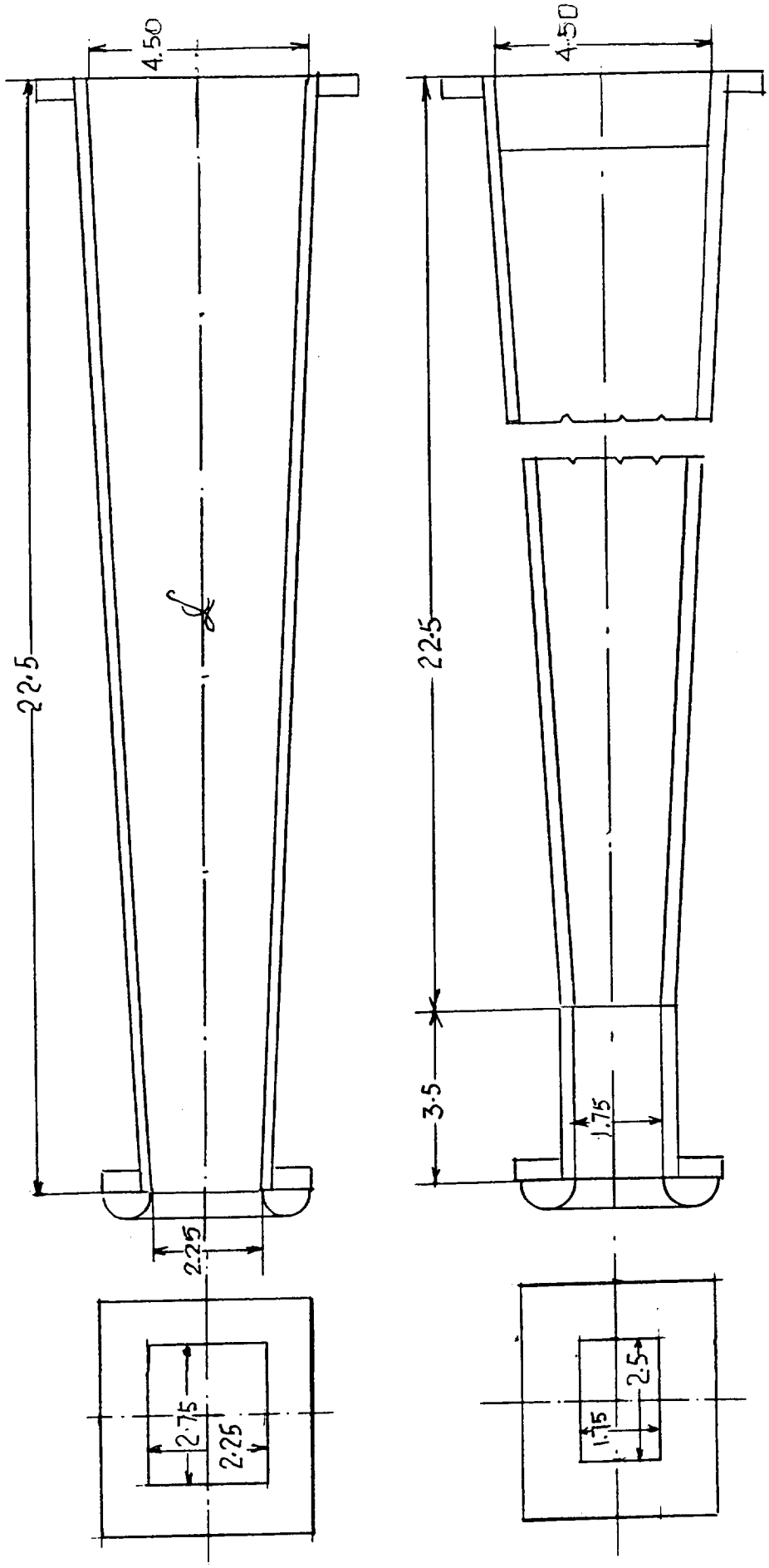

Figure 6. Details of the original and the modified diffuser.

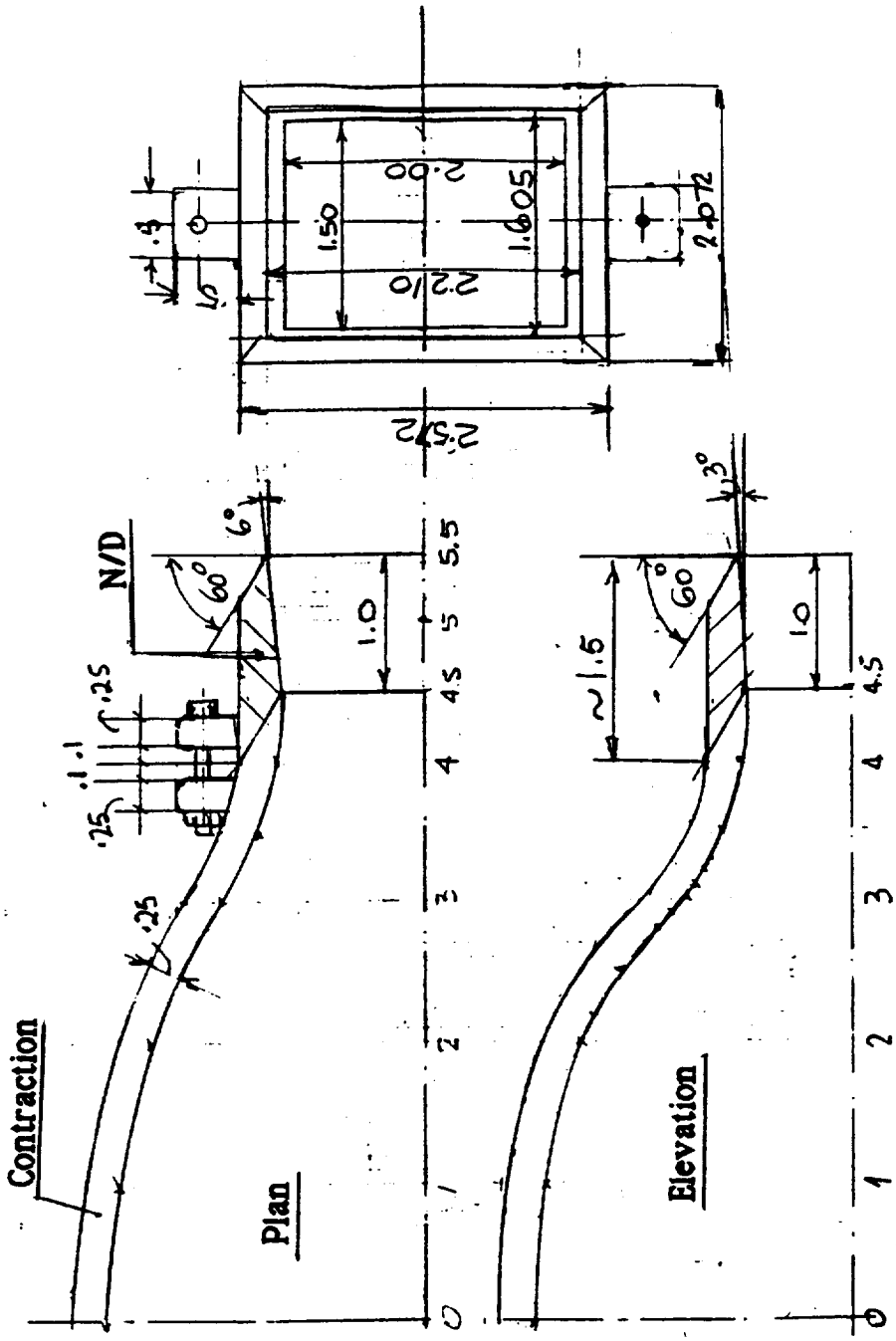

Figure 7. Nozzle-diffuser details

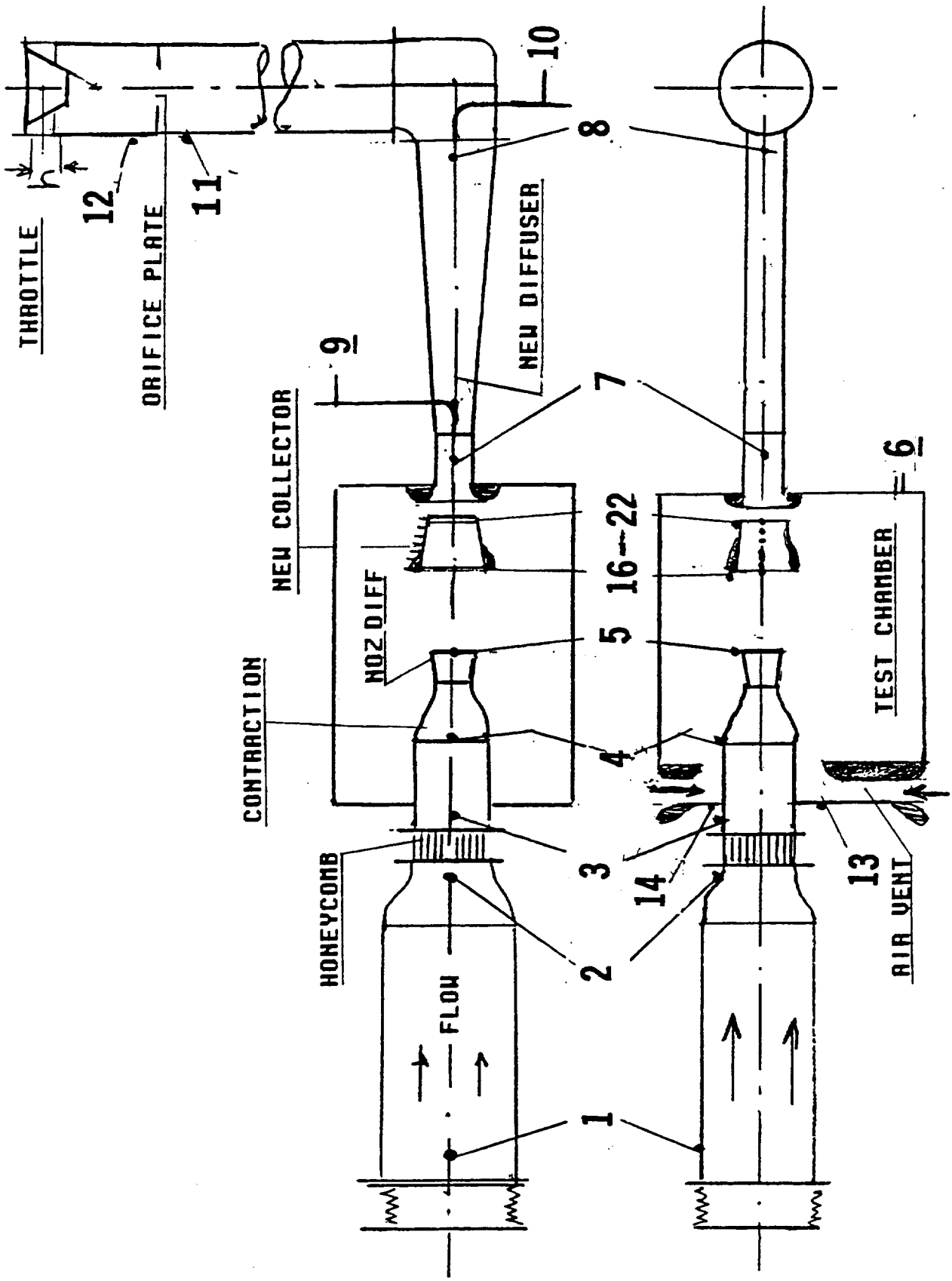

FIGURE 8. DISTRIBUTION OF STATIC PORTS ALONG THE MODIFIED TUNNEL CIRCUIT

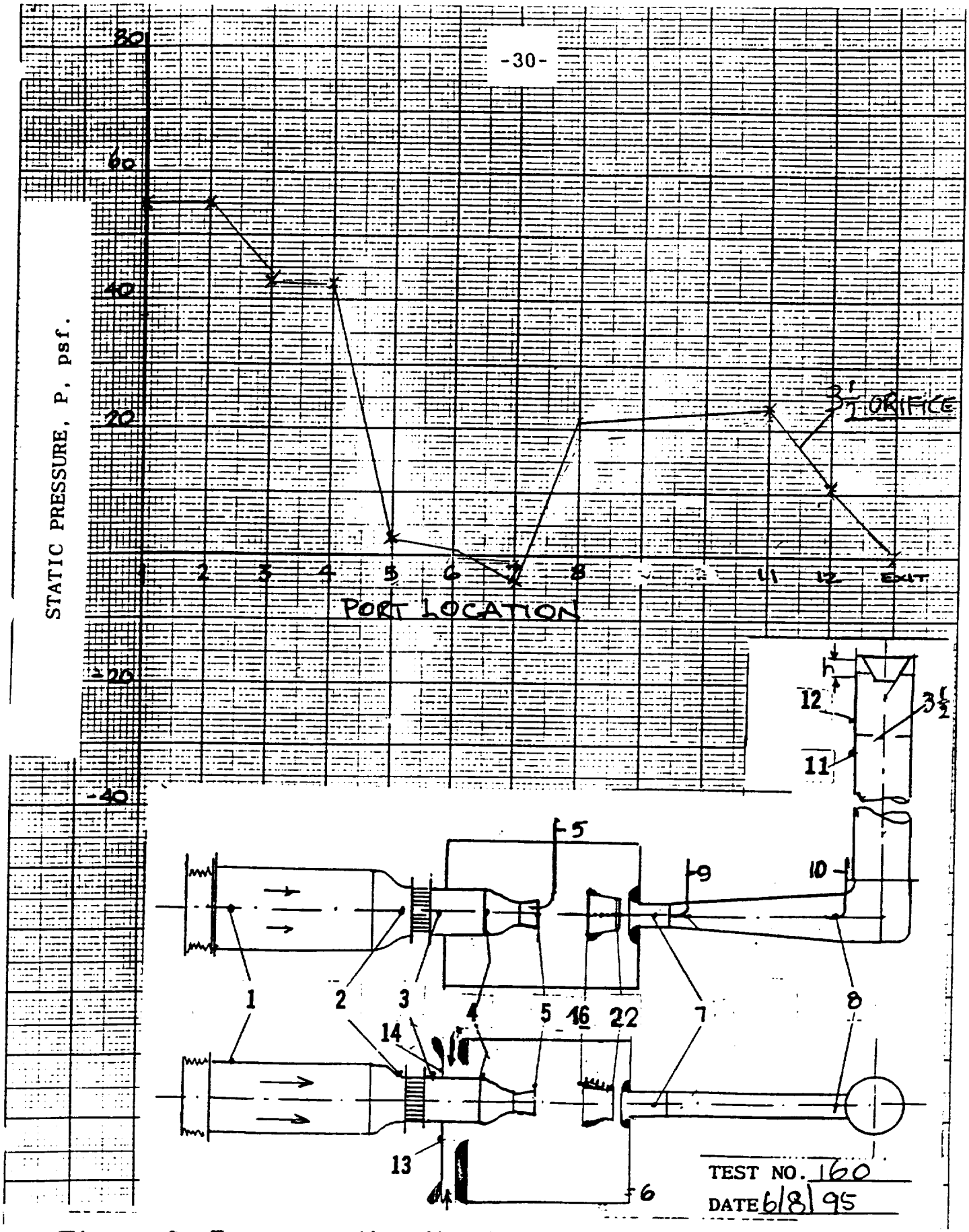

Figure 9. Pressure distribution with the 3.5 inch orifice plate.

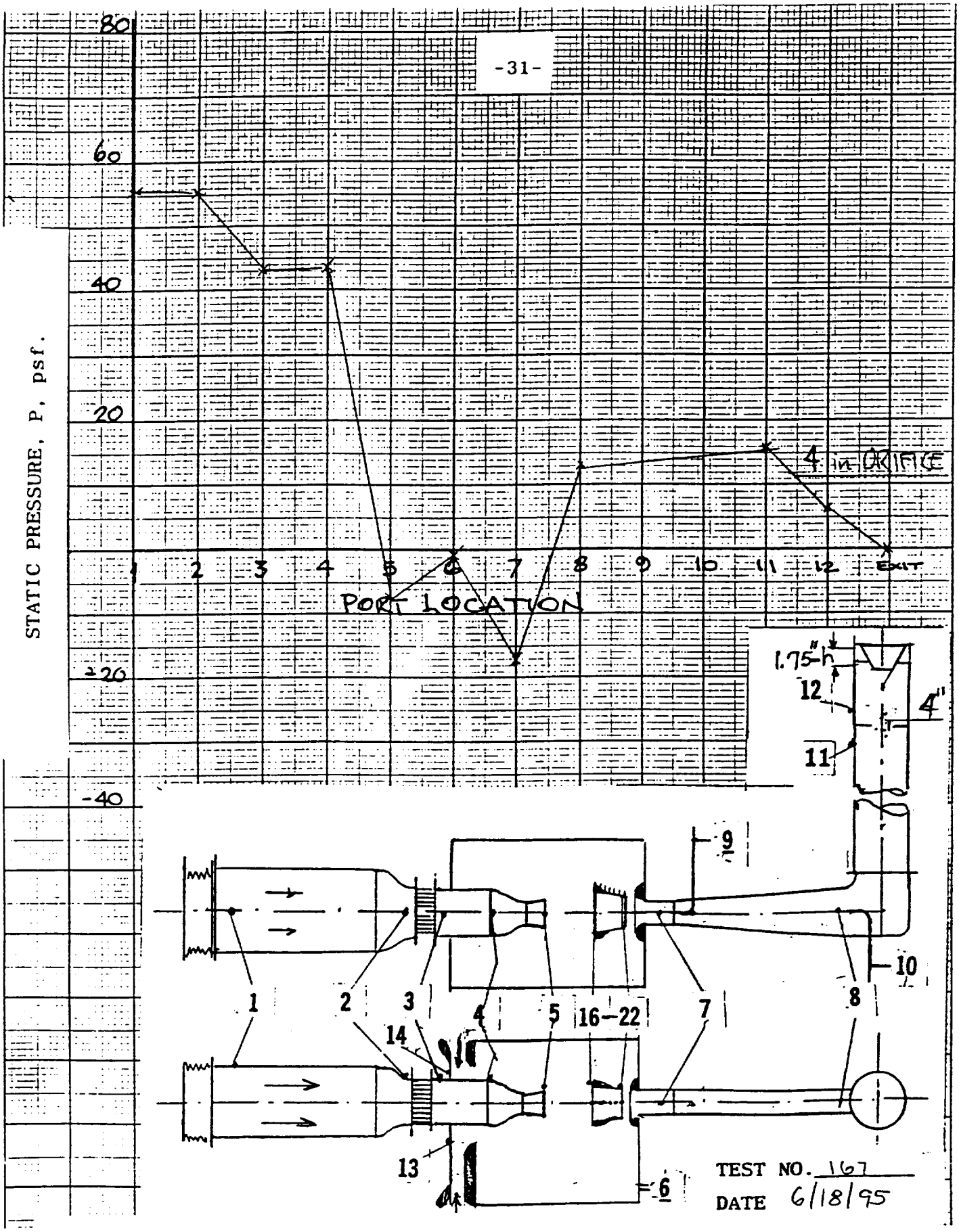

Figure 10. Pressure distribution with the 4 inch orifice plate.

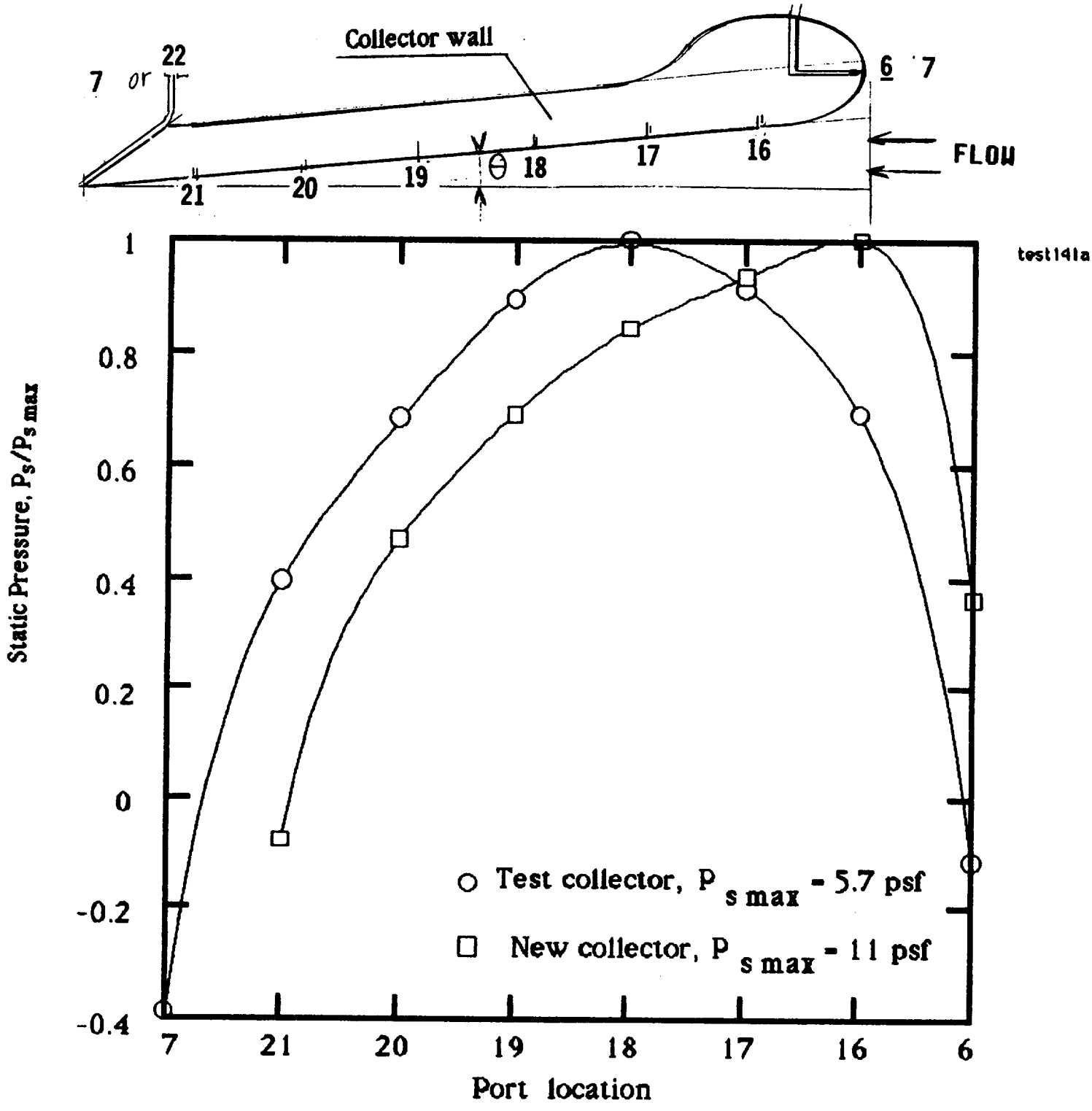

Figure 11. Pressure distribution along the collector walls.

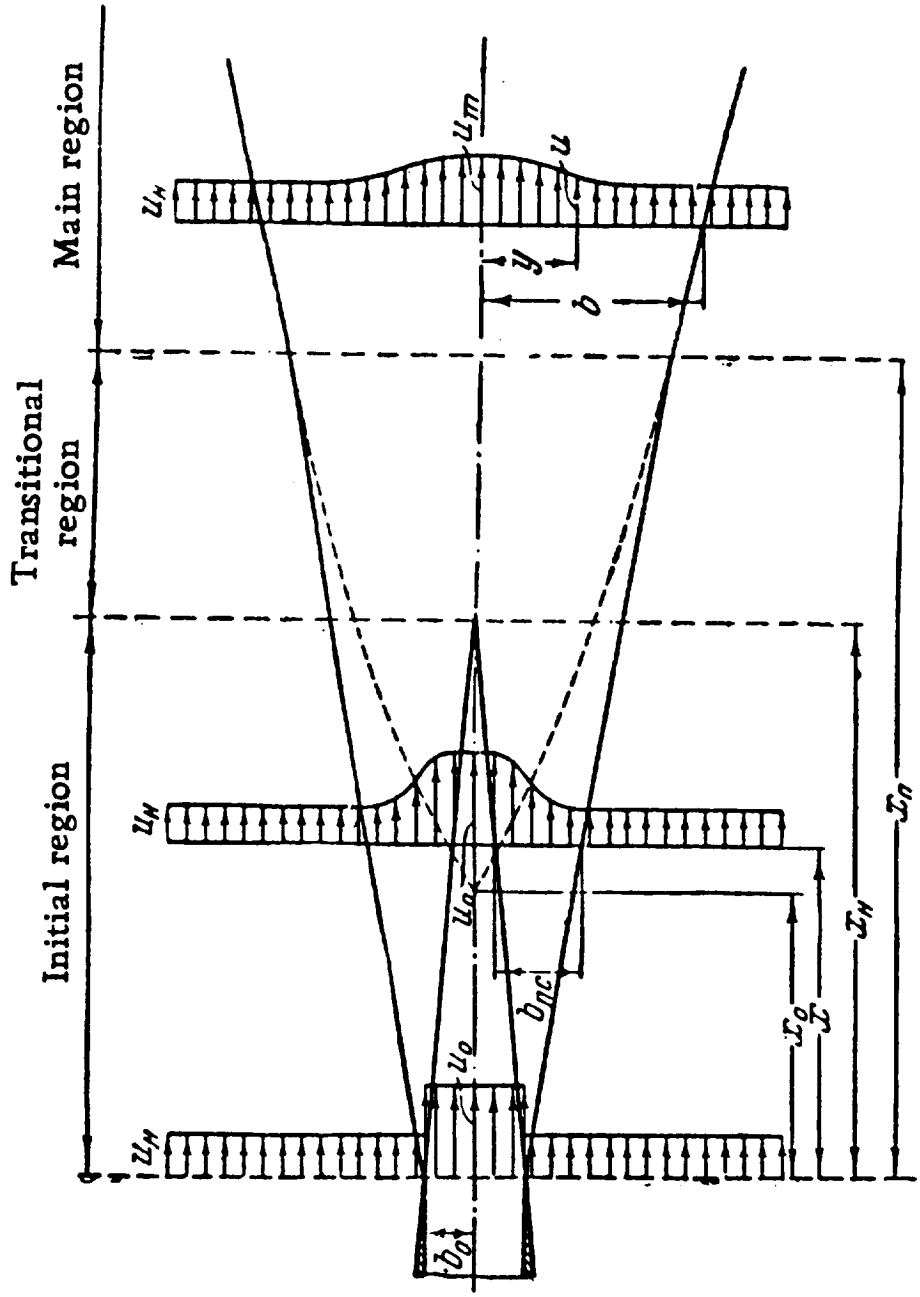

Figure 12. Jet traversing the test area - schematic.

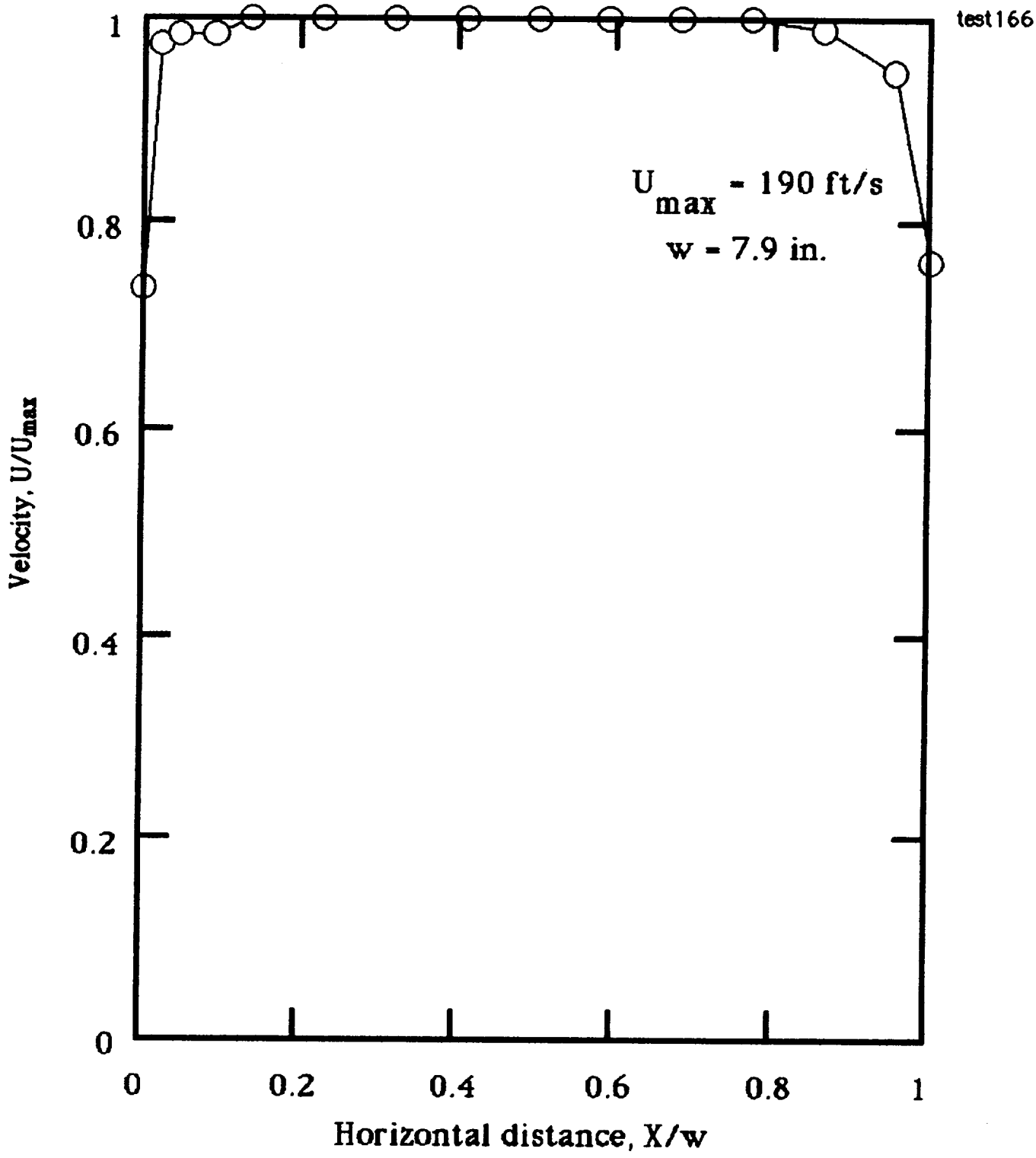

Figure 13. Horizontal flow distribution at N/D exit plane.

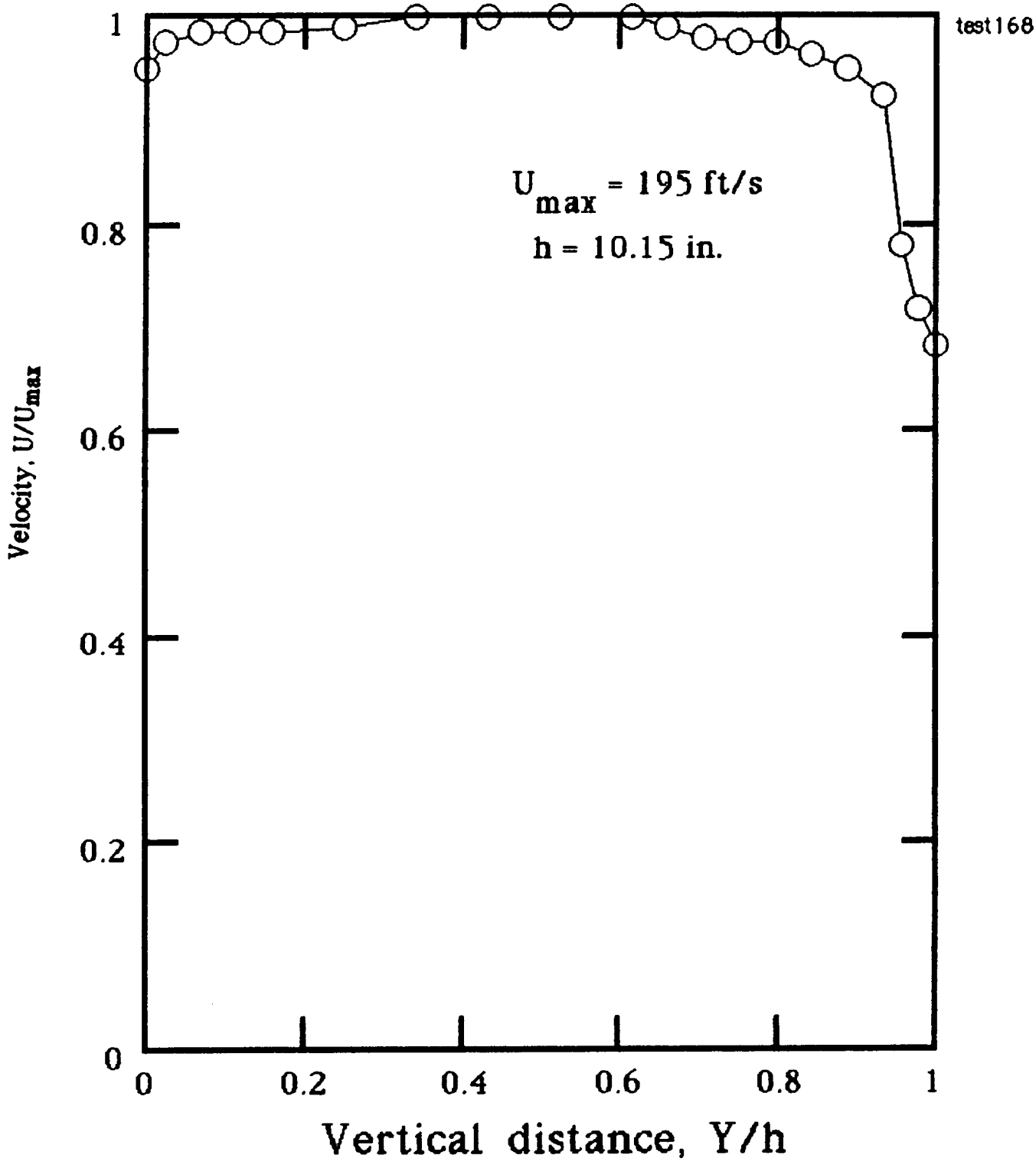

Figure 14. Vertical flow distribution at the N/D exit plane.

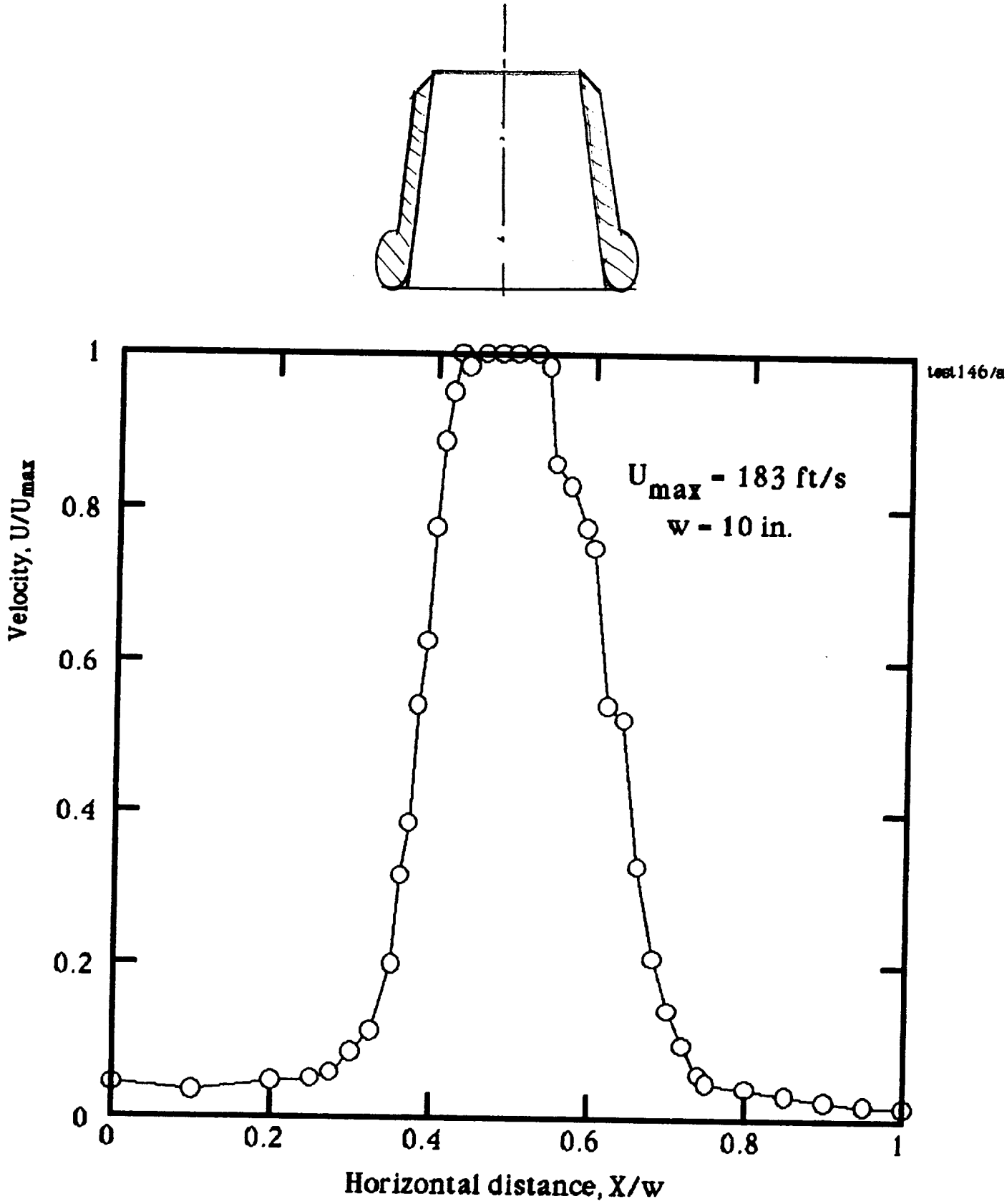

Figure 15. Flow distribution at the collector inlet.

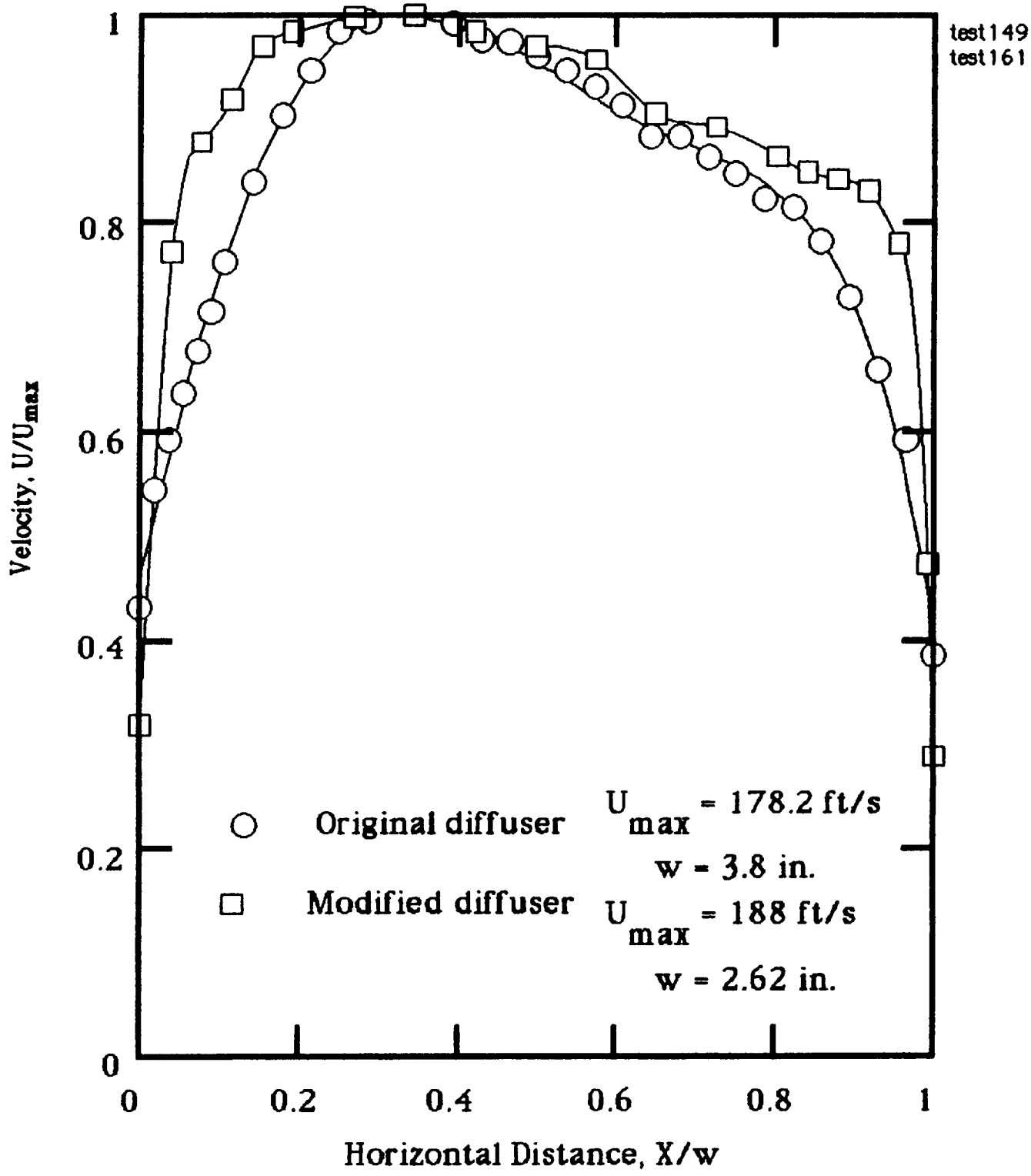

Figure 16. Flow traverses at the diffuser inlet - horizontal.

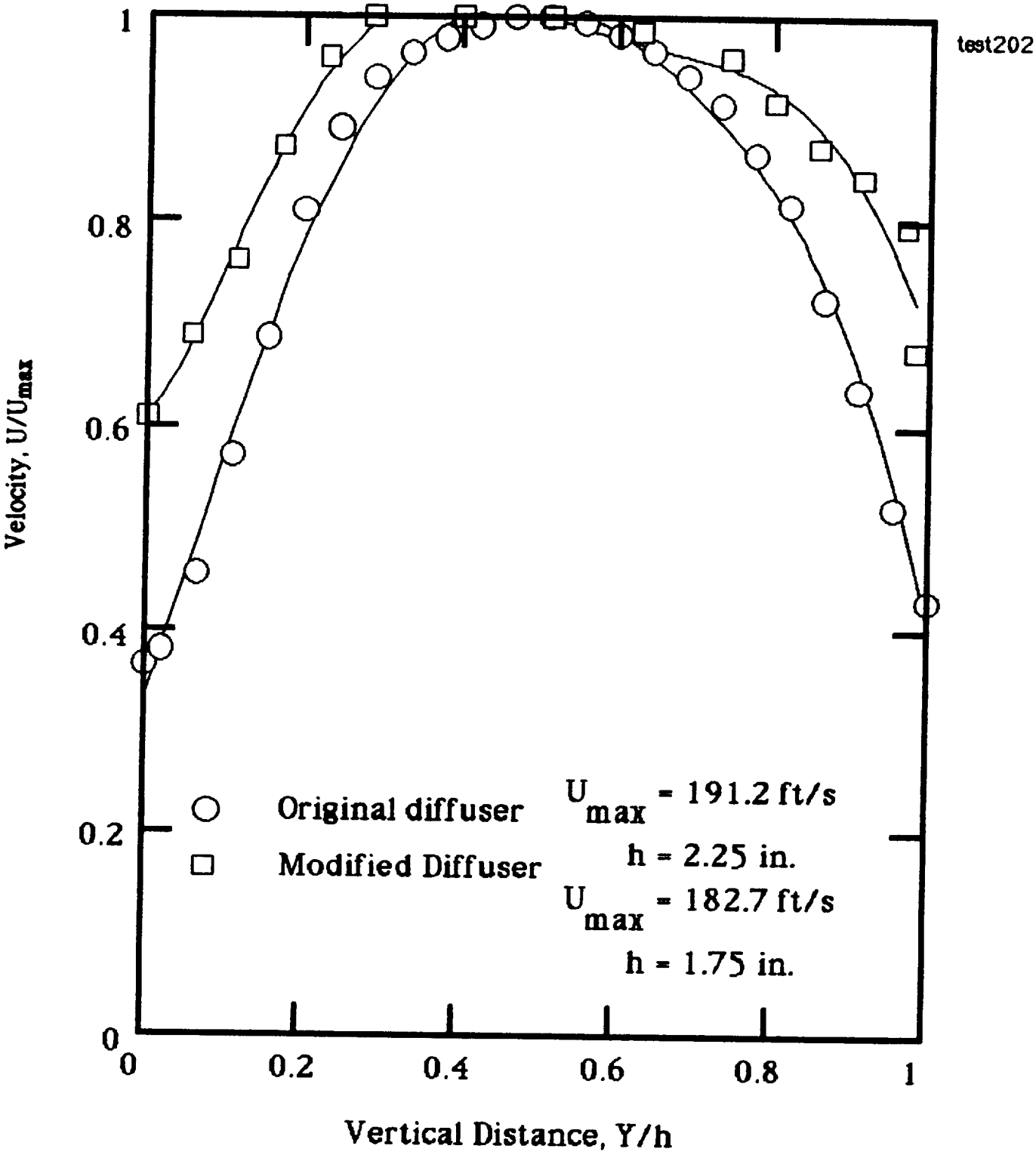

Figure 17. Flow traverses at the diffuser inlet - vertical.

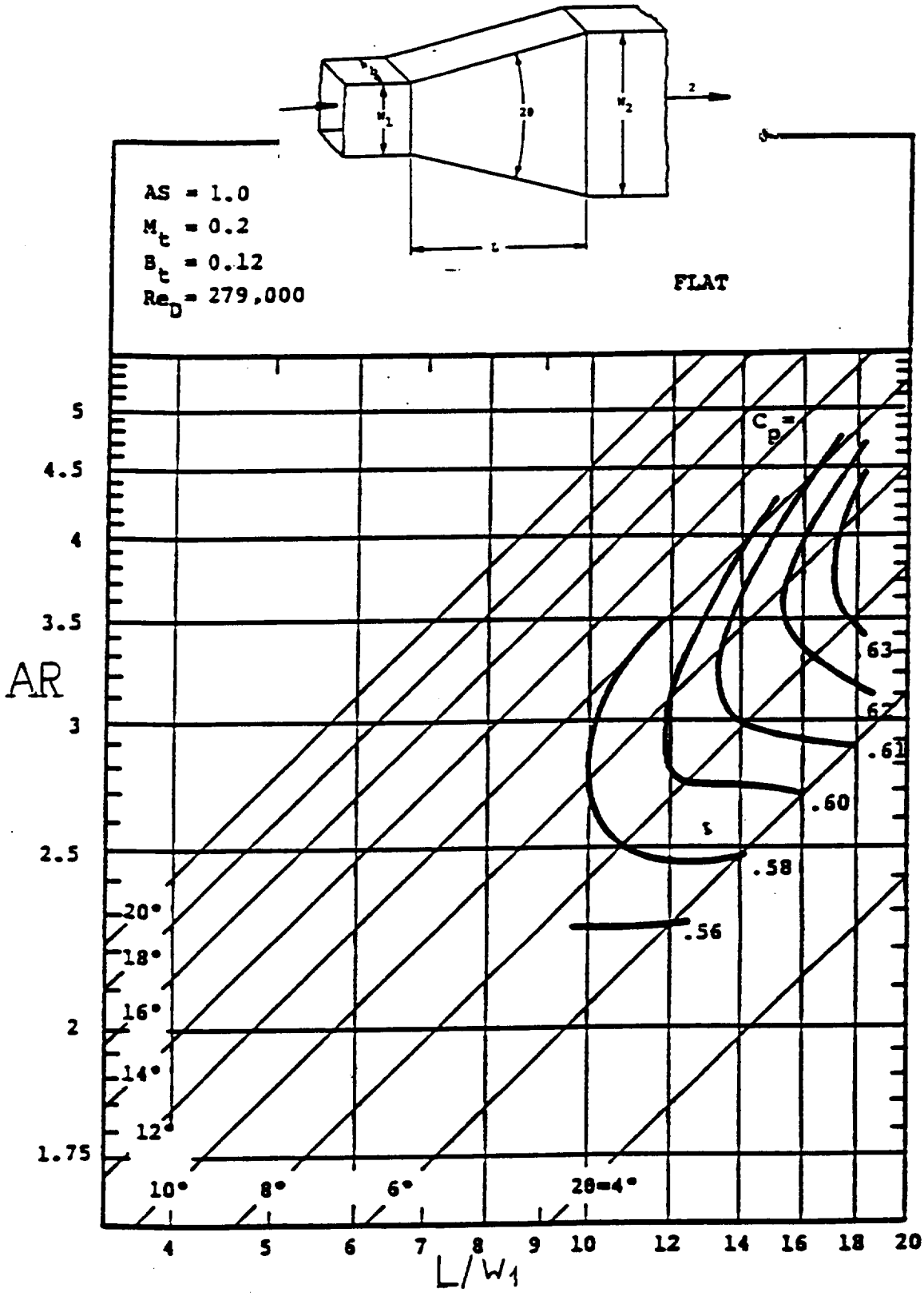

Figure 18. Performance curves of flat diffusers reproduced from DATA BOOK.

SECTION II

VARIATION OF FLOW PARAMETERS INSIDE THE TEST CHAMBER

In this Section the effects of various parameters on the flow quality in- and outside of the jet within the test chamber are discussed. These studies are distinct from those concerning tunnel performance presented in Section I. Measured effects include variations in both, normal and streamwise, distributions of static and total pressure, flow velocity, and turbulence. Turbulence measurements are further supported by flow vizualization.

BRIEF REVIEW OF THE TESTS

The measurements performed within the Test Chamber are presented in the following sequence:

Pressure:

a) Variation of static pressure Ps along the entire tunnel circuit as affected by the presence or absence of the Nozzle/Diffuser (N/D). (Tests #167, 170, 182)

b) Variation of the static pressure normal to the flow at a location as affected by the presence or absence of the N/D.(#171,173,183)

c) Variation of static pressure within the Test Area, that is along the flow between the nozzle exit and the contraction entry.(#172,174, 185,192,198,200, 200/A).

d) Variation of total pressure normal to the flow at a selected location.(#175,184).

e) Variation of total pressure within the Test Area, that is along the flow between nozzle exit and collector entry.(#176,186).

Velocity:(normal to flow)

f) Horizontal variation of velocity (U/Umax) at collector entry, w/ regular N/D.(Taken right across the chamber "wall-to-wall")#165.

g) Horizontal and vertical variation of velocity across the gap, downstream from the collector. (#163,164).

Velocity and Turbulence (normal to flow):

h) Horizontal variation of velocity U/Umax and turbulence u*, wall-to-wall, at N/D exit. (#201).

i) Horizontal and vertical variation of U/Umax and u* at collector entry. (#162, 202).

Velocity and turbulence (along the flow)

j) Variation of U/Umax and u* between N/D exit and collector inlet using the regular 1 1/4 in. N/D. (#190, 195).

k) Same as above, but using the longer, 2.5 in. N/D. (#194)

l) N/D removed (#204).

PRESENTATION OF RESULTS

Because of the large variety of tests performed, only the relevant results are presented in this report. It was prudent to provide some explanation to the nature of the tests and to make reference to the test number as well should some questions arise later on. It is noted that all tests (which were traverses) were obtained along both, the centerline of the area under consideration or along the tunnel centerline. Within the Test Area the horizontal and vertical centerlines normal to the flow are noted as X and Y ,respectively, while the horizontal streamwise centerline is noted as Z. An exception to this was the pressure distribution around the tunnel circuit (or along the collector wall) which was obtained with static pressure tappings. Some traverses spread out from the Test Area and the results obtained showed flow conditions right across the the width or height of the Test Chamber with special reference to turbulence. (In this case reference is made to axis XX, YY, ZZ).

Pressure

a) All pressures were measured relative to the atmosphere. For a fixed fan pressure, variation of static pressure Ps along the entire tunnel circuit was subject to changes of such parameters as the geometry of the contraction exit, orifice size, diffuser design, throttle height, collector gap, etc. When changing only the contraction exit and keeping all other parameters the same, the tests show pressure distribution downstream as affected by the presence or absence of the N/D . Figure 19 shows results of tests #167, 170, 182, presented side-by-side which were obtained for three configurations, namely with the "regular" 1.25 ins. long N/D (#167), with the N/D removed (#170) and with an extended 2.5 ins. N/D (#182).

It appears, that while the chamber pressure remained about atmospheric (location 6), static pressure decreased when the flow was entering the diffuser (location 7). It is noted that the decrease was found more marked in tests #170 and #182 and less marked in test #167. It is also noted that in test #182 the chamber pressure increased

slightly above atmospheric which affected the flow of vent-air.

b) Traverses of static pressure normal to the flow were obtained at the contraction and nozzle-diffuser exits where a very distinct difference and rather unexpected distribution was found, as shown in figure 20. The difference showed up in two facets: first in the shape of the distribution, second in the values experienced at the peaks. In the distribution one notices a shape close to an inverted parabola and in this the three curves appear somewhat similar. However the peaks vastly differ. Test #171 shows results obtained in absence of any N/D with the curve rising from zero to a peak of +4.21 p.s.f. near the center of the traverse, and ending at -1.11 p.s.f. at the end of the traverse. With the regular 1.25 in. N/D, results of test #191 show the curve decreasing from -2.81 to a minimum of -5.74 p.s.f. and ending at -2.52 p.s.f. With the extended 2.5 in. long N/D, results of test #183 show the curve falling from zero to -3.10 p.s.f. ending at zero again, with the plateau of the curve extending over a small distance about the center of the traverse.

These results will be subject to further discussions.

c) Variation of static pressure <u>along</u> the flow was restricted to the Test Area where the traverse distance (z) along the centerline was between contraction exit and collector entry. The traverse distance was the path covered by the static port of the Pitot tube where the port was located 1.125 ins. from the main stem centerline.

With the regular N/D removed, results of test #198 first reveal a marked drop in positive pressure which flattens out after a third of traverse distance 4.45 ins, as shown in figure 21. Noted that the 4.45 ins traverse started at the exit of the contraction with p=6.0 p.s.f. and ended 1.125 ins. from collector entry with p=+0.66 p.s.f. While the flat portion of the pressure curve was slightly below atmospheric, on approaching the collector, the end "kicked up" and became positive again thus signifying the presence of diffusion.

With the regular N/D attached to the contraction, results of test #200 reveal reverse effect of pressure distribution. Starting with

a hefty, -7.15 p.s.f. negative pressure at the N/D exit, it rapidly increases towards atmospheric and continues to increase on approaching the collector, as shown in figure 22. Variation of pressure between locations X/W = 0.3 and 0.8 is relatively small in comparison and may be considered the "flat" part of the distribution, although not as flat as it was in absence of the N/D, figure 21.

With the extended N/D attrached to the contraction, results of test #185 reveal a rapidly increasing pressure that begins with -3.5 p.s.f. at exit and finishes at + 2.15 p.s.f. at the collector entry, figure 23. There is a conspicuous absence of the "flat" portion of the pressure distribution experienced with test #198.

To explore the effects of space on longitudinal pressure distribution the length of the Test Area was increased by 1.25 ins. from 4.5 ins. to 5.75 ins. Figure 24 shows the improvement both, in the length of the flat portion and in its flatness as well.

d) Total pressure traversed normal to the flow at the regular N/D exit was found to remain practically constant at Pt=44.3 p.s.f., test #175, except near the side walls as shown in figure 25. Similar results were obtained with the extended N/D, test #184, as shown in figure 26.

e) Total pressure changes along the flow within the Test Area were found small, approximately 8.5 percent with the regular N/D (test #176) and almost zero percent with the extended N/D (test #186), as shown in figures 27 and 28. Total pressure also remained about constant in the absence of any N/D as shown in figure 29.

Velocity

f) Variation of velocity obtained normal to the flow and located immediately upstream of the collector entry was obtained with hot wire anemometry, test #165. For the regular N/D, the result is shown in figure 30, where U/Umax is plotted against horizontal distance. The traverse, noted as XX, was taken horizontally right across chamber, practically "wall-to-wall".

Figure 30 shows some results of interest for consideration. The high velocity peak was experienced within the jet "core", the region of the immediate vicinity of the tunnel center. Velocities decreased rapidly on both sides and spread out to locations where they became small and leveled off to a minimum. However, near the walls there seems to be a slight increase in the velocity "spectrum" adding to the complexity of the flow pattern outside the main jet.

If one imagines for a moment that the flow is "frozen" (thus independent of time) one may also consider placing the collector on top of the frozen velocity peak, with its shape added to the flow distribution picture, shown in figure 30. Imagine further the process needed to transform this frozen high-peak velocity entering the collector at its intake to emerge at the collector exit with a constant speed, rectangularly shaped velocity distribution. To achieve this, the two dimensional tunnel tests indicated that this process would require a flow adjustment, starting with diffusion first, then followed by acceleration. Apparently, diffusion levels off the "peak" in the center region and acceleration increases the speed outside the main jet. All that is then needed is a collector of the correct design.

g) Horizontal and vertical traverses of velocity were made across the collector exit, along the centerlines, within the gap, to assess the collector's effectiveness, tests #163, and 164. The results are shown in figures 31 and 32 which show a much improved distribution.

Velocity and turbulence (normal to flow)

h) Velocity distribution and turbulence levels were obtained right across the flow (wall-to-wall) at the exit of the regular N/D, test #201, and the results are shown in figure 33. It appears, that highest velocities were found across the width of the N/D exit, where the turbulence levels were the lowest. The highest turbulence was experienced inside a narrow width of the traverse where the velocity gradients were the steepest. Similar results were found earlier with the

two dimensional model. Markedly high levels of turbulence were also found inside the recirculating flow in the neighborhood of the far wall of the Test Chamber, between location xx/w=0.025 and 0.30. This also showed up with flow visualization studies using helium bubbles: the bubbles showed an increased excitation.

i) Having crossed the Test Area, the horizontal distributions of velocity and turbulence at the entrance to the collector, test #196, show changes in both, the jet shape and the turbulence levels created by it. When compared with figure 33, the velocity peak at the collector is more rounded and the velocity gradient is less steep, as shown in figure 34. Accordingly, the turbulence levels are smaller, especially near the far wall of the chamber. However, turbulence increased near the close wall. In the vertical traverse, test #197, the velocity distribution appears about the same as in the horizontal traverse, but the turbulence peaks were found somewhat higher, shown in figure 35.

Velocity and turbulence along the flow

j) Variation of velocity and turbulence with distance along the tunnel centerline were studied with the regular and extended nozzle-diffusers and without any N/D as well; (tests #190, 195 for the regular N/D, #194 for extended N/D and #204 with the N/D removed). Figure 36 shows test results with the 4.5 ins. regular traverse distance (test #195). Three regions appear: betweent Z/Zo=0.0-0.2 there appears a drop in velocity and no change in turbulence; between 0.2-0.8 a slight drop in velocity and a gradual increase in turbulence; between 0.8-1.0 a sharp drop in velocity but little change in turbulence level, ending at Z/Zo=1 with u*=0.027. With the traverse distance increased to 5.5 ins., (test #190) results on velocity remained about the same while turbulence increased to 0.038 at end of the traverse, as shown in figure 37.

k) With the extended N/D the traverse distance was decreased to 4.25 ins. While longitudinal variations of centerlane velocity in test #194 remained about the same as in #195, turbulence decreased, figure 38.

l) In absence of any N/D, test#204, there was hardly any change in

velocity along the flow except near the collector intake. Turbulence sharply increased downstream from the contraction, became somewhat steady, and again increased along the flow until dropping off just upstream of the collector, as shown in figure 39. It is noted that by removing the regular N/D the traverse distance increased by 1.25 ins.

DISCUSSION OF THE RESULTS

All results presented in this report demonstrate that wind-tunnels operating with open test section have a variety of complex problems which, apparently, were not well known before. For example, with reference to the 14-by-22 ft. Low Speed Tunnel at Langley, the various tests performed on collectors of different geometry were aimed, in a 24th scale model, to establish only the lowest turbulence level at one fixed point inside of the open Test Section (testing area). Results of these studies (see Ref.2, in which the author of this report took a part) showed that collectors with straight walls proved far superior to the collectors of the old "bell-mouth" shape. Studies concerning effects of the side-wall angle of incline on flow distribution up- and downstream and within the collector -including reversed flow along the walls- were ignored. The studies presented in this report correct this deficiency and extend the range of application of the results to benefit, in addition to the AQFF, all wind-tunnels operating with an open test section.

While design aspects of collectors were discussed already in Section I, it was observed that upstream effects of the collector on the flow, as evidenced by static pressure rise, became stronger when approaching the intake. In the AQFF scale model tunnel under consideration, the effects were felt over approximately 30 percent of the Test Area length where deceleration accompanied by static pressure increases were observed. Furthermore, static pressure changes also occur downstream from the contraction exit. Tests showed marked changes in static pressure along the flow up to a location where it became about equal to the test chamber pressure (slightly below

atmospheric) . Depending on configuration, the distances over which these marked changes occured were found to differ. With the regular N/D it was found to be about 20 percent of the test length, while it was about 30 percent with the N/D removed.

Having recognized these two effects, the length of the test area may duly be increased to offset the loss of the effective length needed for testing. The realization that the effective length is roughly halved may, in some cases, ultimately require adjustments of the test area length. With regard to the D.S.M.A. design under consideration, the results of tests show a rather tight space sorely in need of some increase in the test area length.

Having discussed the length of the test section, it may be prudent to discussed it's width. Naturally, without the application of the N/D, test section width is largely dictated by the width of the contraction exit. Along the flow, as the jet core width decreases, so does the "effective" width of the stream. As a matter of fact, there are two effects to consider: variations of velocity changes along the flow and across the flow.

Along the flow, the axial velocity varied only slightly in absence of the N/D, while with application of the regular N/D the variations became more significant, although the changes were limited to both ends of the test section. With the extended N/D the changes were continuous. Across the flow, uniform velocity was experienced at exit from the contraction with or without the N/D but the N/D allowed the stream to widen the core thus helping the test section to maintain a wider stream for experimentation. Tests also showed that at entry to the collector the flow distribution was well rounded with the uniform portion almost nil.

Turbulence levels increased along the flow for all configurations, the rate of increase being markedly stronger along the second half of the longitudinal traverse. However, across the flow, turbulence showed a different pattern: it became minimum in the tunnel center and maximum where the gradients of velocity distributions were the largest. Altogether, these experiences show need for a wider contraction exit

as well as a longer test section than the D.S.M.A. design demands.

Ventilation may prove helpful in reducing recirculation in the test chamber by mixing quieter "fresh air" from the outside with noisy air issuing from the contraction. Regarding ventilation, only a slight static pressure depression was required for small amounts of atmospheric air to be drawn into the test chamber through the two openings provided in the sides of the chamber. To achieve this, application of the regular N/D especially proved helpful because at it's exit the static pressure was found sub-atmospheric. With the application of the extended N/D, however, the pressure in the test chamber rose above atmospheric and the ventilating flow was reversed. Further downstream, near the duct exit, replacing the 3.5 ins. orifice plate with a 4 ins. opening also proved helpful maintaining positive ventilation.

While the scale model tunnel was obvously small for acoustic tests, it proved useful to explore energy effects. While maintaining positive ventilation, amounting to about 10-12 percent of the jet mass-flow, the energy of the jet entering the collector needed to be partially converted into pressure to balance the resistance of the duct system, including the diffuser, the elbow and the orifice as well. In addition, adequate energy was needed to maintain flow through the system. To achieve this, efficient energy conversion in the diffuser was required. Application of the regular N/D (Ref.5) helped to attain this goal. (For detail studies of energy, see APPENDIX D.)

Among other variables, <u>total pressure was found practically constant</u> throughout the test area both, along the tunnel centerline and across the flow while <u>static pressure varied a great deal</u>. Specifically, at the exit from the contraction, the variation of static pressure across the flow resembled to an inverted parabola. Remarkably, in absence of the N/D the maximum pressure in the area center was +4.21 p.s.f. in contrast to the regular N/D where the center pressure was -5.74 p.s.f.! This result came as a complete surprise and posed a serious problem! How could the total pressure remain constant and the static pressure vary, when flow traverses taken with hot-wire were showing uniform velocity distribution

(except at the edges).

The most plausible answer to this question may be found when considering radial equilibrium, that is: a fluid stream in a parallel flow cannot support transverse pressure gradient unless there is curvature in the path of the motion. Since motion along a curvature sets up a centrifugal force, in fluids this must be balanced by a pressure "gradient" equal and opposite to the force. This being the case, the flow from the contraction cannot be parallel.

Two cases present themselves:

In absence of the N/D, the flow leaving the contraction is affected by the wall curvature near the contraction exit in such a way that the streamlines at the exit are still converging towards the tunnel centerline so that the flow becomes parallel with it only at some distance downstream. One can calculate the "instantaneous" radius of the curvature R at various locations in the exit plane by using the radial equilibrium equation for that location

$$\frac{dP}{dR} = \rho \frac{U^2}{R}$$

Omitting details of calculations given in APPENDIX E, the radius of curvature at the edge was found Re = 9.775 ins. assuming a flow velocity U = 200 ft/s, This may be considered as an inward curvature, because the radius vector points towards the centerline, shown in in figure 40/a. In this case the pressure gradient is positive and acts to curve the flow outwardly from the centerline.

With the regular N/D, an attached flow aligns with the walls of the N/D which are inclined at 6 degrees with the centerline and supposedly leaves at that angle. However, at some distance downstream from the N/D exit the flow must align with the centerline. This time the curvature is considered outward because the radius vector points away from the centerline, shown in figure 40/b. This accounts for the negative pressure distribution and the pressure gradient acts to curve the flow back toward the centerline.

When compared to the jet size, the radius of curvature appears

several times larger. (Jet width at contraction exit is 2 ins.).

As far as recirculation is concerned, two areas, one on each side of the jet perimeter were observed. These two areas were two sides of the test chamber, one wide and one narrow, where recirculation was observed. Within these two spaces flow velocities were found roughly two order of magnitudes smaller than in the jet itself. Hot wire techniques were used for measuring both, velocity and turbulence, yet even the hot wire measurements proved inaccurate in places where the velocity fell below 3 ft/s. Furthermore, the 2-D hot wire probes were insufficient to measure direction. Ultimately, to explore the recirculation pattern, helium bubbles were introduced into the wide side of the test chamber and the movement of these bubbles was recorded photographically using fast speed movie cameras. These records are available for inspection.

Since only the wide side of the test chamber was available for the photo studies (because neither the narrow side nor the top and bottom were accessible,) the picture of recirculation all around the jet remains incomplete. There is, however, evidence of a clockwise circulatory motion of the bubbles with an estimated speed of about 3 ft/s.

CONCLUSIONS

Tests performed on the scale model of the AQFF wind-tunnel operating with an open test section show a variety of complex problems. These problems were partly due to original design flaws as well as to the complexity of the flow of a jet first moving into an empty space and finally discharging through a duct system into the atmosphere. Studies on the model show that certain steps taken could correct the design and that the flow problems could be solved by a better understanding of the underlying flow phenomena. It appears from the studies performed, that design and flow are interconnected.

The following suggestion may lead to a much improved design:

1. Between the two options available, namely either sucking or blowing air through the duct system, blowing seems to have the advantage to allow the test chamber to operate under slightly below atmospheric pressure. When sucking air the test chamber must operate under a considerable sub-atmospheric pressure, which has numerous disadvantages. All of test results presented in this report were obtained in the blowing mode and no models were placed inside the Test Area.

2. The jet, having crossed the Test Area and being accompanied by the co-flowing air, has to be "collected" first before it is allowed to enter a diffuser.

3. Collection must take place in a suitably shaped "collector" that is located at some distance upstream of the diffuser intake.

4. A suitably shaped collector is designed on the basis of flow distribution at its intake and should be free of reverse-flow effects.

5. The distance between collector exit and diffuser intake -called the "gap"- needs to be wide enough to allow "breathing", that is to allow the flow of any air that missed collection.

6. The jet issuing from the contraction may flow either parallel with the tunnel axis, or may slightly diverge. In the first case, the contraction exit needs to have an extension with a parallel duct of some length to ensure perfectly parallel flow from its exit. In the second case, the exit of the contraction may be fitted with a slightly divergent duct, called the "nozzle-diffuser", which proved helpful to both, widen the jet core and improve recovery in the diffuser as well.

7. The flow of ventilating air, originally intended to stabilize the jet, amounted to roughly 10-12 percent of the mass flow of the main jet in the tests. However, this amount of flow could be manipulated by a well designed throttling valve located at the very end of the duct system. In addition, it also could be manipulated with the nozzle-diffuser. (The original design called for an air vent located at the top of the chamber but in order ensure more uniform flow, this was later changed to vents located in both sides of the chamber).

8. Recirculating air motion in a 1:48 scale model was rather difficult to trace partly due to the lack of space and partly to instrument sensitivity. Helium bubbles introduced through the sides of the Test Chamber showed qualitatively a rather irregular motion superimposed on an average circulatory path which could not be traced with hot wire measurements. High speed cinematography did the trick.

9. Turbulence levels were found varied and relatively high when compared with the center of the jet, where it was the lowest as indicated by traverses taken <u>across</u> the flow. However, <u>along</u> the flow turbulence levels measured in the tunnel centerline consistently increased from the lowest at contraction exit, to the highewt level near the collector intake.

10. With consideration to streamwise variation of some flow parameters, the length of the Test Area needs further attention. While this aspect needs further studies, in the light of the test results the proposed length of AQFF tunnel may prove rather short.

APPENDIX D

ENERGY CONSIDERATIONS
PART 1
JET ENERGY

It appears from the tests performed on the scale model tunnel that in the blowing mode near atmospheric conditions can be maintained inside the Test Chamber. In other words, only a small depression below atmospheric pressure is require to induce adequate ventilation. Thus the jet energy for the specified Mach number, M = 0.4, of the full-scale tunnel may be roughly estimated by conveniently assuming at the exit from the contraction, a static pressure and temperature.

$$p_e = 14.7 \text{psia}$$

$$\Theta_e = 74 \text{ deg. F.} = 534 \text{ deg. R.}$$

Since the stagnation temperature, T, remains constant along the flow in the contraction, one finds from Compressible Flow Tables (CFT) for isentropic flow (k = 1.4) at $M_e = 0.4$

$$\frac{\Theta_e}{T_e} = 0.96899$$

Hence the stagnation temperature $T_e = 534/0.96899 = 551.08$ Deg. R.

Similarly , one can establish at the contraction exit the stagnation pressure P from CFT data

$$\frac{p_e}{P_e} = 0.89562$$

Hence the stagnation pressure

$$P_e = 14.7/0.89562 = 16.413 \text{ psia}$$

It is noted that the stagnation pressure at the contraction inlet needs to be adjusted for losses inside the contraction.

The Mach number at the inlet to the contraction may be established from the inlet-to-outlet area ratio AR = 8.10 .

From the CFT one finds at the contraction exit for M_e = 0.4 the area ratio A/A^* = 1.590. Using the area ratio AR = 8.1, one calculates at the contraction inlet A/A^* = 1.59 · 8.1 = 12.88. With this value, the inlet Mach number (with extrapolation) becomes M_i = 0.045. For this inlet Mach number, the static temperature

$$\Theta_i = 551.08 \cdot 0.9996 = 550.85 \text{ deg. R.}$$

The jet power, P_j, is obtained from the product of the mass flow and the change in enthalpy

$$P_j = \dot{W}\Delta h$$

The mass flow may be calculated from the expression, frequently called the "Fanno equation",

$$\dot{W} = \sqrt{k \cdot g/R} \cdot \left(\frac{p \cdot A}{\sqrt{T_e}} \right) \cdot M_e \sqrt{1 + \frac{(k-1)}{2} \cdot M_e}$$

Substitution of A_e = 40 sqft and other relevant quantities at the contraction exit, one obtains

$$\dot{W} = 1347.8 \text{ lbs/sec.}$$

The change in enthalpy is proportional to the change in static temperature between the inlet and outlet of the contraction, thus

$$\Delta h = J \cdot C_p \cdot (\Theta_i - \Theta_e)$$

Substitution of the relevant quantities yields

$$\Delta h = 3146.23 \text{ ft} \cdot \text{lbs/lb}$$

Hence the jet power

$$P_j = 1347.8 \cdot 3146.23 / 550 = 7710 \text{ HP}$$

PART II

FAN POWER

In order to estimate the power required to drive the fan, one needs to estimate first the losses experienced between the fan and the contraction. However, at this point, one cannot estimate theses losses due to insufficient data[1]. Even so, by ignoring these loses, one can, at least, estimate the ideal fan shaft power required based on the stagnation pressure rise across the fan, the volumetric flow rate, and the fan efficiency.

Accordingly:

fan pressure rise = 16.413 - 14.7 = 1.713 psi = 246.67 psf;

volumetric flow rate = 1347.8/0.0744 = 18,115.6 cfs.

Hence ideal shaft power, assuming an 85% fan efficiency

$$P_{fan} = \frac{18115.6 \cdot 246.67}{550 \cdot 0.85} = 9558.44 \text{ HP}$$

[1] Note DSMA calculated power, 9827.4 HP, with a 'loss factor' of 1.1618.

PART III

FLOW THROUGH THE EXHAUST DUCT SYSTEM

Flow through the exhaust duct system consists of two parts: the flow through the contraction, and the flow through the air-vents. The test performed on the model tunnel showed that no additional power was require for maintaining the combined flow. However, it was observed that positive ventilation was attained only if the amount of energy recovered from the jet was sufficient to overcome the resistance of the exhaust duct system. If the resistance proved too high, negative ventilation ensued and some air flowed out through the vents instead of the exhaust duct system.

In the three-dimensional model tests efficient energy recovery was achieved by first redesigning and subsequently installing , both, a collector - absent in the original DSMA design - and a new diffuser. Flow rate through the exhaust system, and consequently through the air vents, could be controlled by a throttling device attached to the system exit. The throttling device would effectively determine the resistance in the exhaust duct, thereby determining the flow rate, and direction of the vent air. Although the vent air flow rate may also be controlled at the vents themselves, a throttling device should prove more practical.

APPENDIX E

RADIAL EQUILIBRIUM ON A CIRCULAR PATH.

In circular fluid motion under radial equilibrium

$$\frac{\delta p}{\delta r} = \rho \frac{V^2}{r} .$$

From this the radius of curvature, r, can be calculated. For the case of the contraction alone - no Nozzle-Diffuser - the data presented in figure 20/a can be a used to approximate the pressure gradient

$$\frac{\delta p}{\delta r} \equiv \frac{\Delta p}{\Delta x} = \frac{0.42 \cdot 4.21}{0.1 \cdot 1.85/12}$$

$$\therefore \frac{\delta p}{\delta r} \equiv \frac{\Delta p}{\Delta x} = 114.93 \text{ lb/ft}^3$$

Assuming a density of $\rho = 0.00234$ slug/ft^3, and an air speed of $V \equiv 200$ ft/sec^3,

$$\frac{\delta p}{\delta r} = 114.93 = \frac{0.00234 \cdot (200)^2}{r}$$

$$\therefore r = \frac{0.00234 \cdot (200)^2}{114.93} = 0.814 \text{ ft} = \underline{9.773 \text{ in.}}$$

Similarly, the curvature of the flow issuing from the regular and extended nozzle-diffusers is found first by estimating the pressure gradient

$$\frac{\delta p}{\delta r} = 207.97, \text{ and } \frac{\delta p}{\delta r} = 123.14$$

respectively. Then from the radial equilibrium equation,

$$r = \underline{5.401 \text{ in.}}, \text{ and, } r = \underline{9.121 \text{ in.}}$$

for the regular, and extended nozzle-diffuser respectively. A sketch of the hypothetical streamlines is presented in figure 40.

FIGURES ACCOMPANYING TEXT

PART II SECTION II

19. The effect of contraction exit geometry on static pressure in tunnel.
20. Distribution of static pressure across exit of contraction and N/D.
21. Variation of static pressure along tunnel centerline downstream...
22. Ditto...downstream from the regular nozzle-diffuser.
23. Ditto...downstream from the extended N/D.
24. Ditto...downstream from the regular N/D w/ extended test section.
25. Total pressure variation across exit of the regular N/D.
26. Ditto...across exit of the extended N/D.
27. Variation of total pressure along tunnel centerline w/ reg. N/D.
28. Ditto...w/ the extended N/D.
29. Ditto...downstream from the contraction with N/D removed.
30. Horizontal variation of flow velocity at entrance to the collector.
31. Horizontal variation of velocity across gap...
32. Vertical variation ofvelocity across gap...
33. Velocity and turbulence 1/2 ins. downs. from reg. N/D exit.
34. Ditto...V and t at entrance to the collector, with regular N/D.
35. Ditto...V and t vertical distribution at collector entrance.
36. Longitudinal variation of V and t between reg. N/D and collector.
37. Ditto...except with 5.5 ins. test area length.
38. Ditto...extended N/D exit and collector.
39. Ditto...between contraction and collector (N/D removed).
40. Sketch of hypothetical streamlines entering test area.

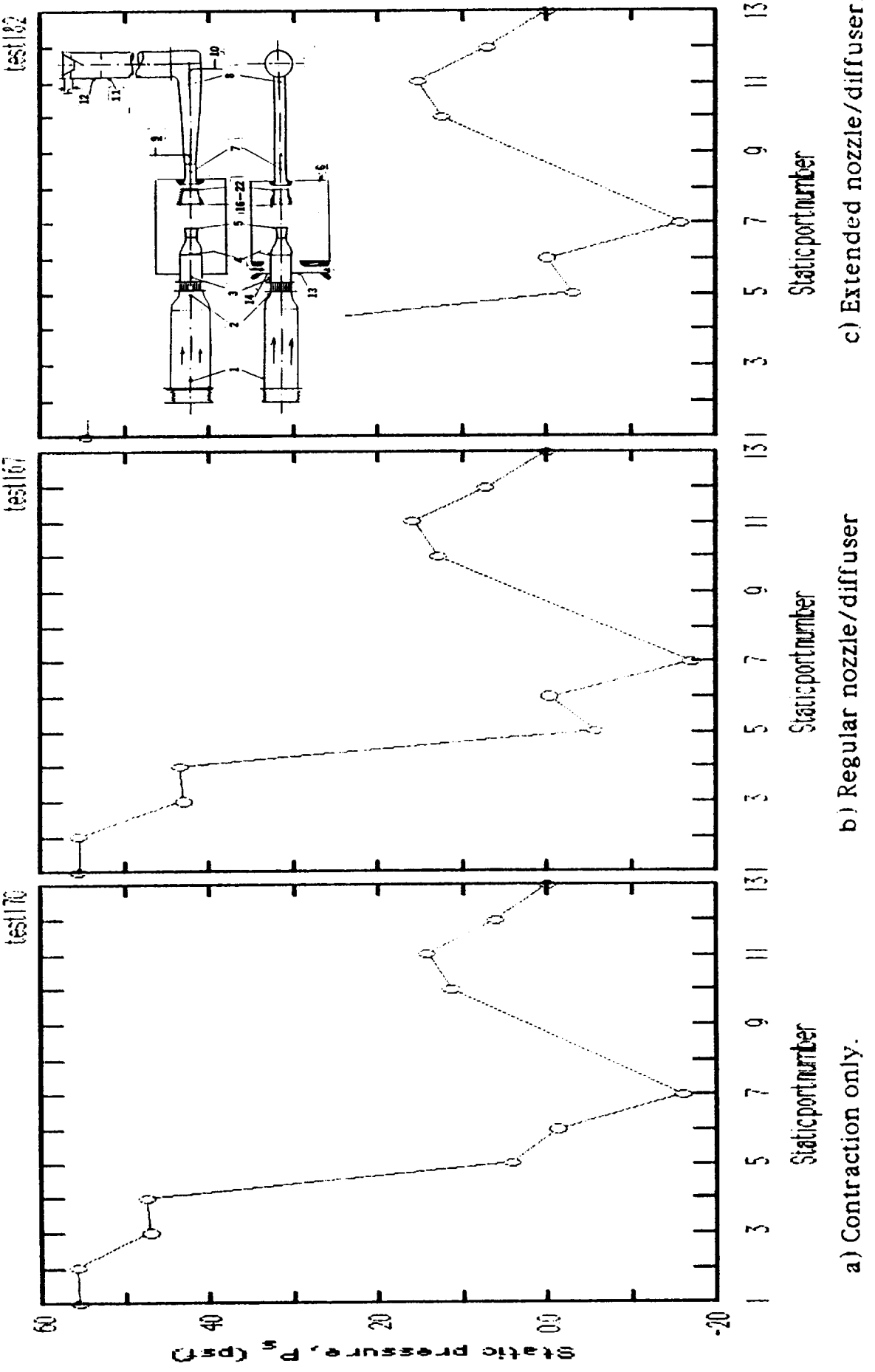

Figure 19. The effect of contraction exit geometry on static pressure throughout the tunnel circuit.

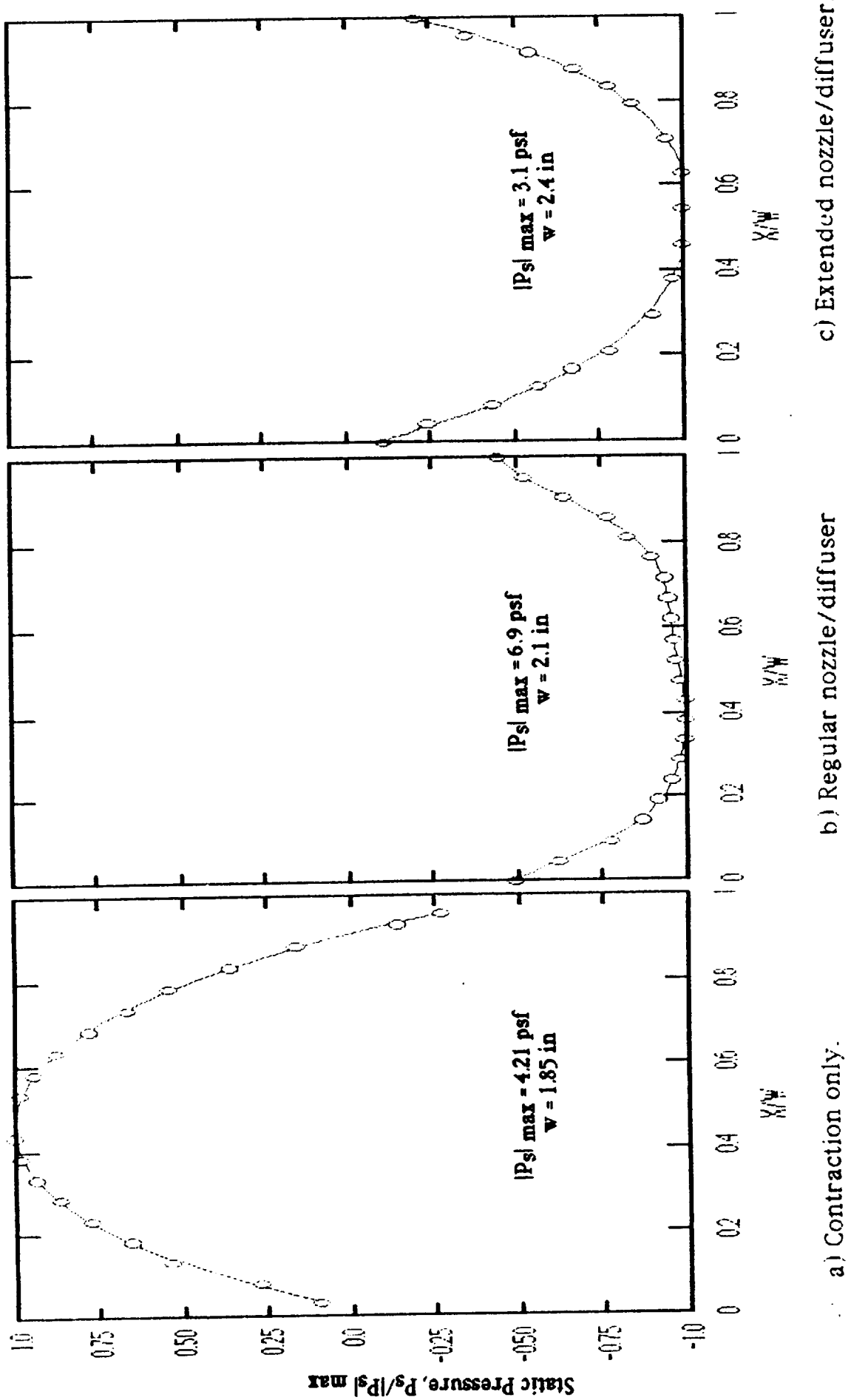

a) Contraction only. b) Regular nozzle/diffuser c) Extended nozzle/diffuser.

Figure 20. The effect of contraction exit geometry on the distribution of static pressure across the exit of the contraction, or nozzle/diffuser.

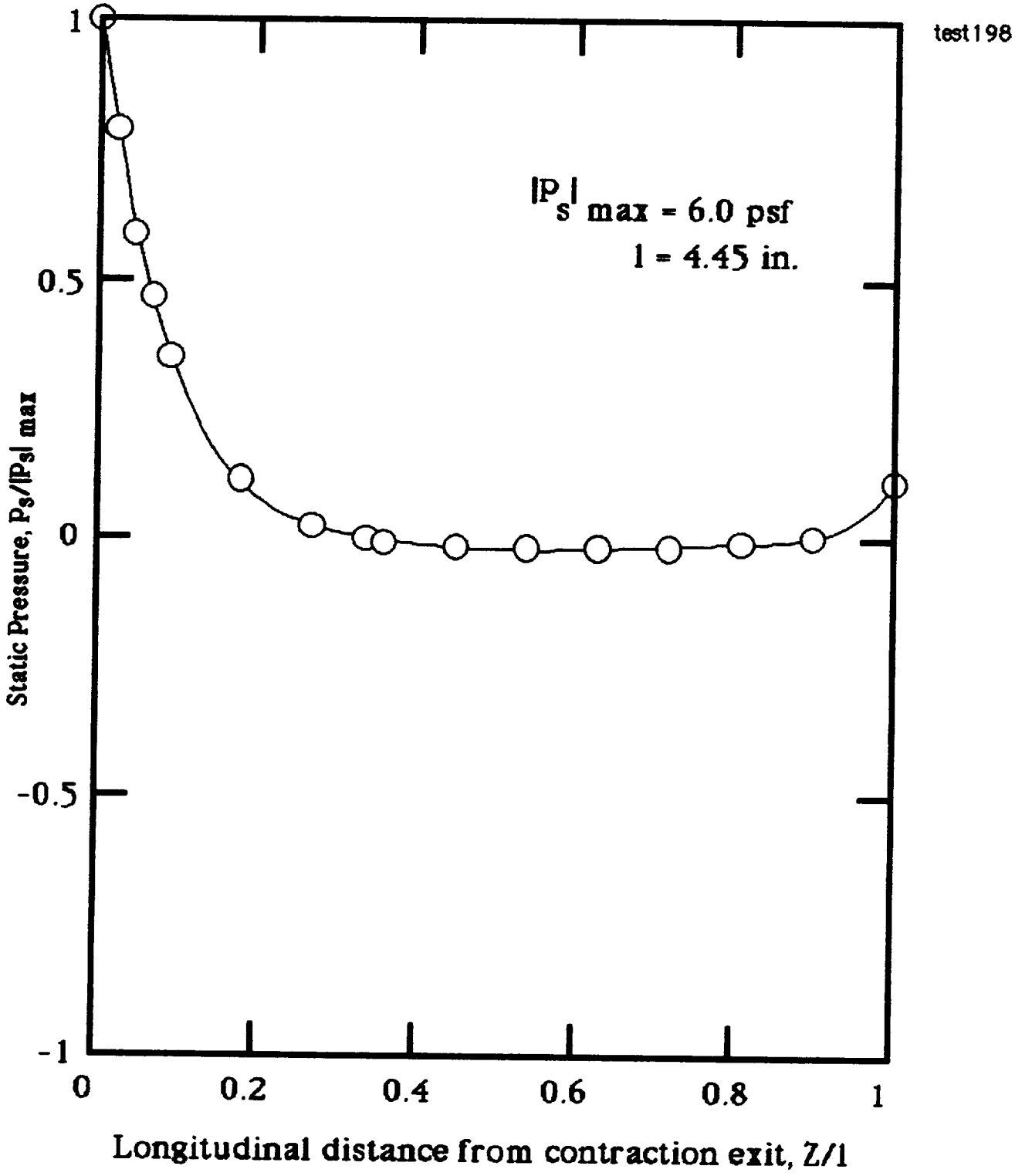

Figure 21. Variation of static pressure along tunnel centerline downstream of the contraction (noz/dif removed).

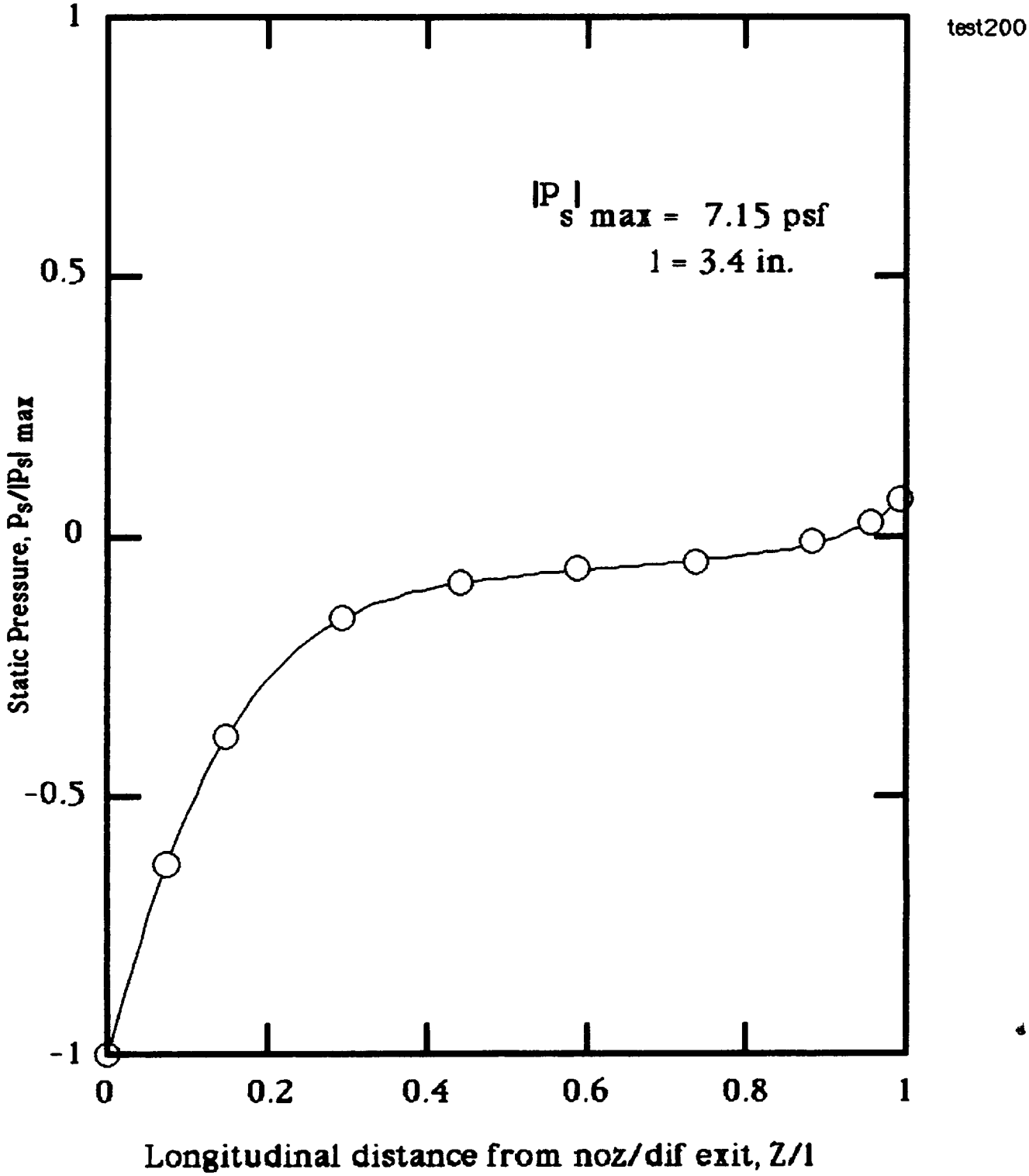

Figure 22. Variation of static pressure along tunnel centerline downstream of the regular noz/dif.

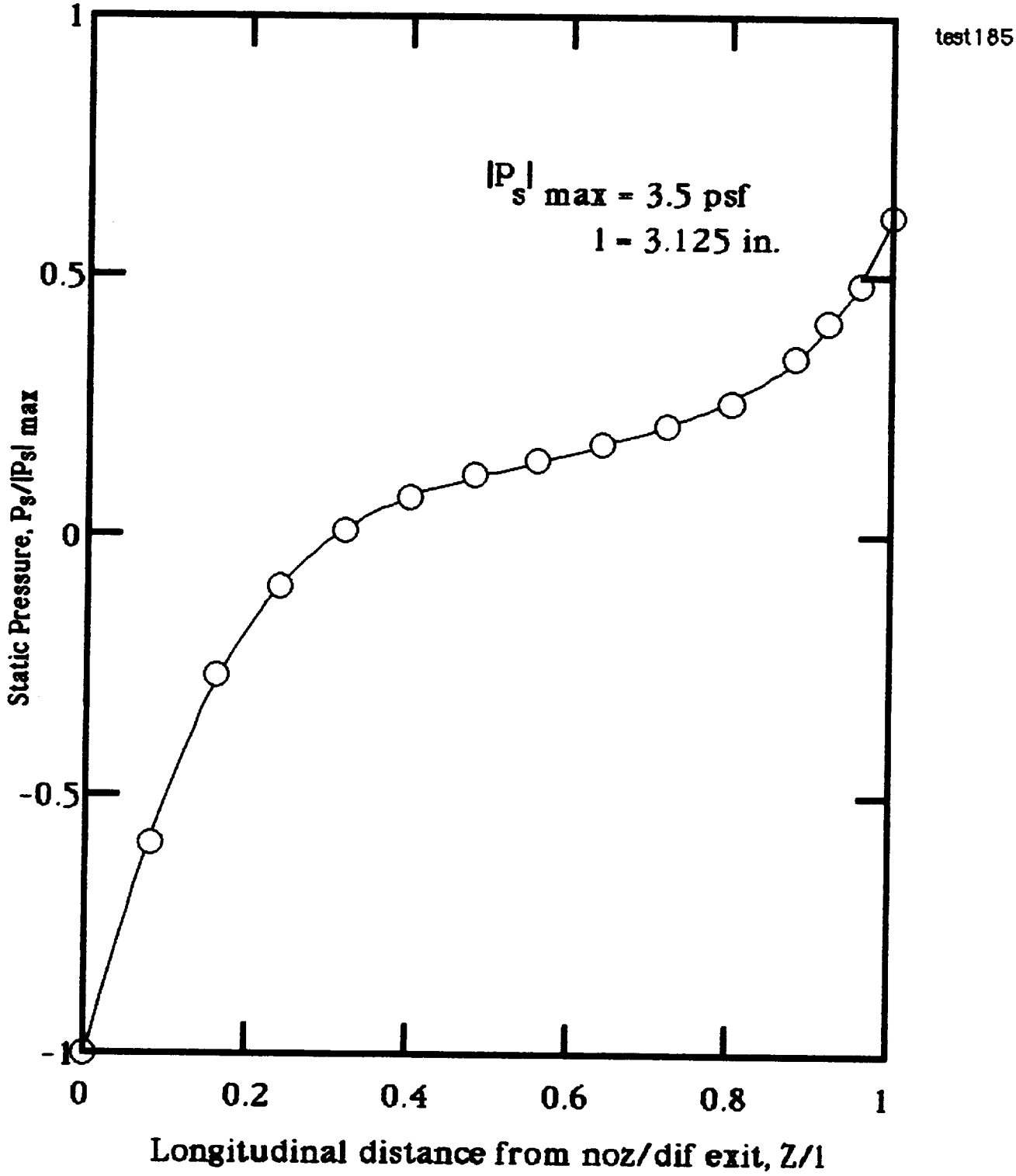

Figure 23. Variation of static pressure along tunnel centerline downstream of the extended noz/dif.

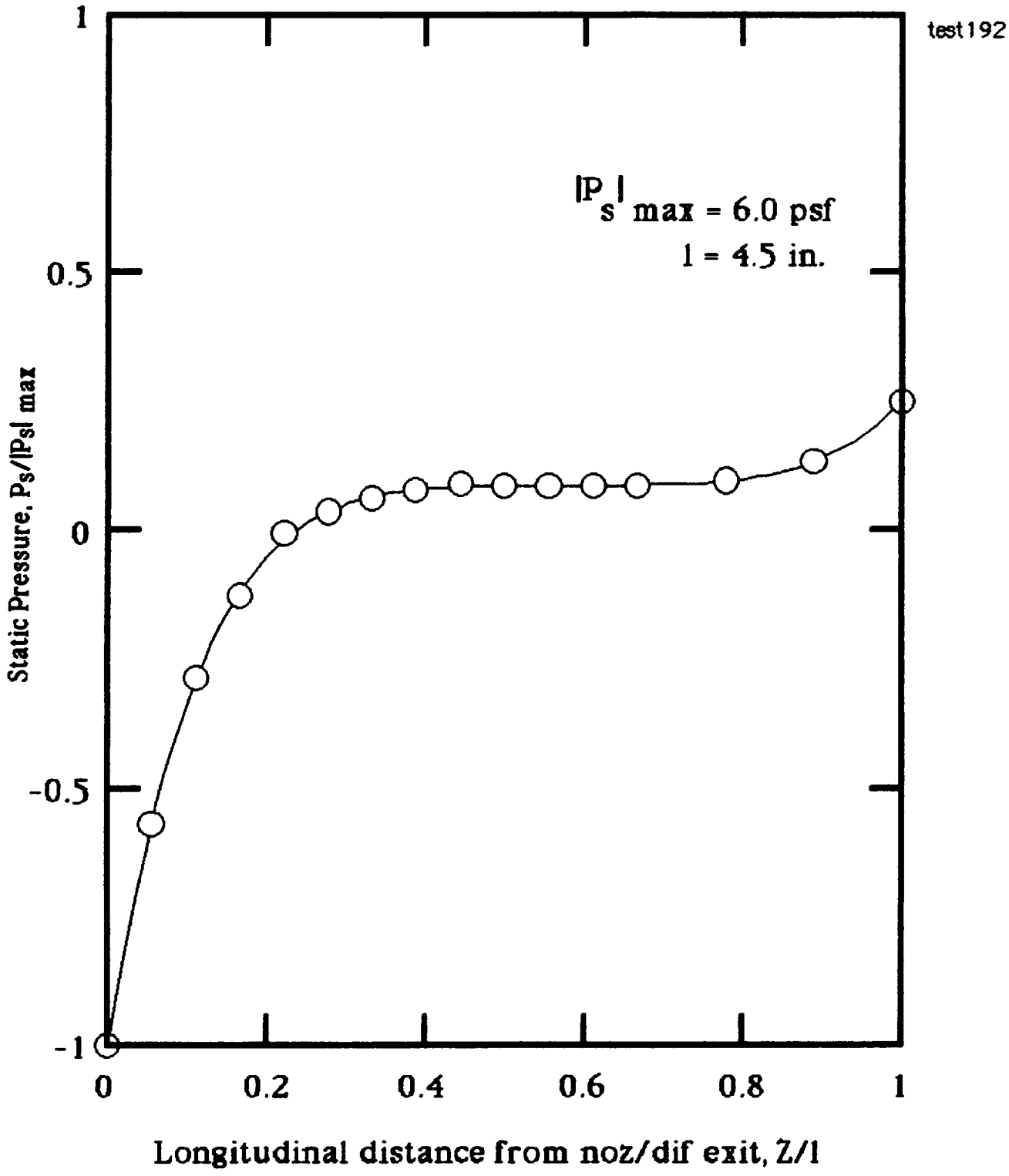

Figure 24. Variation of static pressure along tunnel centerline downstream of the regular noz/dif (extended test section).

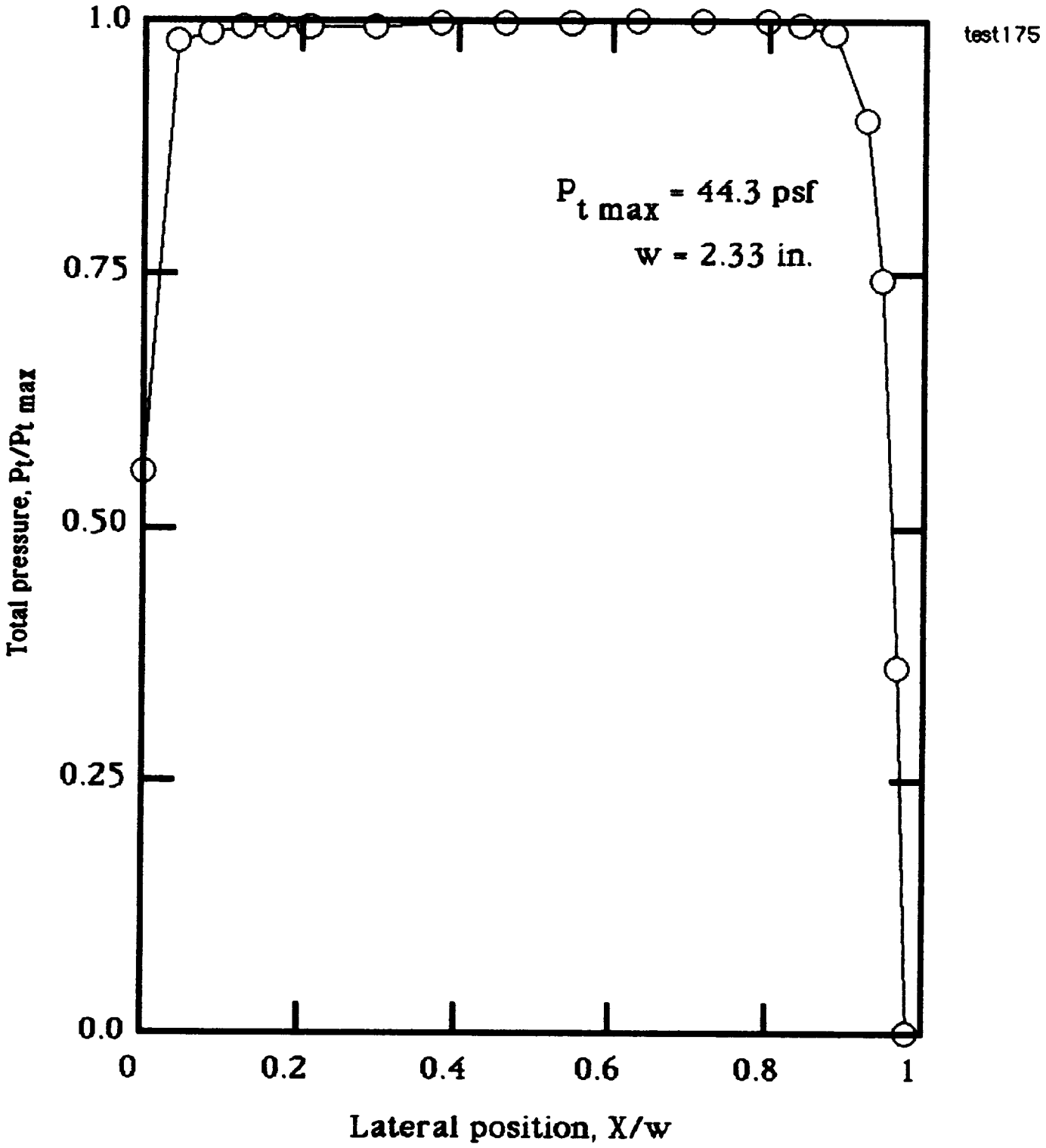

Figure 25. Horizontal variation of total pressure across the exit of the regular noz/dif.

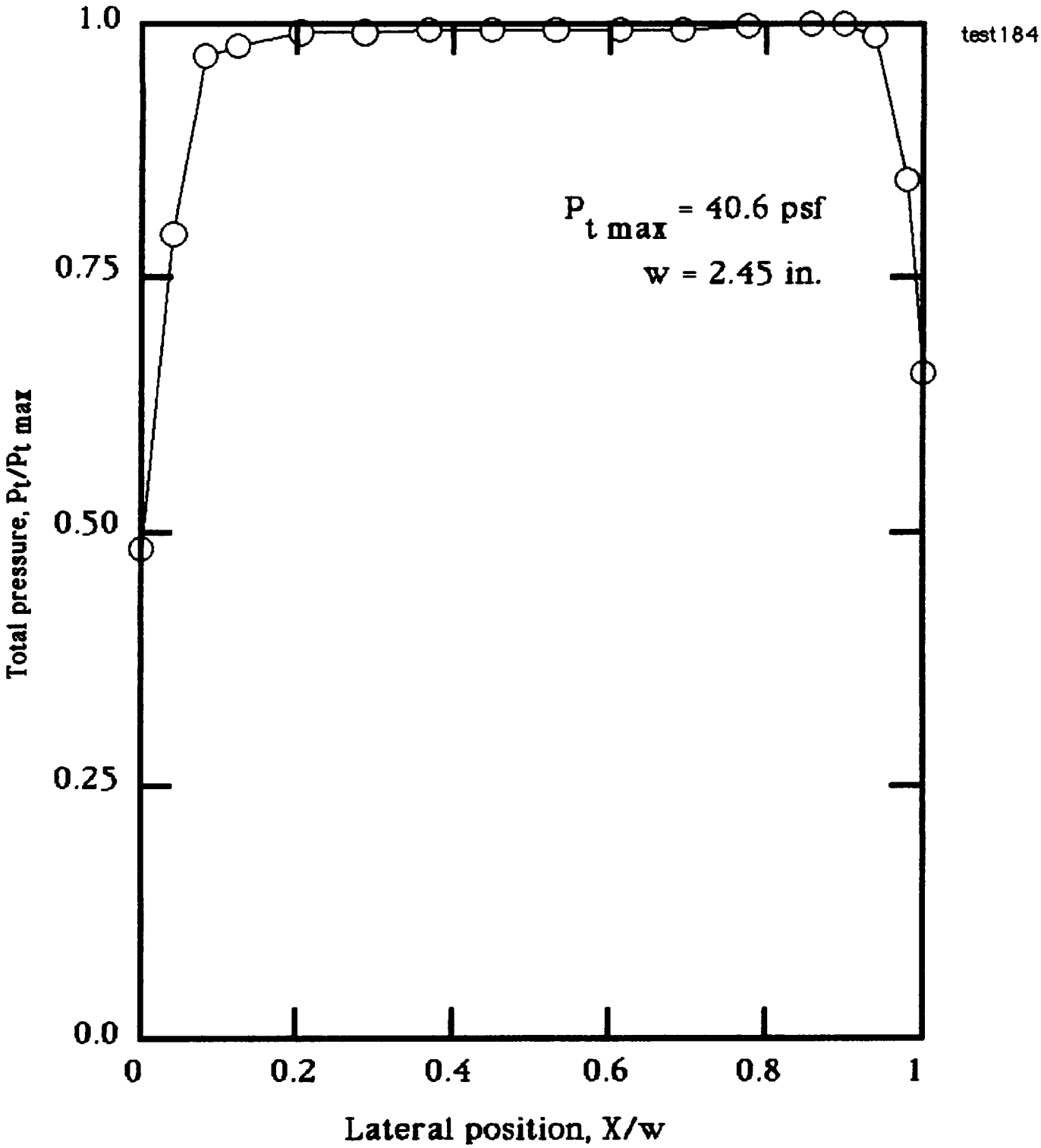

Figure 26. Horizontal variation of total pressure across the exit of the extended noz/dif.

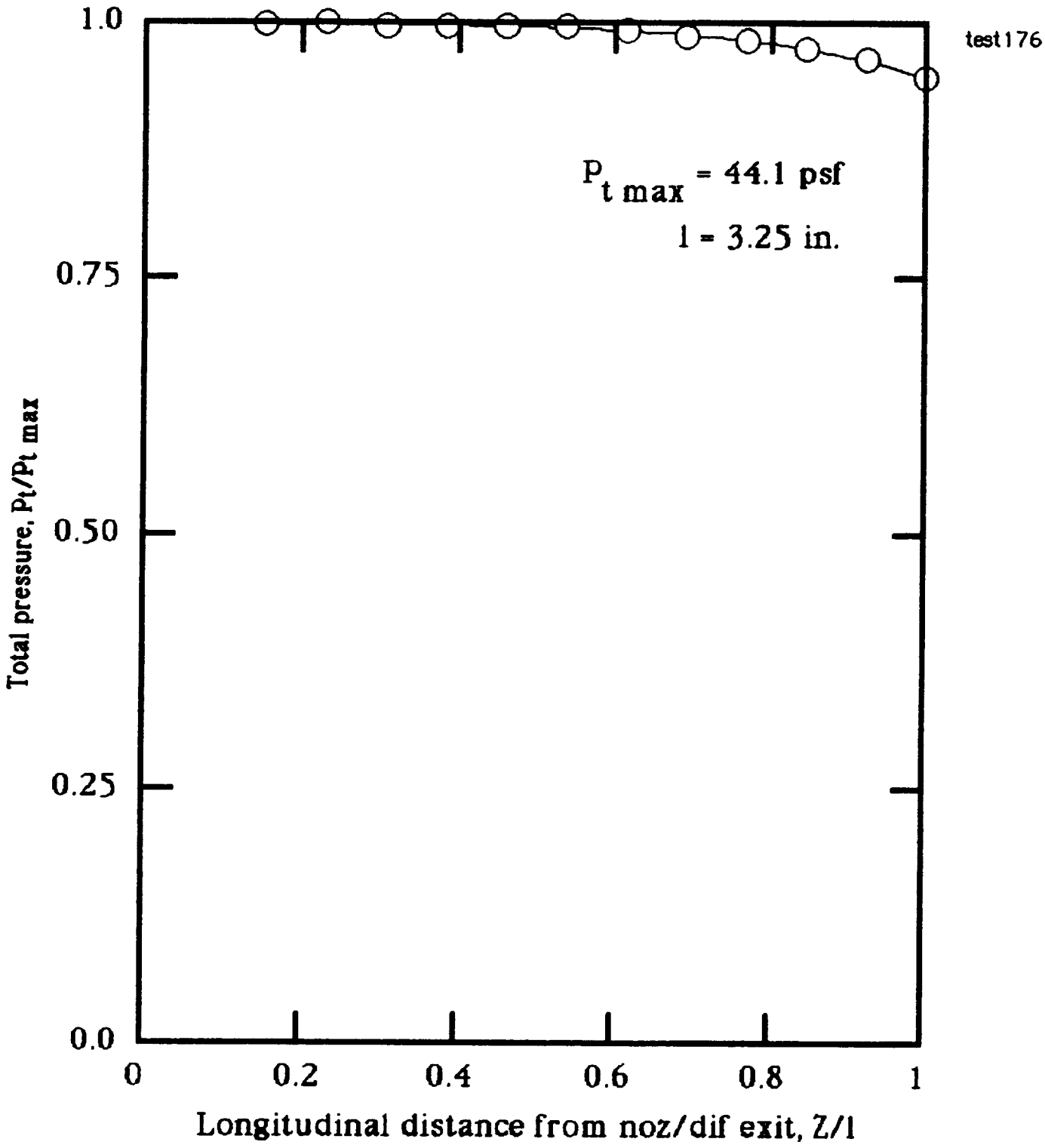

Figure 27. Variation of total pressure along tunnel centerline downstream of the regular noz/dif.

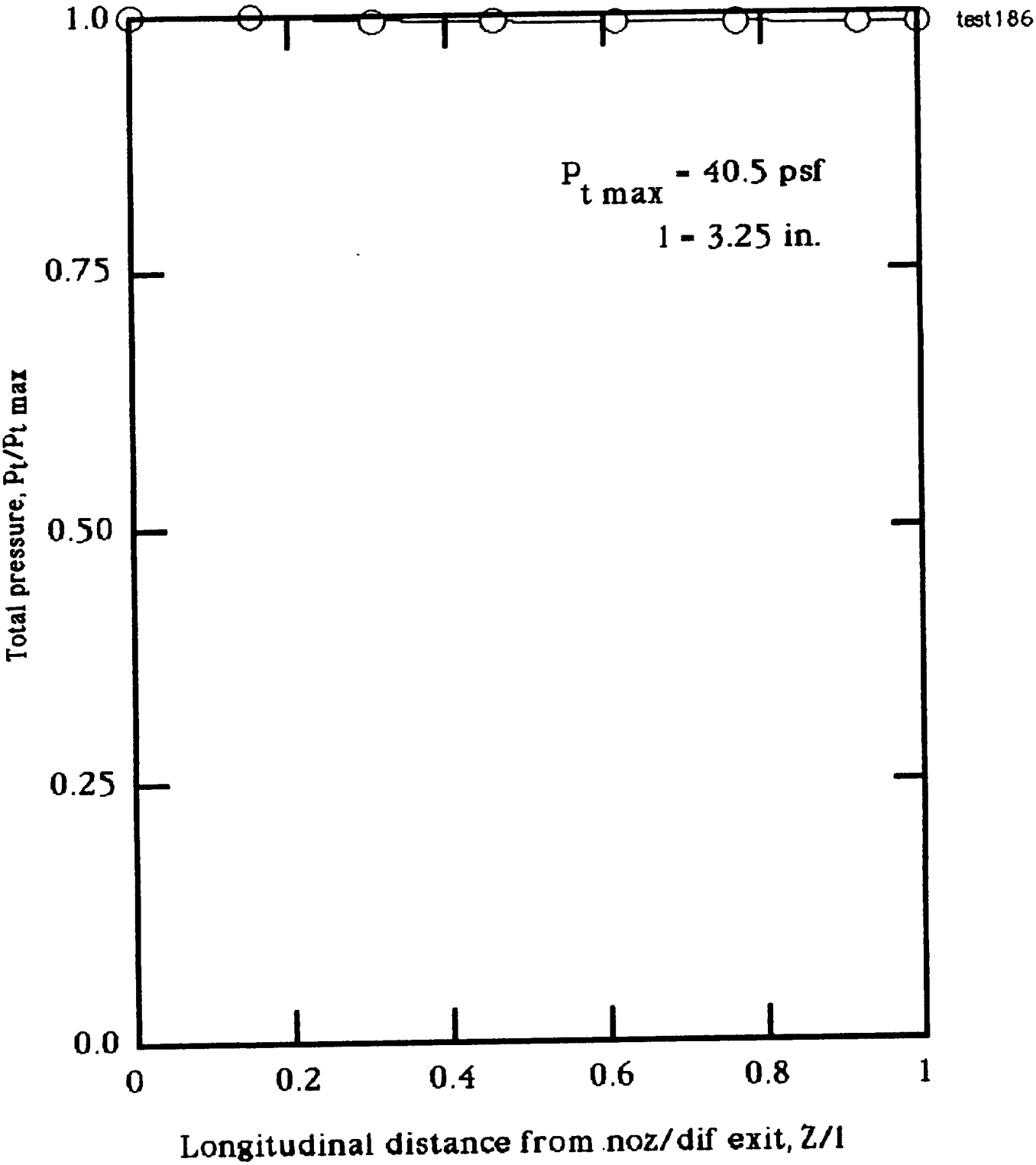

Figure 28. Variation of total pressure along tunnel centerline downstream of the extended noz/dif.

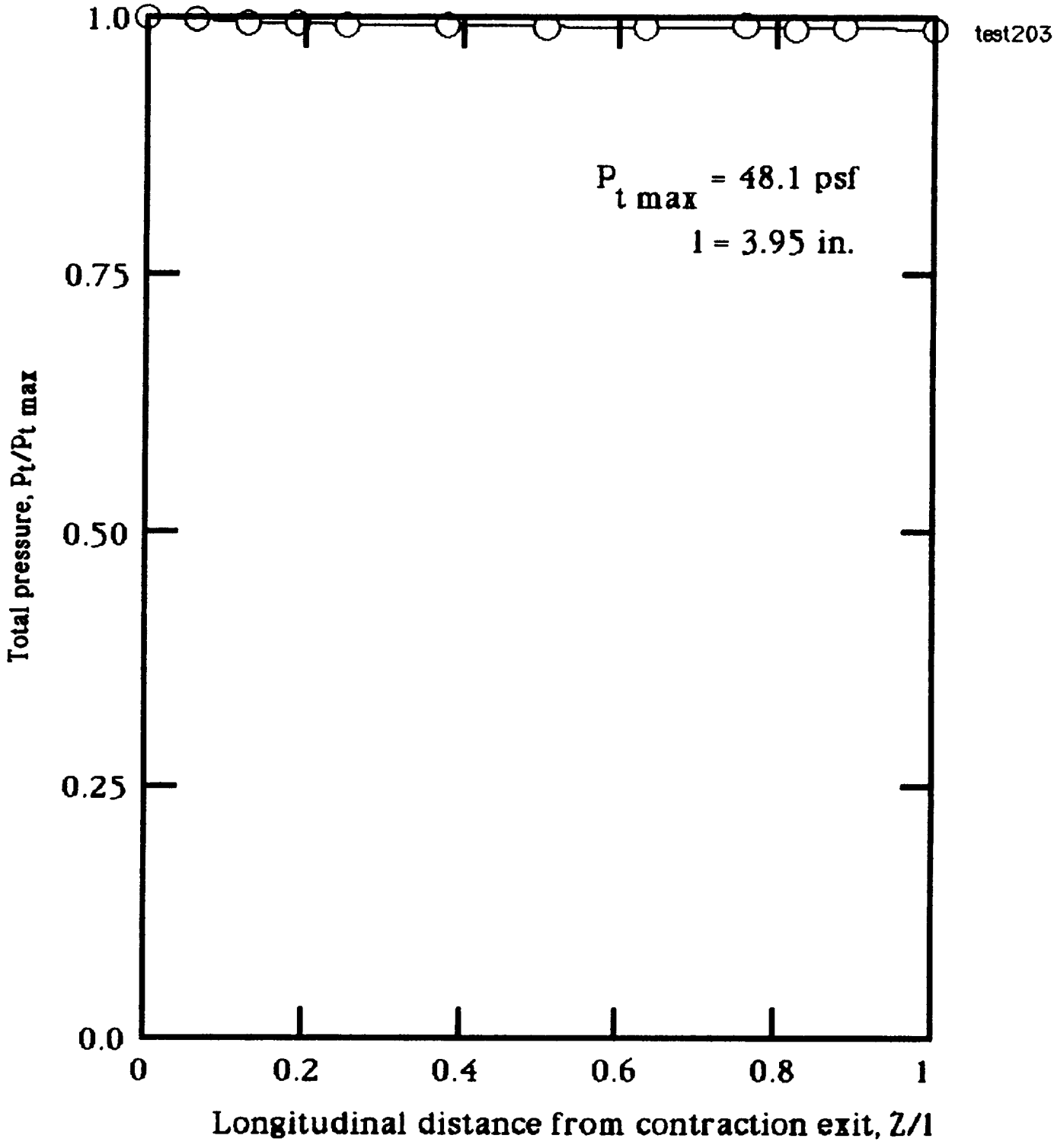

Figure 29. Variation of total pressure along tunnel centerline downstream of the contraction (no noz/dif).

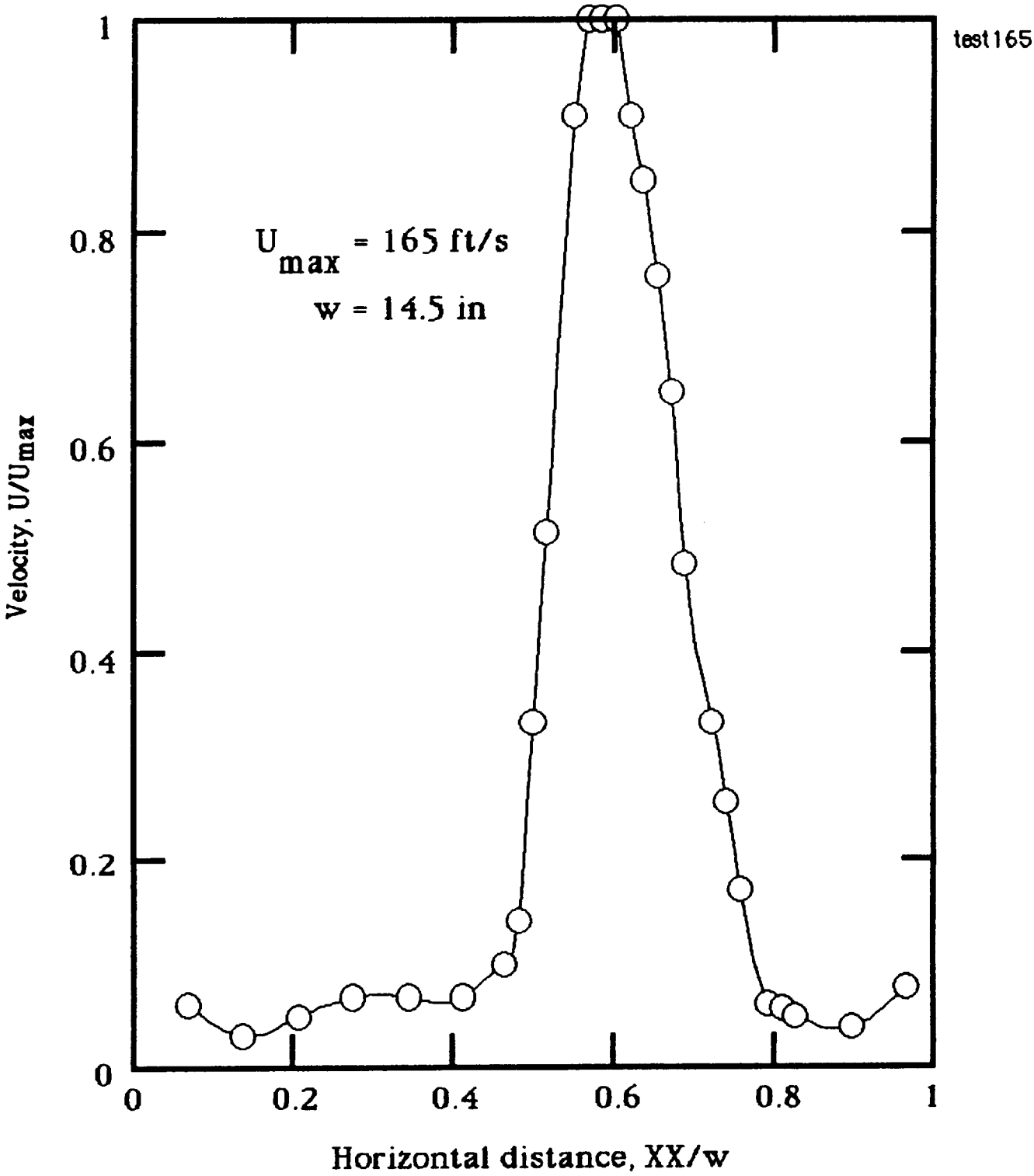

Figure 30. Horizontal variation of flow velocity at the enterance to the new collector.

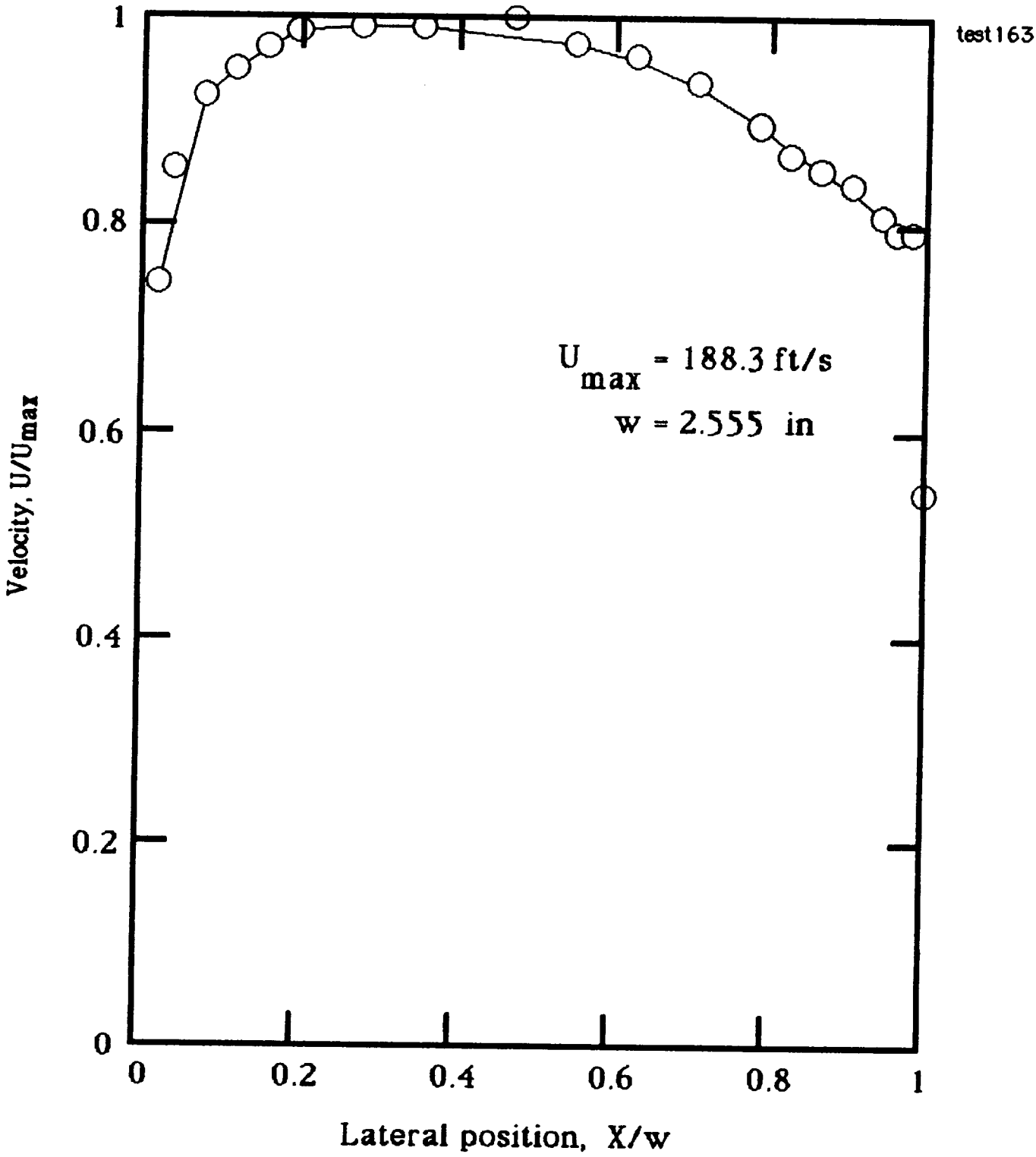

Figure 31. Horizontal variation of velocity across the gap between the collector and diffuser.

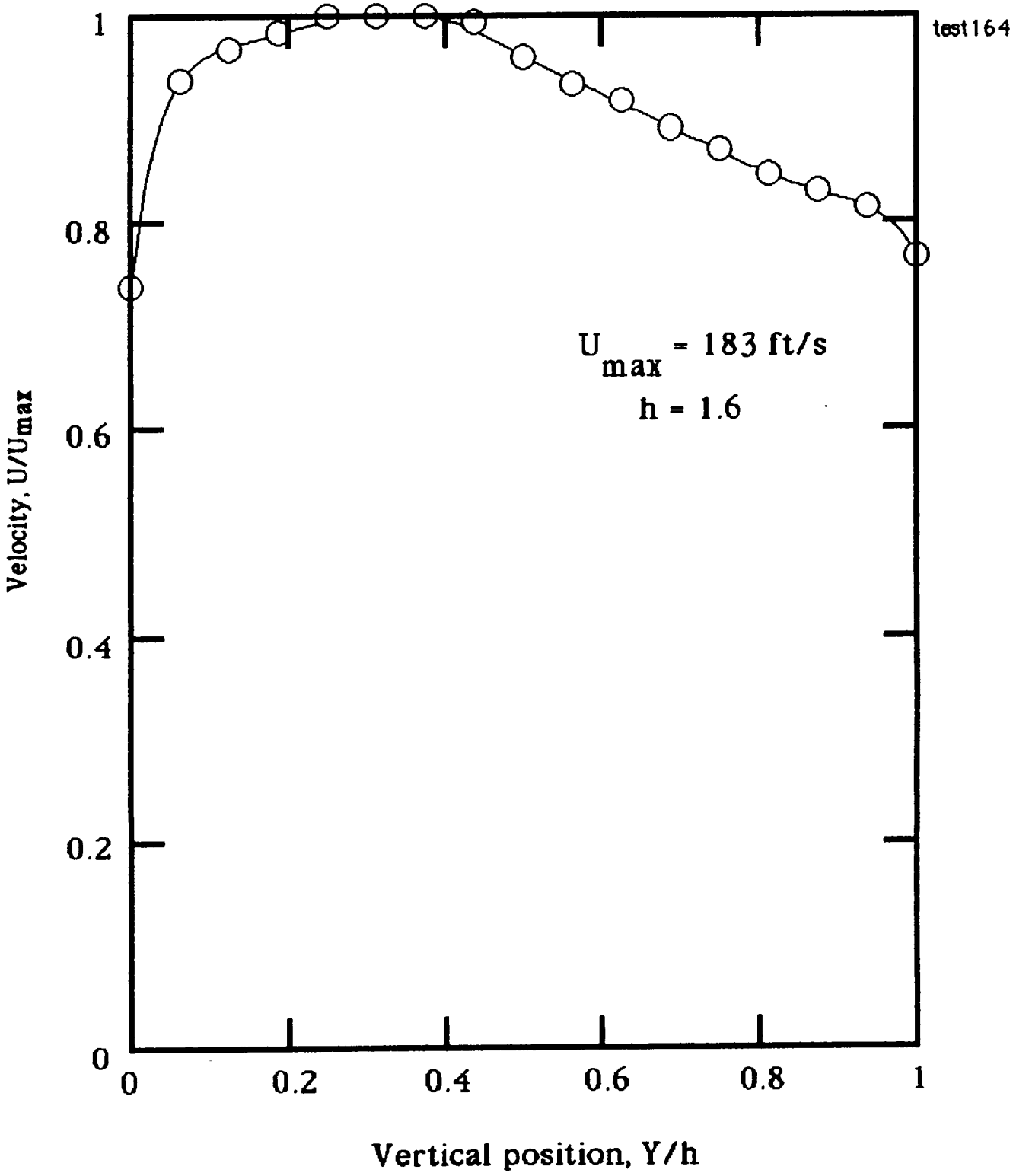

Figure 32. Vertical variation of velocity across the gap between the collector and diffuser.

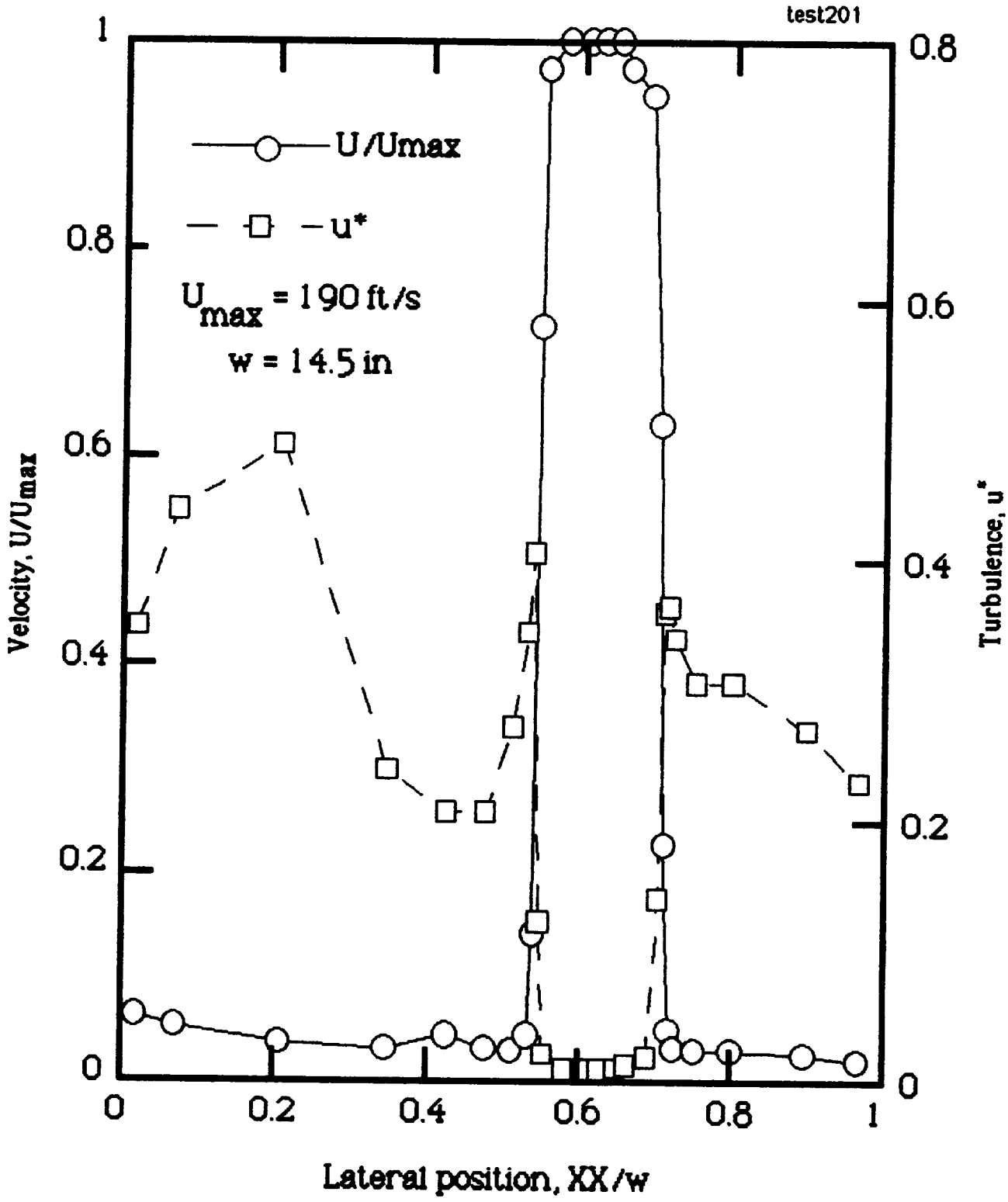

Figure 33. Horizontal variation of velocity and turbulence, 1/2 " downstream from the regular N/D exit.

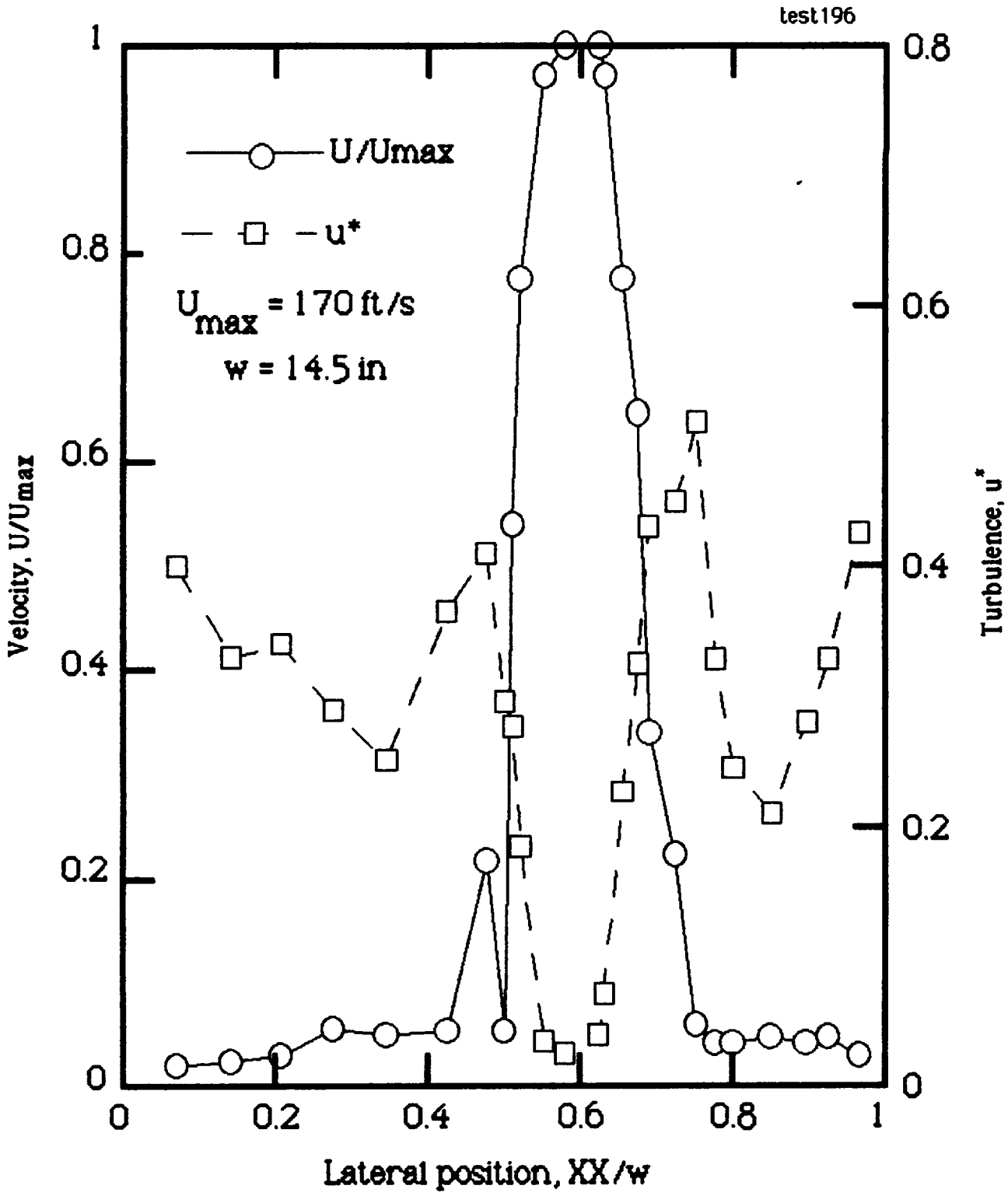

Figure 34. Horizontal variation of velocity, and turbulence at the enterance to the new collector, with the regular N/D.

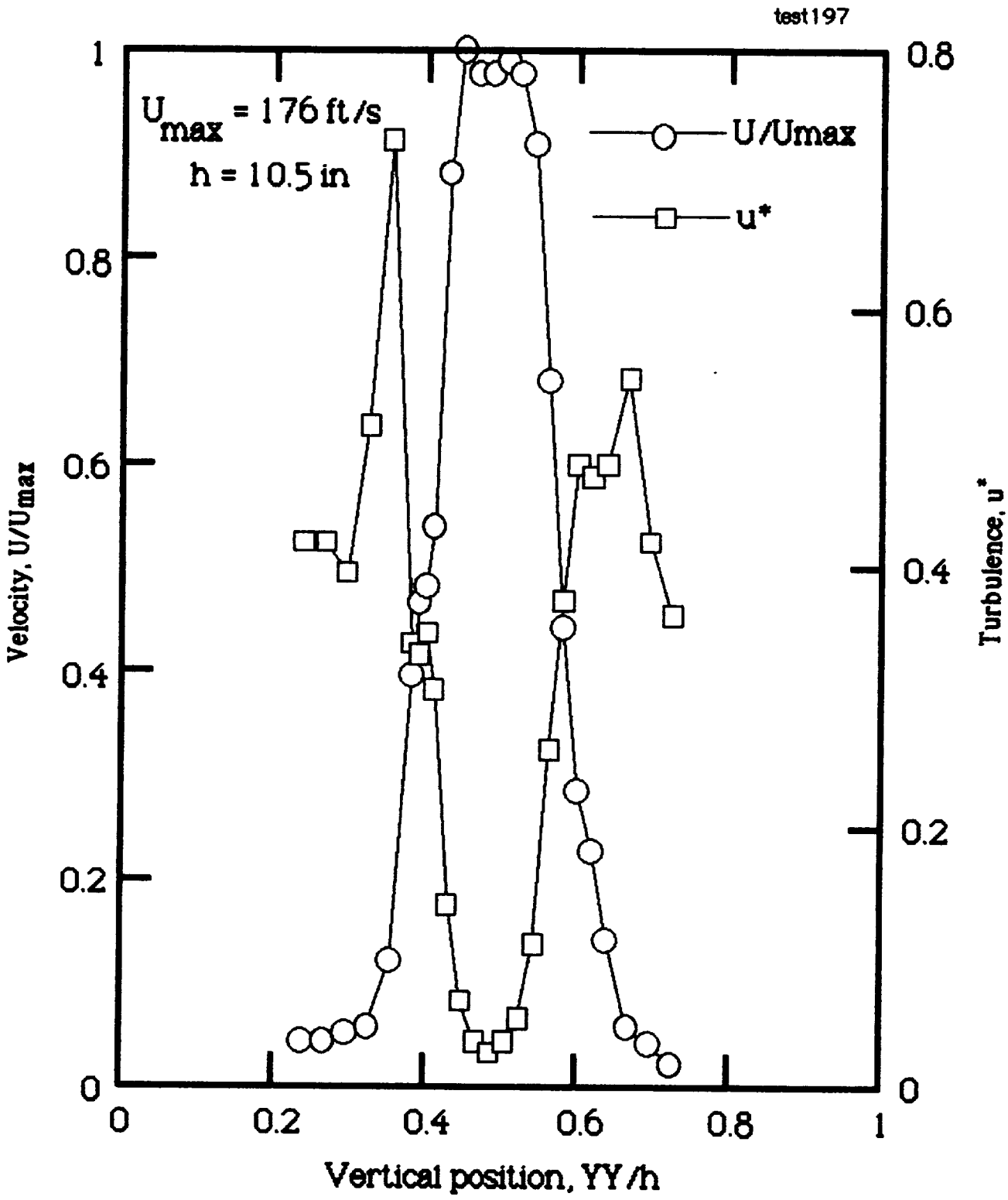

Figure 35. Vertical variation of velocity, and turbulence at the enterance to the new collector, with the regular N/D.

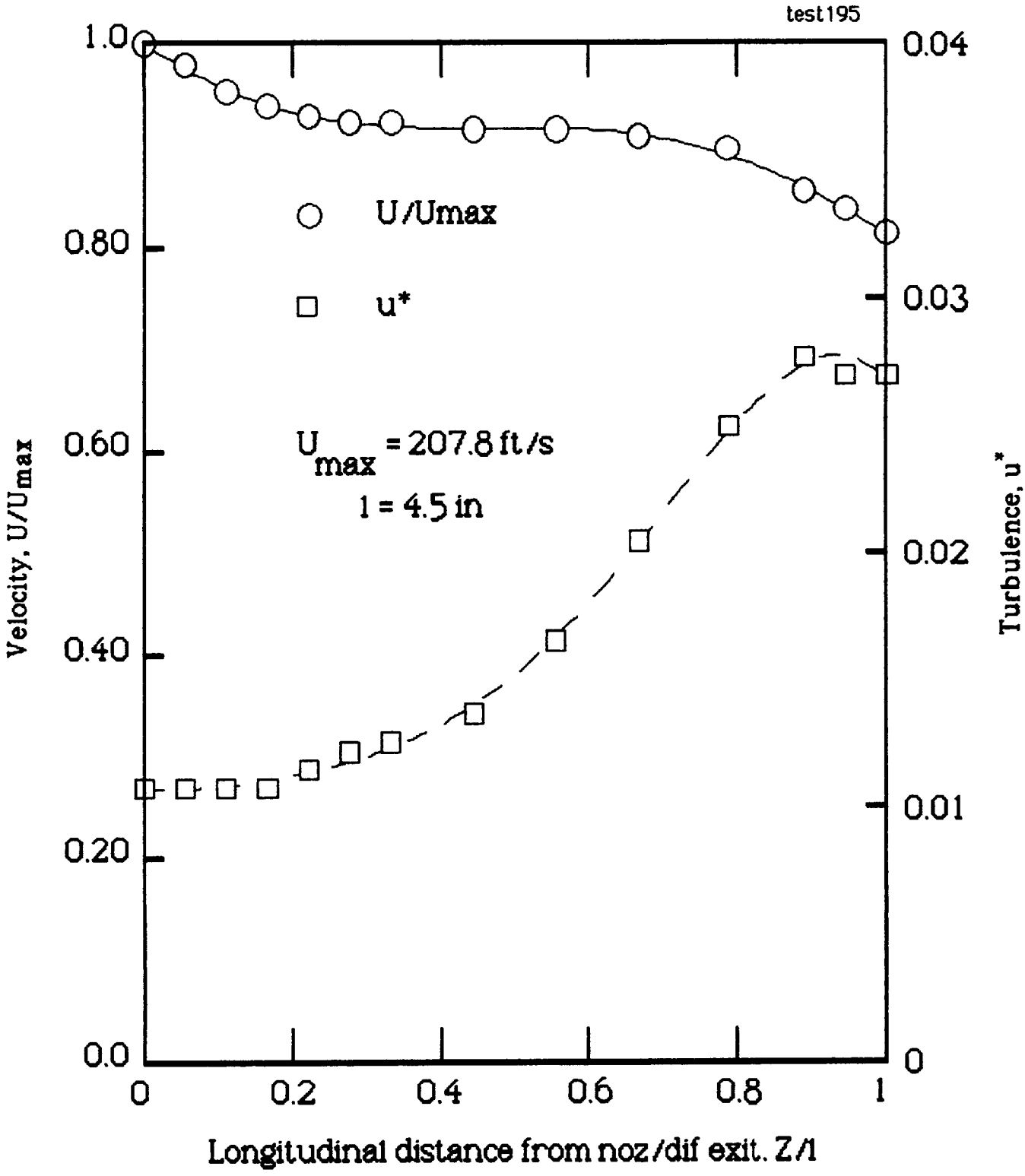

Figure 36. Longitudinal variation of velocity and turbulence between the regular N/D exit and collector inlet along the jet centerline.

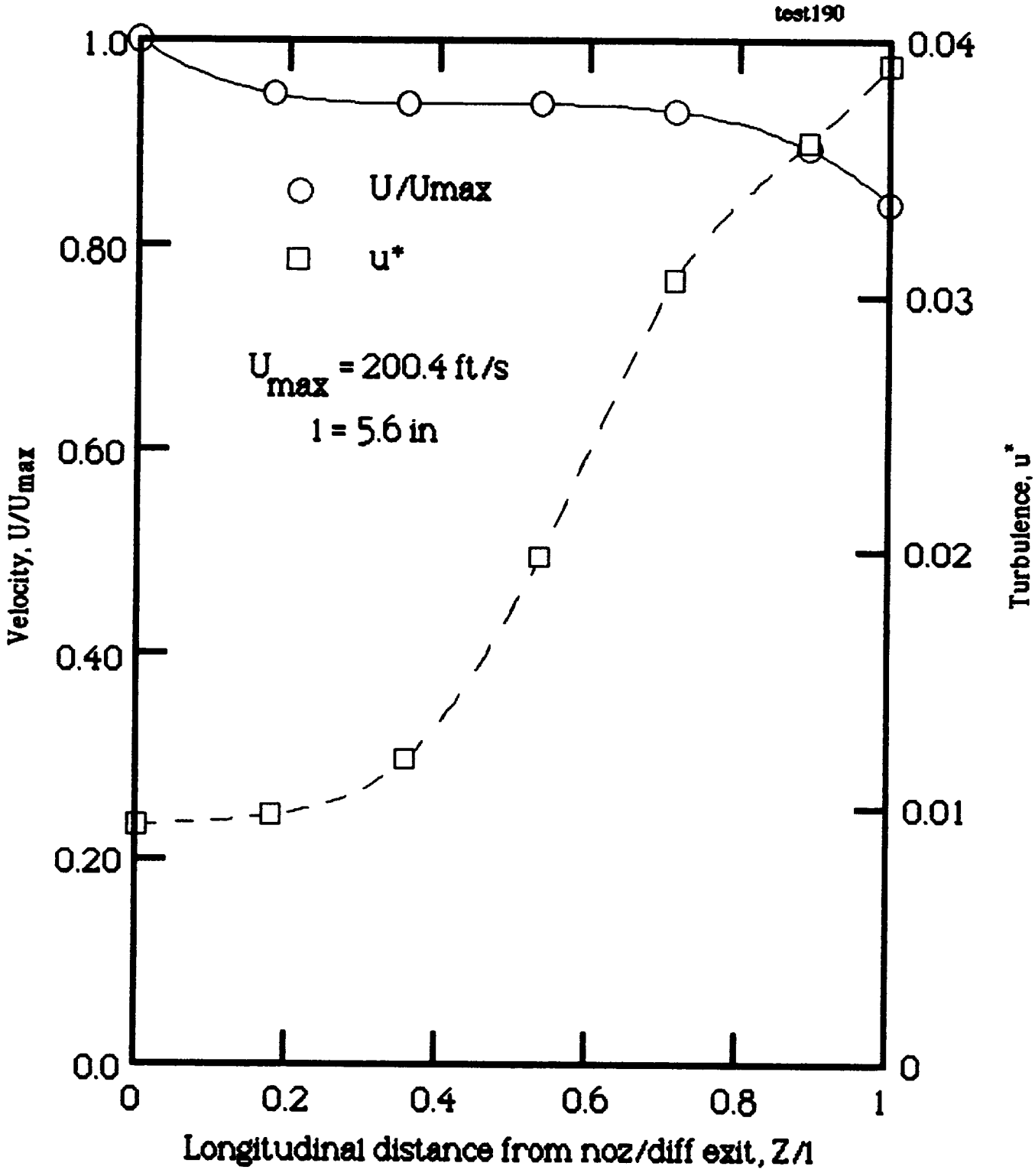

Figure 37. Longitudinal variation of velocity and turbulence, over the extended test area, between the regular N/D exit and collector inlet along the jet centerline.

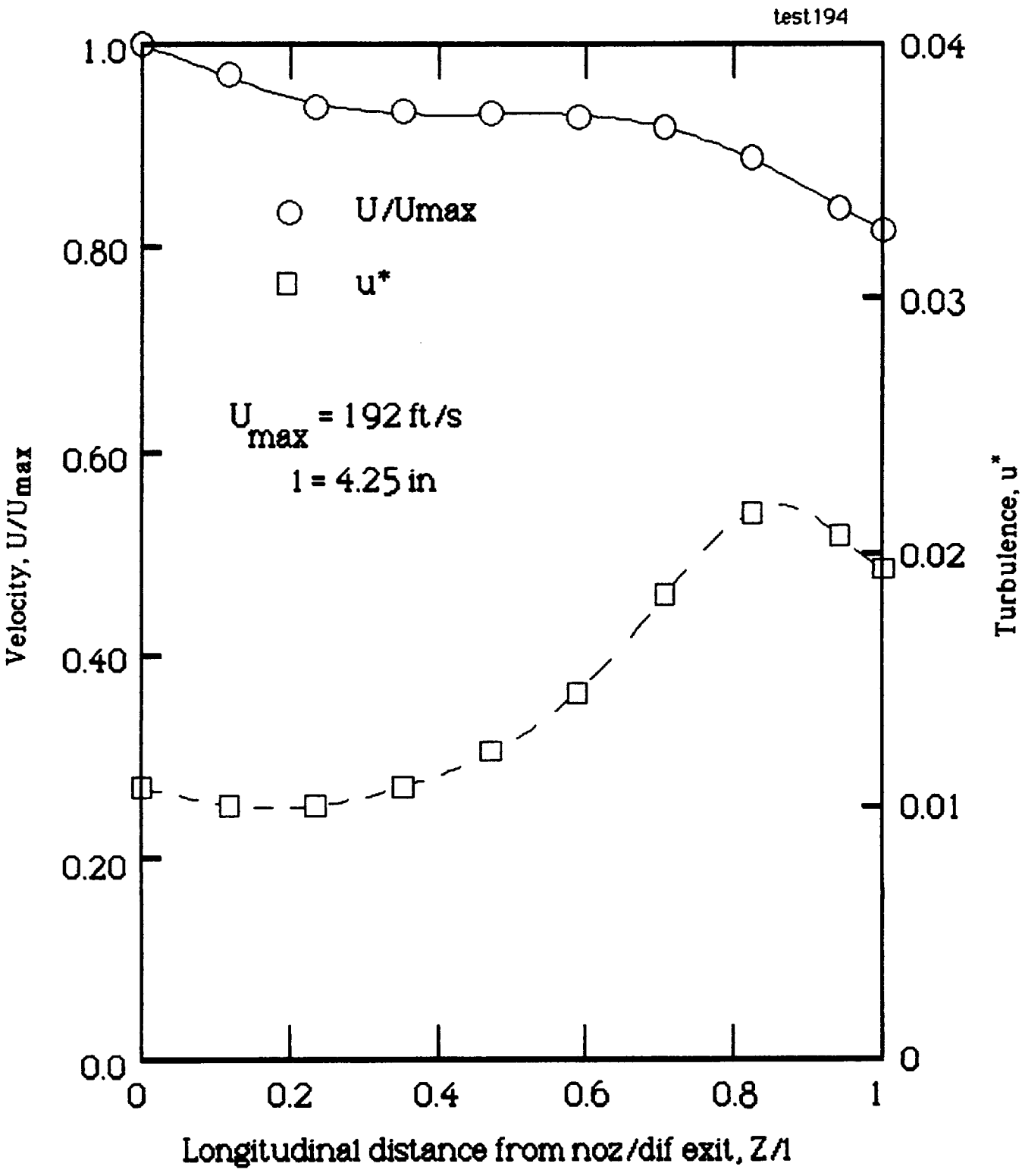

Figure 38. Longitudinal variation of velocity and turbulence between the extended N/D exit and collector inlet along the jet centerline.

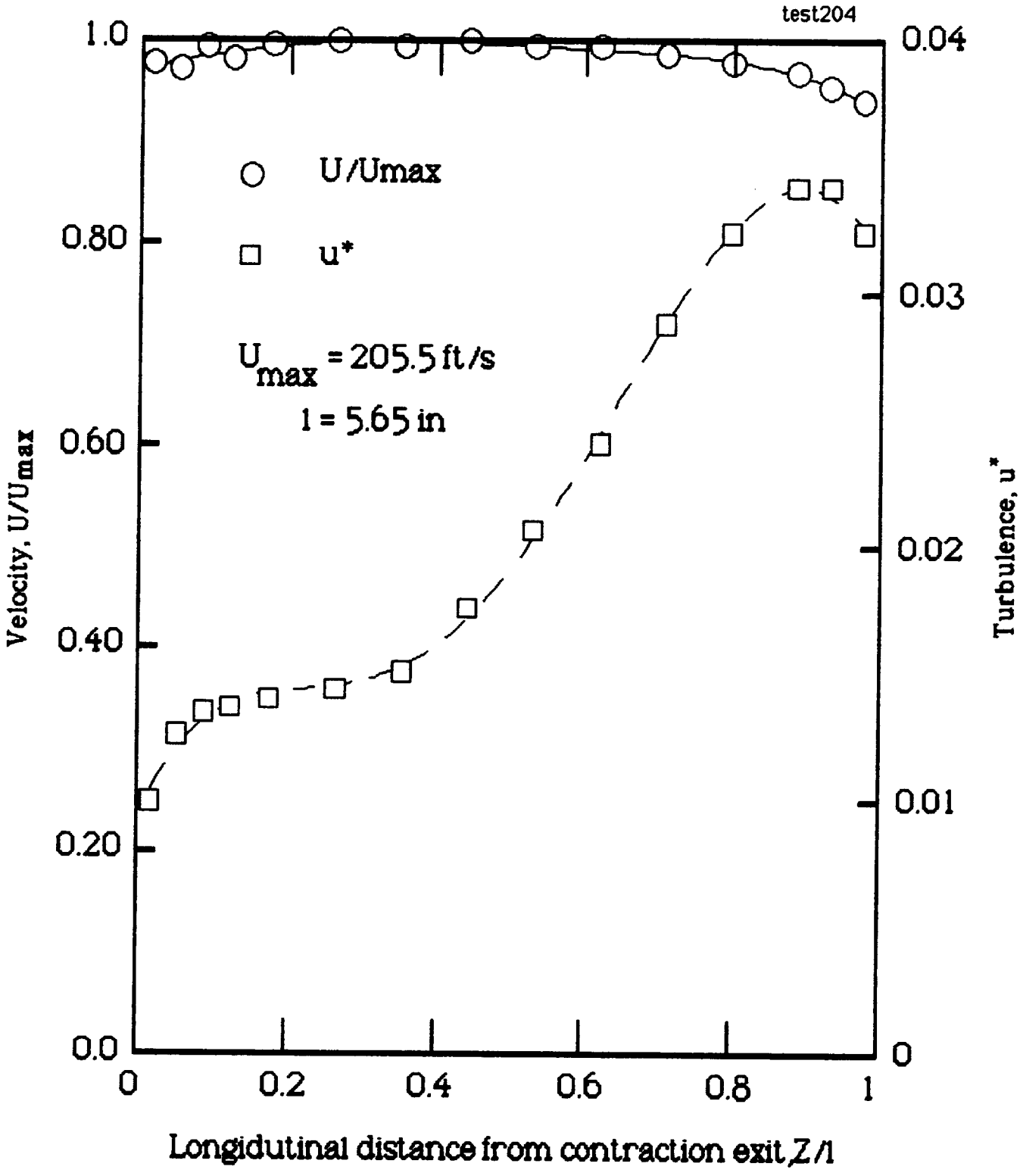

Figure 39. Longitudinal variation of velocity and turbulence between the contraction exit and collector inlet along the jet centerline.

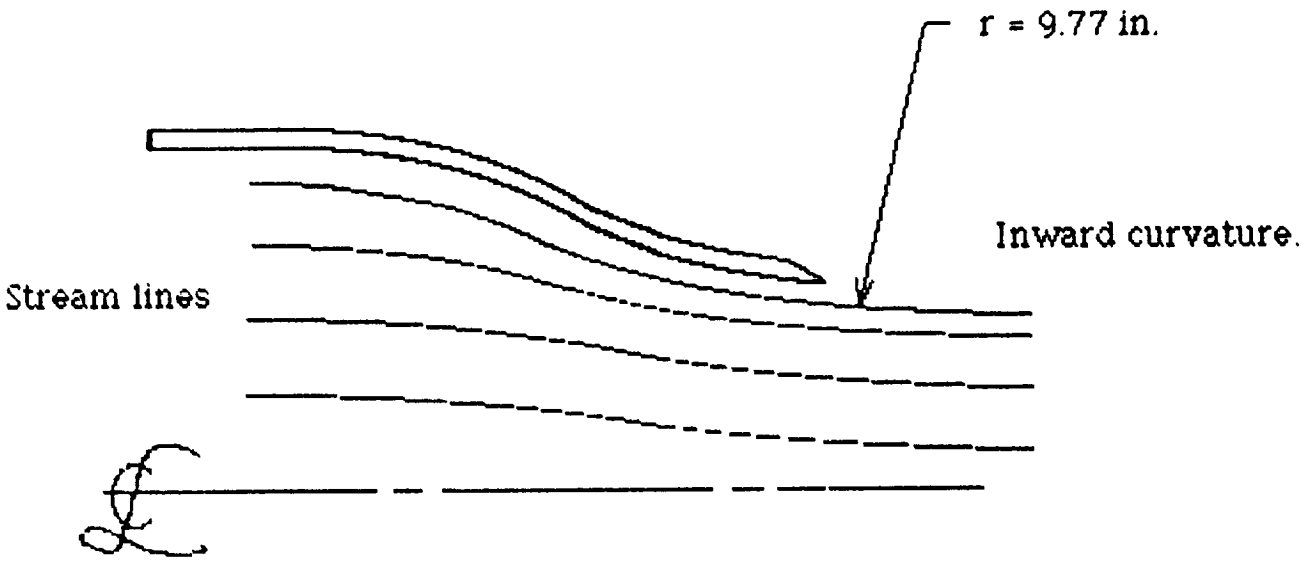

a) Contraction only.

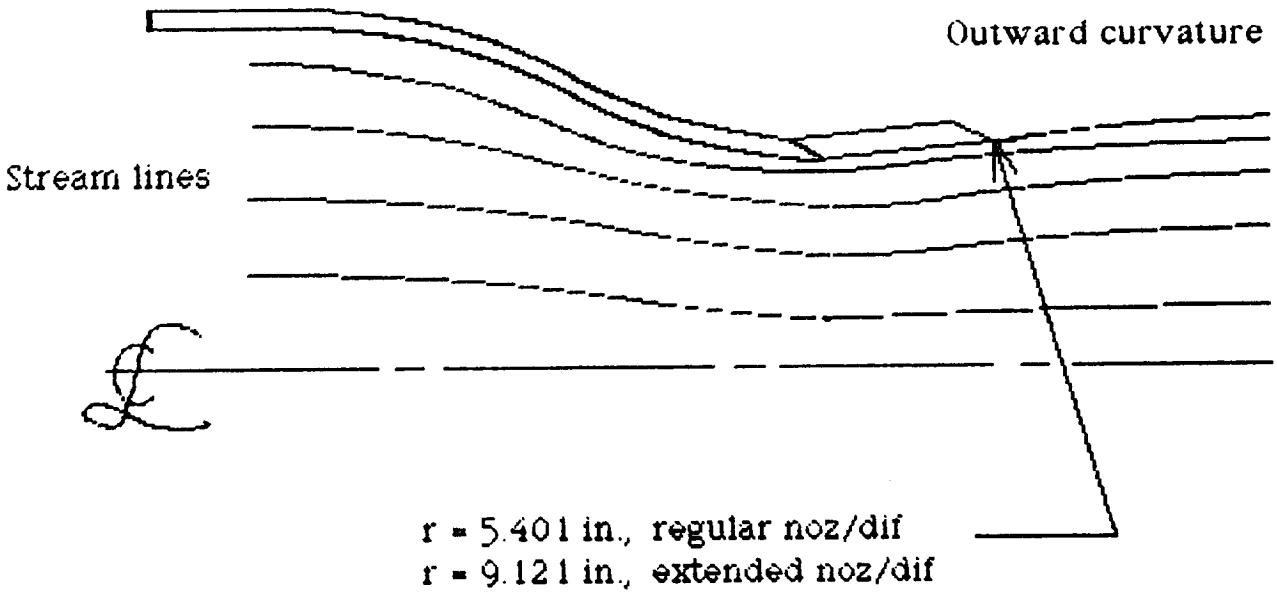

b) Regular or extended noz/dif.

Figure 40. Sketch of hypothetical streamlines entering the test area.

REPORT DOCUMENTATION PAGE

Form Approved
OMB No. 0704-0188

1. AGENCY USE ONLY (*Leave blank*)	2. REPORT DATE	3. REPORT TYPE AND DATES COVERED
	April 1996	Contractor Report

4. TITLE AND SUBTITLE

Results of Tests Performed on the Acoustic Quiet Flow Facility Three-Dimensional Model Tunnel
Final Report on the Modified D.S.M.A. Design

5. FUNDING NUMBERS

C NAS1-19000
WU 538-03-12-01

6. AUTHOR(S)

P. S. Barna*

7. PERFORMING ORGANIZATION NAME(S) AND ADDRESS(ES)

Lockheed Martin Engineering & Sciences Company
Hampton, VA 23666

8. PERFORMING ORGANIZATION REPORT NUMBER

9. SPONSORING / MONITORING AGENCY NAME(S) AND ADDRESS(ES)

National Aeronautics and Space Administration
Langley Research Center
Hampton, VA 23681–0001

10. SPONSORING / MONITORING AGENCY REPORT NUMBER

NASA CR-198312

11. SUPPLEMENTARY NOTES

Langley Technical Monitor: J. W. Posey; Final Report

12a. DISTRIBUTION / AVAILABILITY STATEMENT

Unclassified-Unlimited
Subject Category: 71

12b. DISTRIBUTION CODE

13. ABSTRACT (*Maximum 200 words*)

Numerous tests were performed on the original ACOUSTIC QUIET FLOW FACILITY THREE-DIMENSIONAL MODEL TUNNEL, scaled down from the full-scale plans, shown in figure 1, which were submitted to NASA by Messrs. D.S.M.A. Corporation in July 1992 (1). Results of tests performed on the original scale model tunnel were reported in April 1995, which clearly showed that this model was lacking in performance.

Subsequently this scale model was modified to attempt to possibly improve the tunnel performance.

The modification included: (a) redisigned diffuser; (b) addition of a collector; (c) addition of a Nozzle-Diffuser; (d) changes in location of vent-air.

Tests performed on the modified tunnel showed a marked improvement in performance amounting to a nominal increase of pressure recovery in the diffuser from 34 percent to 54 percent.

Results obtained in the tests have wider application. They may also be applied to other tunnels operating with an open test section not necessarily having similar geometry as the model under consideration.

14. SUBJECT TERMS	15. NUMBER OF PAGES
wind tunnel, open jet, jet entrainment, scale model flow facility, nozzle-diffuser, jet collector	84
	16. PRICE CODE: A05

17. SECURITY CLASSIFICATION OF REPORT	18. SECURITY CLASSIFICATION OF THIS PAGE	19. SECURITY CLASSIFICATION OF ABSTRACT	20. LIMITATION OF ABSTRACT
Unclassified	Unclassified	Unclassified	